2013-01-01

Interaction Of CeO2 And ZnO Nanoparticles Towards The Symbiotic Association Of Alfalfa (Medicago Sativa) And Sinorhizobium Meliloti In Soil

Susmita Bandyopadhyay
University of Texas at El Paso, sbandyopadhyay2@miners.utep.edu

INTERACTION OF CeO_2 AND ZnO NANOPARTICLES TOWARDS THE SYMBIOTIC ASSOCIATION OF ALFALFA (*MEDICAGO SATIVA*) AND *SINORHIZOBIUM MELILOTI* IN SOIL

SUSMITA BANDYOPADHYAY

Environmental Science and Engineering

APPROVED:

Jorge L. Gardea-Torresdey, Ph.D., Chair

Jose R. Peralta-Videa, Ph.D.

Mahesh Narayan, Ph.D.

John Walton, PhD. PE.

Benjamin C. Flores, Ph.D.
Dean of the Graduate School

Dedication

To my beloved parents, for their endless love, support, and encouragement and who helped shape me into the person I am.

&

To my sweet and supportive in-laws!

INTERACTION OF CeO_2 AND ZnO NANOPARTICLES TOWARDS THE SYMBIOTIC ASSOCIATION OF ALFALFA (*MEDICAGO SATIVA*) AND *SINORHIZOBIUM MELILOTI* IN SOIL

by

SUSMITA BANDYOPADHYAY, MSc

DISSERTATION

Presented to the Faculty of the Graduate School of

The University of Texas at El Paso

in Partial Fulfillment

of the Requirements

for the Degree of

DOCTOR OF PHILOSOPHY

Environmental Science and Engineering

THE UNIVERSITY OF TEXAS AT EL PASO

December 2013

Acknowledgements

I would like to express my heartfelt gratitude to my Guru, Dr. Jorge L. Gardea-Torresdey, my research supervisor, for his patient guidance, enthusiastic encouragement, and useful critiques. I would like to thank you for giving me the privilege to work with one of the most famous research groups in the field of environmental chemistry. You are one of the most intelligent, smart, energetic, and caring people I know. During these past three years of my doctoral studies, I have learnt how to publish, how to formulate projects, how to write scientific journal articles, and how to review manuscripts/proposal/grants. You have taught me to think and work independently. Probably, the most important lesions I get from you are to think positive, believe in my abilities, and humbleness. You showed me how to become successful in both professional and personal lives. I consider myself extremely fortunate to get the chance to be associated with you for the last three years. Working with you was fun and challenging. Thanks for being such a great mentor. I am honored to be a part of your research group. All the credit of my successful postgraduate career is directly attributed to you.

I would also like to thank Dr. Jose R. Peralta-Videa, for your advice and assistance in keeping my progress on schedule. I am fortunate to be associated with an expert like you. I learnt a lot about plant related research and the test plant “alfalfa”, which helped me to conduct my experiments in the laboratory. Thanks for your patience while correcting my manuscripts and teaching me how to improve scientific writing. Your training is one of the major facts, which made me an independent writer and reviewer. You also taught me how to finish everything before the deadline and I will remember your suggestions and the *mantra: “If 24 h are not enough, work more than 24 h.*” Thanks for your support, cooperation, and guidance.

I would also like to extend my thanks to Dr. Mahesh Narayan for serving my committee and thanks for all your valuable suggestions and critiques for my doctoral research. Thanks for being an awesome teacher. A special thanks to him for being very supportive and friendly to me and my family.

I am thankful to my committee member Dr. John Walton for his valuable suggestions and teaching the awesome class “fate and transport’. So far this is one of the great classes where I learnt a lot and improved my scientific skills as an environmental professional.

My completion of the projects could not have been accomplished without the support of Dr. Gardea’s group members. Thank you all for your collaboration, cooperation.

In addition, a big thank to all my collaborators, especially to Dr. Miguel Jose Yacaman and Dr. Germán Plascencia Villa of The University of Texas at San Antonio, whose association helped me to complete my projects by obtaining outstanding electron microscopy imaging.

I would also like to thank the Environmental Science and Engineering Program of UTEP for accepting me and giving a chance to pursue my PhD career. A special thanks to the Chemistry Department for allowing me to use necessary resources.

I wish to thank my parents for their support and encouragement throughout my study. Thanks for such an awesome teacher and teaching me the chemistry of life. I am also grateful to my in-laws for their support during my study. Nothing could have been possible without your support.

Special thanks to my friend Dr. Rajib Paul. Thanks for being a great support to me in my personal and professional life; especially helping me with the statistical analysis.

My deepest gratitude goes to my caring, loving, and supportive husband, Arnab Mukherjee. Your encouragements, especially when the times got rough, are much appreciated.

Thanks for taking care of our son Ashmit during my absence in summer. Thanks for being an amazing friend for last sixteen years and a great husband. My life is complete with your presence along with our son Ashmit. Thanks for your support in my personal and professional life.

Finally, I would like to thank my cute, smart, and little *big boy* Ashmit for making my life so colorful and enjoyable. You are one of my greatest inspirations towards my future endeavors.

Abstract

The production of engineered nanoparticles (ENPs) has rapidly increased due to their wide range of applications in the field of electronics, medicine, chemistry and biology. Consequently, concerns have risen about the environmental release and potential negative impact of NPs. A few reports have described the effects of TiO_2 NPs and quantum dots upon nitrogen fixing bacteria. However, the understanding of the interaction of NPs in plant-microbe interface (symbiotic association), like alfalfa (*Medicago sativa* L.)-*Sinorhizobium meliloti*, is still in its infancy. Alfalfa is the world's most important forage crop. It grows in association with *S. meliloti*, which is very important in terms of nitrogen fixation and, hence, global nitrogen cycling. This research project was aimed at understanding the effect of two ENPs (CeO_2 and ZnO) on *S. meliloti* and alfalfa, separately, and on their symbiosis. This investigation was completed in three phases. Initially, the associated bacterium was treated, separately, with CeO_2 and ZnO NPs. Ten nm CeO_2 and ZnO NPs were exposed towards *S. meliloti* at 10, 31, 62.5,125, and 250 mg/l in liquid Yeast Mannitol Broth (YMB). Toxicological parameters evaluated included UV/Vis measurement of minimum inhibitory concentration, disk diffusion tests, and dynamic growth. Advanced scanning transmission electron microscope (STEM) and infrared spectroscopy (FTIR) were utilized to determine the spatial distribution of NPs and macromolecule changes in bacterial cells, respectively. Results indicate that ZnO NPs were more toxic than CeO_2 NPs in terms of inhibition of dynamic growth and viable cells counts. STEM images revealed that CeO_2 and ZnO NPs were found on bacterial cell surfaces and ZnO NPs were internalized into the periplasmic space of the cells. FTIR spectra showed changes in protein and polysaccharide structures of extra cellular polymeric substances present in bacterial cell walls treated with both NPs. The growth data showed a bacteriostatic effect of CeO_2 NPs, whereas ZnO NPs was bactericidal to *S.*

meliloti. Overall, ZnO NPs were found to be more toxic than CeO_2 NPs to *S. meliloti*. In phase II, the alfalfa plant in association with *S. meliloti,* were cultivated for 30 d in soil treated with ZnO NPs, ionic ($ZnCl_2$) and bulk ZnO, concentrations ranging from 0 (control)-750 mg kg^{-1}. Plant growth, Zn bioaccumulation, dry biomass, leaf area, total protein, and catalase (CAT) activity were measured. Results showed 50% germination reduction by bulk ZnO at 500 and 750 mg/kg and all $ZnCl_2$ concentrations. ZnO NPs and ionic Zn reduced root and shoot biomass by 80% and 25%, respectively. Conversely, bulk ZnO at 750 mg/kg increased shoot and root biomass by 225% and 10%, respectively, compared to control. At 500 and 750 mg/kg, $ZnCl_2$ reduced CAT activity in stems and leaves. Total leaf protein significantly decreased as external $ZnCl_2$ concentrations increased. STEM analysis revealed the presence of ZnO particles in tissues, suggesting the uptake of NPs. However, ZnO NPs showed less toxicity compared to $ZnCl_2$ on measured traits. Phase III was performed in soil treated with either ZnO or CeO_2 NPs at 0, 250, 500, and 750mg/kg for 30 days to study the toxicity effect of ZnO and CeO_2 towards alfalfa's secondary metabolites and antioxidative properties. The toxicity was evaluated for leaf using chlorophyll (*a* & *b*), carotenoids, phenolic, and flavonoid contents. Results showed that, compared to control, leaf chlorophyll *a* content reduced to 60% and 40% at 750 mg/kg of CeO_2 and ZnO NP treatments, respectively. Chlorophyll *b* reduced by 64%, 48%, and 60% at 250, 500 and 750 mg/kg CeO_2 NP treatments, while chlorophyll *b* remained the same except 40% reduction at 750 mg/kg bulk ZnO treatment. CeO_2 NPs enhanced the root flavonoids content by 34% at 750 mg/kg treatment and 86% in shoot at 500 mg/kg treatment, compared to control. Total root flavonoids decreased by 49% in plants treated with 750 mg/kg of ZnO NP treatment, whereas total flavonoids in shoots remained similar to control in all treatments, except 250 mg/kg ZnO NP treatment, where the flavonoid content decreased to 77%. This is the first

complete study in a symbiotic system in terms of nano, bulk and ionic Zn species comparison in soil matrix. In addition, to the best of the authors' knowledge, this is the first report on the effects ZnO and CeO_2 on alfalfa's secondary metabolites and chlorophyll content. Our results will help to reveal the toxicity of CeO_2 and ZnO NPs on alfalfa and *S. meliloti* species, as well as to understand the eco-toxicity of NPs in plant-microbe symbiosis.

Table of Contents

List of Tables

List of Figures

Chapter 1

Introduction

Nanoparticles (NPs) are natural or manmade materials with at least two dimensions between 1 and 100 nm (*1*). Mostly, there are two groups of NPs, carbon-containing and metal-containing particles and metal oxide NPs are one of widely used NPs in the market. The most well-known carbon-containing NPs are carbon nanotubes (CNTs) and fullerenes, and TiO_2, ZnO, CeO_2, are among the most popular metal-oxide NPs (*2*). These particles can be in different shapes and sizes. For example, asymmetrical like nanorods or more symmetrical like spheres, shells, cubes, or cages (*3*), with a wide range of application in the fields of medicine, electronics, manufacturing and energy production is due to their high surface to volume ratio and higher numbers of atoms at the grain boundaries, which make them more reactive (*4-6*). Conversely, these unique properties are responsible for their potential toxicity to living organisms. Recent literature has shown that NPs affect in different ways animals, plants, and microorganisms, including fungi and bacteria (*7-11*). But the understanding of the impact of ENPs on the edible/crop plants is limited. Only few reports describe the toxicity of ENPs on crop plants such as rape (*Brassica napus*), radish (*Raphanus sativus*), lettuce (*Lactuca sativa*), corn (*Zea mays*), cucumber (*Cucumis sativus*) and alfalfa (*Medicago sativa*), among others (*12-14*).

It has been evidenced that these NPs adversely affect plant growth of green pea, corn, cucumber, rye, zucchini, soybean, and wheat, depending on the concentration of the NPs used (*15, 16, 17-20*). Dimpka et al. reported reduced wheat plant growth with increased production of ROS with the application of ZnO NPs (*15*). On the other hand, Lin and Xing (*18*) reported that ZnO NPs affected root elongation in ryegrass (*Lolium perenne*), radish (*Raphanus sativus*) and

rape (*Brassica napus*) (*18*). The reported phytotoxicity was due to disruption in water and nutrient pathways (*19*). They also confirmed the adsorption and aggregation of the ZnO NPs to the root surface of ryegrass where the high magnification TEM images showed the presence of NPs in the apoplast, cytoplasm and nuclei of the endodermal cells and the vascular cylinder (*18, 19*). However, X-ray absorption confirmed the nonexistence of the NPs. Later, Kim et al (*21*), reported phytotoxic effects of ZnO NPs in *Cucumis sativus* due to excess Zn bioaccumulation (*21*); whereas, Lopez-Moreno et al.(*22*) reported the genotoxic effect of ZnO NPs to soybean (*Glycine max*) (*22*). The authors also reported the toxicity of CeO_2 NPs to alfalfa seedlings and confirmed the presence of CeO_2 NPs in plants cells through XRF (*22*). Recently, Mukherjee et al. (*17*) reported the phytotoxic effect of ZnO NPs in green peas where ZnO NPs were found to be more toxic (compared to bulk ZnO) due to higher accumulation of ROS in different plant tissues (*17*). However, only one report was found where the interaction of NPs (CeO_2 and ZnO) on symbiotic association (important in terms of nitrogen fixation) was studied (*23*). The authors reported that higher Zn and Ce was accumulated in above and below ground parts of soybean plants, including the nodules, which was confirmed through ICP analysis and electron microscopy imaging. The result showed that CeO_2 and ZnO NPs adversely affect the plant growth; however the effect on nodulation/nitrogen fixation remained unaltered in case of ZnO. But, CeO_2 negatively impacted on the nitrogen fixation process. The authors also confirm the Zn ions/ZnO NPs accumulation in different parts of plants through ESEM and STEM (*23*).

However, the interaction of NPs with the environmentally benign microbial community is still in its infancy. Few reports have described the effects of NPs upon nitrogen fixing bacteria. For example, TiO_2 NPs was reported to have bactericidal effects in nitrogen fixing soil bacteria *Anabaena variabilis* (*24*, *25*). However, a more recent study (*26*) has shown that quantum dots

do not produce significant negative effect in several nitrogen cycling bacteria including *Azotobacter vinelandii. Nitrosomonas europaea, Rhizobium etli, Azospirillum lipoferum* and denitrifying bacteria such as *Pseudomonas stutzeri* (*26*).

Studies have shown that NPs and/or ionic species released from NPs affect bacteria in different ways, including surface attachment, membrane disorganization, surface coating-related photocatalytic oxidation, and reactive oxygen species (ROS) production through lipid peroxidation (*5, 9 27-30*). It has been reported that the toxicity of ZnO NPs towards the Gram-negative *Escherichia coli* (*E. coli*) is mainly due to the presence of free zinc ions (Zn^{2+}) in the aqueous media (*31*). Nevertheless, other NPs show toxicity to bacteria through surface attachment or internalization through cell wall. For instances, Pelletier et al. (2011) reported the bactericidal effect of CeO_2 NPs on *E. coli* and the authors mentioned the related toxicity was due to the surface attachment (of NPs). But, Thill et al. (2006) suggested a different toxicity pathway; they mentioned that these NPs affect *E. coli* cells through membrane damage (*5, 28*). The differences in toxicity mechanisms induced by NPs is attributed to several factors including the source of NPs, stabilizing/capping agents used, and other physicochemical properties (pH, ionic strength, ionic composition and organic matter of the media) (*5, 31, 32).*

To the best of the author's knowledge, there are no reports on the effects of ZnO and CeO_2 NPs on *Sinorhizobium meliloti*, a soil bacterium which fix nitrogen in symbiotic association with the host plant alfalfa, one of the most important crops worldwide (*33, 34).* It has been evidenced that *S. meliloti* interacts with alfalfa roots through the extra cellular polysaccharides (EPS) which allow bacterial cells to attach on the root surface and hence induce the nodulation. In addition, EPS also help in nutrient acquisition and protect the bacterial cells from environmental

stresses (*33*). Therefore, any effect on the bacterial EPS will alter the nodulation; hence, the nitrogen fixation will be distressed.

While it is known that CeO_2 and ZnO nanoparticles can be toxic to many different bacteria (*2, 27-30*) and plants (*6, 9, 10, 12, 15-23*) their effects on environmentally important process of nitrogen fixation through symbiosis are unknown. Most of the available literatures are based on hyperaccumulation of heavy metals (3*5-39*). Alfalfa is well known as metal accumulator, capable of absorbing heavy metals at high concentrations with no toxicity observed (*35, 39*). Studies have demonstrated, that the symbiotic interaction between plants and bacteria, have an effect on the tolerance and uptake of heavy metals, but little is known about this (*30, 41*). On the other hand, it has been previously reported alfalfa is able to germinate in the presence of CeO_2 NPs and accumulate Ce in seedling tissues (*9*). Nevertheless, to our knowledge the proposed plant's ability to uptake ENPs (CeO_2 and ZnO) by itself and its symbiotic interactions with *S. meliloti* have not been studied beyond germination. In addition, uptake, translocation and localization of CeO_2 and ZnO NPs are desired in order to understand the physical and physiological mechanisms between the host plant (*M. sativa)* and the bacteria (*S. meliloti).*

This study was aimed to use the plant-bacterial model to define the effect of CeO_2 and ZnO NPs on environmentally significant bacterial processes of nitrogen fixation. We focused to find out the effect of these ENPs (CeO_2 and ZnO) on symbiotic nitrogen fixation by characterizing the effect of CeO_2 and ZnO NPs on both members of the *S.meliloti-M. sativa* symbiosis. This is an interesting system to study the toxicity of NPs as both the partners have been well studied in their own and the symbiosis relationship between *Sinorhizobium* and *M. sativa* has been a subject of robust investigation for many decades. *Medicago sativa* is a model

or reference species for legume genetics, genomics, and breeding. Thus, the information acquired through the proposed studies could be pioneering in this field. Consequently, the main objective of this study was to understand how the bacterial nodulation is affecting the uptake/interaction of ENPs towards *M. sativa*.

The association of both the species would affect the CeO_2 and ZnO uptake capacity by the host plant, bacteria, and the association of host plant and the *S. meliloti*. The elemental (Ce^{4+} and Zn^{2+}) uptake and translocation in plant tissue, bacterial cells, and soil was determined by using an inductively coupled plasma optical emission spectrometer (ICP-OES). Furthermore, other techniques including scanning transmission electron microscopy (STEM) and energy diffraction system (EDS), X-ray absorption spectroscopy (XAS) was used to find out the localization/accumulation of NPs inside the bacterial cells, plant tissues. The biochemical assays (Catalase activity, total protein content along with phenolic content and flavonoids in roots and shoots) was used to determine the NPs induce stress and enzyme activity in the plants. Fourier Transformed Infrared Spectrometer (FTIR) was used to study the changes associated with bacterial cell and changes associated with the protein and carbohydrates structure of plants cells wall upon treatment of CeO_2 and ZnO.

Chapter 2

Comparative toxicity assessment of CeO_2 and ZnO nanoparticles towards *Sinorhizobium meliloti*, a symbiotic alfalfa associated bacterium

Abstract

Cerium oxide (CeO_2) and zinc oxide (ZnO) nanoparticles (NPs) are extensively used in a variety of instruments and consumer goods. These NPs are of great concern because of potential toxicity towards human health and the environment. The present work aimed to assess the toxic effects of 10 nm CeO_2 and ZnO NPs towards the nitrogen fixing bacterium *Sinorhizobium meliloti*. Toxicological parameters evaluated included UV/Vis measurement of minimum inhibitory concentration, disk diffusion tests, and dynamic growth. Advanced scanning transmission electron microscope (STEM) and infrared spectroscopy (FTIR) were utilized to determine the spatial distribution of NPs and macromolecule changes in bacterial cells, respectively. Results indicate that ZnO NPs were more toxic than CeO_2 NPs in terms of inhibition of dynamic growth and viable cells counts. STEM images revealed that CeO_2 and ZnO NPs were found on bacterial cell surfaces and ZnO NPs were internalized into the periplasmic space of the cells. FTIR spectra showed changes in protein and polysaccharide structures of extra cellular polymeric substances present in bacterial cell walls treated with both NPs. The growth data showed that CeO_2 NPs have a bacteriostatic effect, whereas ZnO NPs is bactericidal to *S. meliloti*. Overall, ZnO NPs were found to be more toxic than CeO_2 NPs.

Keywords: CeO_2, ZnO, *Sinorhizobium meliloti*, bactericidal, bacteriostatic, Extracellular Polymeric Substances

2.1. Introduction

The unique properties of the nanomaterials are responsible for their potential toxicity to living organisms (*1-3*). Recent literature has shown that NPs affect/interact differently to animals, plants, and microorganisms, including fungi and bacteria (*4-8*). A number of studies have shown that NPs and/or ionic species released from NPs affect bacteria in different ways, including surface attachment, membrane disorganization, surface coating-related photocatalytic oxidation, and reactive oxygen species (ROS) production through lipid peroxidation (*2, 9-12)*. The differences in toxicity mechanisms are attributed to several factors including the source of NPs, stabilizing/capping agents used, and other physicochemical properties (pH, ionic strength, ionic composition and organic matter present in the media) (*2, 13)*. Laboratory studies have shown that the toxicity of ZnO NPs towards the Gram-negative *Escherichia coli* (*E. coli*) is mainly due to the presence of free zinc ions (Zn^{2+}) in the aqueous media (*13)*. This was further corroborated by Li et al. for the aquatic bacteria *Bacillus subtilis* and the Gram-negative *Pseudomonas putida* (*14*). However, other NPs show toxicity to bacteria through surface attachment or internalization through the cell walls. For instance, Pelletier et al. (*2*) reported that CeO_2 NPs exerted bactericidal effect on *E. coli* due to the surface attachment, while Thill et al. (*10)* suggested that these NPs affect *E. coli* cells through membrane damage.

Our understanding of the interaction of NPs with the soil microbial community is still in its infancy. Johansen et al. (*15)* reported the toxicity of C_{60} fullerenes (50 nm to μm-size) on the soil microbiota in terms of total respiration, biomass production, and number and diversity of bacteria. Ge et al. (*16)* reported that both TiO_2 and ZnO NPs were toxic to soil microbial communities (as bulk) in terms of reduced biomass and the reported toxicity of ZnO NPs was higher than that of TiO_2 NPs. Few reports have described the effects of NPs upon nitrogen

fixing bacteria. These groups of bacteria are very important in terms of soil health and fertility. Cherchi et al. (*17, 18*) reported cellular internalization of TiO_2 NPs in nitrogen fixing soil bacterium *Anabaena variabilis* with bactericidal effects. A more recent study (*19)* has shown that quantum dots do not produce significant negative effects in several nitrogen cycling bacteria including *Azotobacter vinelandii. Nitrosomonas europaea*, *Rhizobium etli*, *Azospirillum lipoferum* and denitrifying bacteria *Pseudomonas stutzeri*.

To the best of the authors' knowledge, there are no reports on the effects of NPs on *Sinorhizobium meliloti*, a soil bacterium, which fixes nitrogen in symbiotic association with alfalfa (*Medicago sativa*), one of the most important crops worldwide (*20, 21). S. meliloti* interacts with alfalfa roots through the extra cellular polysaccharides (EPS), which allow bacterial cells to attach on the root surface and hence induce nodulation and thus nitrogen fixation. The EPS also facilitate in nutrient acquisition and protect the bacterial cells from environmental stresses (*20).*

The main objective of this work was to determine the toxicological effects of CeO_2 and ZnO NPs on *S. meliloti* and to uncover the mechanism of toxicity towards this nitrogen fixing bacterium. The working hypothesis was that both NPs exerted toxicity towards *S. meliloti* by affecting EPS through surface attachment or internalization into the periplasmic space of the bacteria. Cells of *S. meliloti* were treated in liquid medium with different concentrations of CeO_2 and ZnO NPs an analyzed for changes in growth. In addition, STEM and FTIR were used to study the localization/accumulation of NPs outside/inside the cell walls and the effects on bacterial EPS, respectively.

2.2. Experimental Procedures

2.2.1. Nanoparticles

Ten nm CeO_2 and ZnO NPs (Meliorum Technologies, Rochester, NY) were obtained from the University of California Center for Environmental Implications of Nanotechnology (UC-CEIN). Characterization of these NPs in different media had been previously published by Keller et al. (*22*). For the present research, the size and zeta potential (ζ) of the CeO_2 and ZnO NPs suspended in distilled water and yeast mannitol broth (YMB) were determined by using a NanoSizer 90 (Malvern Instruments, Worcestershire, UK). Initially, all the experiments were performed in a range of concentrations starting from 31 mg/L to 500 mg/L. But, in higher concentrations of both NPs, e.g., 250 to 500 mg/L, the bacteria did not grow. Thus, we dropped two of the higher concentrations and worked with 31, 62.5 and 125 mg/L of NPs. The suspensions were sonicated for 30 minutes in 250 ml Erlenmeyer flasks before dynamic light scattering (DLS) measurements. The pH of the suspensions was also recorded (see Supplementary Information, SI).

2.2.2. Ionic Species

The toxicity of corresponding ionic species was also measured. Two ionic compounds were selected, i.e., cerium sulfate tetrahydrate ($Ce(SO_4)_2 \cdot 4H_2O$) and zinc acetate dihydrate ($Zn(OOCCH_3)_2 \cdot 2H_2O$. Three different concentrations (31, 62.5, and 125 mg/L) of cerium and zinc salts (Sigma–Aldrich and Alfa Aesar, respectively) were prepared simultaneously in YMB without sonication.

2.2.3. Bacterial Culture

S. meliloti strain Rm 1021 was obtained from the Postgraduate College of Chapingo, Mexico. The bacterial stocks were stored at 4 °C in solid medium before use. Bacterial cells were grown aerobically by overnight shaking at 200 rpm (REVCO, Thermo Scientific) at 30 °C. After 24 h incubation (YMB, pH 6.8), the UV–Vis was taken at 600 nm (Cary 50 UV–Vis

Spectrophotometer, Agilent Technologies) to confirm the bacterial growth in YMB in terms of cell density. The bacterial cells were collected by centrifugation at 4000 rpm at 25 °C for 5 min (Marathon 8K, Fischer Scientific), followed by washing with sterilized DI and stored in centrifuge tubes for further analysis.

2.2.4. Dynamic growth curves

To obtain the bacterial growth curves, the cells were grown at 30°C under continuous shaking at 200 rpm for 36 h. The growth was monitored by measuring the UV/Vis optical density (OD) at 600 nm (OD_{600}) every two h. A negative control (flask containing inoculum and nutrient medium, without NPs) and a positive control (flask containing NPs and nutrient medium, without bacteria) were included. The negative controls indicated the bacterial growth profile in the absence of any NPs. The OD of positive controls was subtracted from the experimental OD values, flasks containing nutrient medium, NPs and bacteria. All treatments were set in triplicate. The actual absorbance was calculated as described by Wu et al. (*23*).

2.3.5. Disk Diffusion Tests (DDT)

The sensitivity of *S. meliloti* Rm1021 to both the NPs was measured by DDT as per Ruparelia et al. (*24*). Initially, three concentrations of CeO_2 and ZnO NPs (31, 62.5, and 125 mg/L) were prepared by suspending a desired amount of NPs in DI and then sonicated for 15 min. Subsequently, uniform disks (6 mm diameter) of Whatman 48 filter paper were damped with the NP suspension for 10 min and placed in Petri dishes previously inoculated with 1 ml of inoculum containing approximately 10^5 colony forming units (CFU). Four disks were distributed in each plate and overnight incubated at 30^oC. Diameter of inhibition zone (DIZ) was measured to assess the toxicity of CeO_2 and ZnO NPs on *S. meliloti*.

2.3.6. Minimum Inhibition Concentration (MIC)

The MIC is the lowest concentration of a compound that inhibits the growth of an organism. In this research, the MIC of CeO_2 and ZnO NPs over *S. meliloti* was determined as described earlier (*25*) Briefly, 10 ml of the bacterial stock culture in logarithmic phase were inoculated in 250 ml Erlenmeyer flasks containing the YMB amended with CeO_2 and ZnO NPs, separately, at 31, 62.5 and 125 mg/L. In this point, we introduced lower a concentration of 10 mg/L along with two higher concentrations (250 and 500 mg/L) as mentioned earlier. All treatments, including control (YMB without NPs) were performed in triplicate. The turbidity was visually inspected in each flask and the bacterial growth was measured with a UV-Vis spectrophotometer after 24 h at 600 nm.

2.3.7. Live/Dead Viability Assay

To determine the live/dead viability, *S. meliloti* cells were grown in liquid YMB with different concentration (31, 62.5 and 125 mg/L) of CeO_2 and ZnO NPs through overnight incubation at 30^oC to the logarithmic phase. Then, a 2 ml aliquot of each sample was dispersed in clean sterile solid YMB plates and kept overnight to see the growth recovery. The plates were observed next day visually to see any colony formation.

2.3.8. Extraction of Extracellular Polysaccharides (EPS)

S. meliloti cells were cultivated aerobically in YMB at 30^oC under continuous shaking at 200 rpm in 250 ml flasks. The cells were grown overnight and supernatants were collected by centrifugation at 8000 rpm for 10 min at 4^oC. The extraction of EPS was performed according to Kumar et al. (*26*) with minor modifications. Three volumes of 95%, 200 proof ethanol (Sigma-Aldrich) were added to the supernatants to precipitate out the EPS. Then, the samples were placed at -20^oC for 24 h. The crude EPS was recovered from the solution by centrifugation at

10,000 rpm for 10 min at 4^{o}C. The pellet was then washed with 95% ethanol and air dried for further analysis (*26*). The weight of the extracted EPS was determined after air drying the pellets at room temperature (for 72 hours). All extractions and measurements, including control (bacterium without NPs) were performed in triplicate.

2.3.9. Field Emission- Scanning Electron Microscopy (FE-SEM) Imaging and Energy Dispersive X-ray (EDX) Analysis

The SEM analysis was carried out with a HITACHI S-5500 In-Lens FE-SEM coupled with LABE (Low Angle Backscattered Electron), YAG-BSE (Yttrium-Aluminum-Garnet Backscattered Electron), BF/DF-STEM detectors and EDX spectrometer (Bruker), operated with an accelerating voltage of 5-30 kV. Further information is presented in SI.

2.3.10. FTIR Analysis

The FTIR spectra of dry EPS samples were collected at a frequency range 4000-500 cm^{-1} and at a resolution of 4 cm^{-1} using a Spectrum 100 (Perkin Elmer, Shelton, CT). All FTIR spectra presented were average of 400 scans with a collection time of 495 sec. A background spectrum was taken before every sample spectrum. Each spectrum was the sum of three representative spectra in FTIR measurements.

2.3.11. Dissolution of the NPs

To find out the release of Ce^{4+} and Zn^{2+} ions in different NP suspensions, we determine the concentration of Zn and Ce in supernatants by inductively coupled plasma- optical emission spectrometer (ICP-OES). Desired amounts of NPs were dispersed into YMB and sonicated for 15 min. Then, the flasks were shaken continuously at 200 rpm for 24 h. Next day, the NP dispersions were centrifuged at 10,000 rpm for 30 min until a clear supernatant was obtained. The dissolved

Ce^{4+} and Zn^{2+} species in the supernatant were determined using an ICP-OES Optima 4300 DV (Perkin Elmer, Shelton CT).

2.3.12. Statistical Analyses.

The growth data was analyzed using a one-way analysis of variance (ANOVA) followed by Tukey-honestly significant difference test using the Statistical Analysis System (SAS).

2.4. Results and Discussion

2.4.1. Characterization of CeO_2 and ZnO NPs

The initial diameter of the CeO_2 and ZnO NPs was 10 nm, however, upon dispersion, the NPs formed aggregates of different sizes. The DLS measurements showed the size distribution ranges from 500 to 1350 nm for ZnO and 800 to 2200 nm for CeO_2 (Table S1 and S2, Supplemental Information). The zeta potential of particles in DI water was positive but negative in the culture media (Table S1 and S2, SI). The Powder X-Ray Diffraction (pXRD) patterns showed that CeO_2 NPs were pure but ZnO NPs had some impurities (Figure S1A-B, SI). Metal oxide NPs in suspension have the tendency to agglomerate due to particle size, composition of the medium and ionic strength, among others (*27*, *28*). It can also be inferred that electric charges on bacterial cells impart some effects on the particle distribution in suspension (*29*). Also, negative ions (PO_4^{3-}, SO_4^{2-} and Cl^-) present in the media might be adsorbed on the surface of the NPs leading to the negative zeta potential (*30-32*).

2.4.2. Bacteriological Toxicity Tests of CeO_2 and ZnO NPs

The growth profile of NP treated and control cells of *S. meliloti* grown for 36 h showed that both NPs were able to reduce/inhibit the growth of *S. meliloti* compared to the control (Figure 2.1. A-

D). As shown in Figure 2.1A, at all concentrations CeO_2 NPs reduced bacterial growth to some extent. The ANOVA test showed differences between treatments at $\alpha \leq 0.01$ and the Tukey test showed that the growth was in the following order: control > 31 mg/L > 62.5 mg/L~125mg/L. The OD values for the bacterial growth curve at 62.5 mg/L and 125 mg/L were similar. We observed that at higher concentrations (>62.5 mg/L), the particles gravitate/precipitate from the suspension, which might be resulting in the same growth profiles for 62.5 and 125 mg/L of CeO_2 treatments. The growth profile for ionic cerium (Ce^{4+}) is exhibited in Figure 1B. These results imply that inhibitory effects of Ce^{4+} and CeO_2 NPs are very similar.

Figure 2.1-C shows the growth of *S. meliloti* cells exposed to ZnO NPs. As seen in figure, all the concentrations of NPs used inhibited the growth of *S. meliloti*, suggesting a bactericidal effect. This is in accordance to previous reports, which indicate that ZnO NPs were bactericidal towards *Bacillus subtilies*, *Streptococcus pyogenes*, *Staphylococcus epidermis* (*32*) and *Escherichia coli* (*33*, *34*).

The bacteria were treated with both ZnO NP suspension and ($Zn(OOCCH_3)_2 \cdot 2H_2O$ solution in order to compare the toxicity of ZnO NPs to ionic zinc. Figure 2.1C-D shows that ZnO NPs produced higher toxicity than ionic Zn. This is not in accordance with other studies where the toxicity was attributed to Zn^{2+} ions for *Escherichia coli* and *Pseudomonas putida* respectively (*13*, *14*). At higher ZnO NP concentrations, partial dissolution of ZnO NPs was observed (Figure S3-A, SI). For example, at 125mg/L of ZnO NPs in YMB, we determined that only ~11.85 mg/L of free Zn ions are present (see Figure S3-B, SI). Therefore, it is hypothesized that the higher toxicity of ZnO NPs may be attributed to the presence and uptake of ZnO NPs by the bacterial cells, as explained below.

The MIC and viability assays support the dynamic growth curve results. CeO_2 NPs were toxic at higher concentrations with MIC values higher than 125 mg/L, while at lower concentrations, no acute toxicity was observed (Figure 2.1A). As observed in this figure, the bacterial cells grew well (65%) at 31 mg/L and 50% at 62.5 mg/L at CeO_2 NP treatments. However, the cells were unable to grow after 125 mg/L and no bacterial growth was observed at 250 mg/L or higher.

In spite of the attachment of CeO_2 NP aggregates onto the outer surface/cell wall of the *S. meliloti* (Figure 2.1A-B), no acute toxicity was observed at 125 mg/L. Conversely, ZnO NPs showed a broader range of toxicity towards *S. meliloti* at lower concentrations compared to CeO_2 NPs. The MIC study showed that *S. meliloti* was very sensitive to ZnO NPs at concentrations as low as 31 mg/L (Figure 1C). The DDT also showed higher inhibition zones (DIZ) of 15.5±.5 mm for 31 mg/L ZnO treatments compared to CeO_2 treatments (Table S3, SI). But, no bacterial colonies were observed at higher concentration of ZnO NPs (62.5 and 125 mg/L) around the disks (Table S3, SI).

However, no inhibition zones were observed at lower concentrations of CeO_2 NPs (10 and 31 mg/L). Nonetheless, it should be mentioned that the DIZ measurements are susceptible to artifacts generated from the particle's hydrophobic/hydrophilic nature, adsorption of NPs onto the disc and the diffusion rate of the NPs from the discs (*2*).

A decreased bacterial viability was observed with increase in CeO_2 concentration compared to control. After 24 h of exposure to 31, 62.5, and 125 mg/L of CeO_2 NPs, the numbers of viable bacterial cells were 55, 40, and 30% respectively. In contrast, ZnO NP treatments had very less viable cells (<10%) due to the higher antibacterial activity.

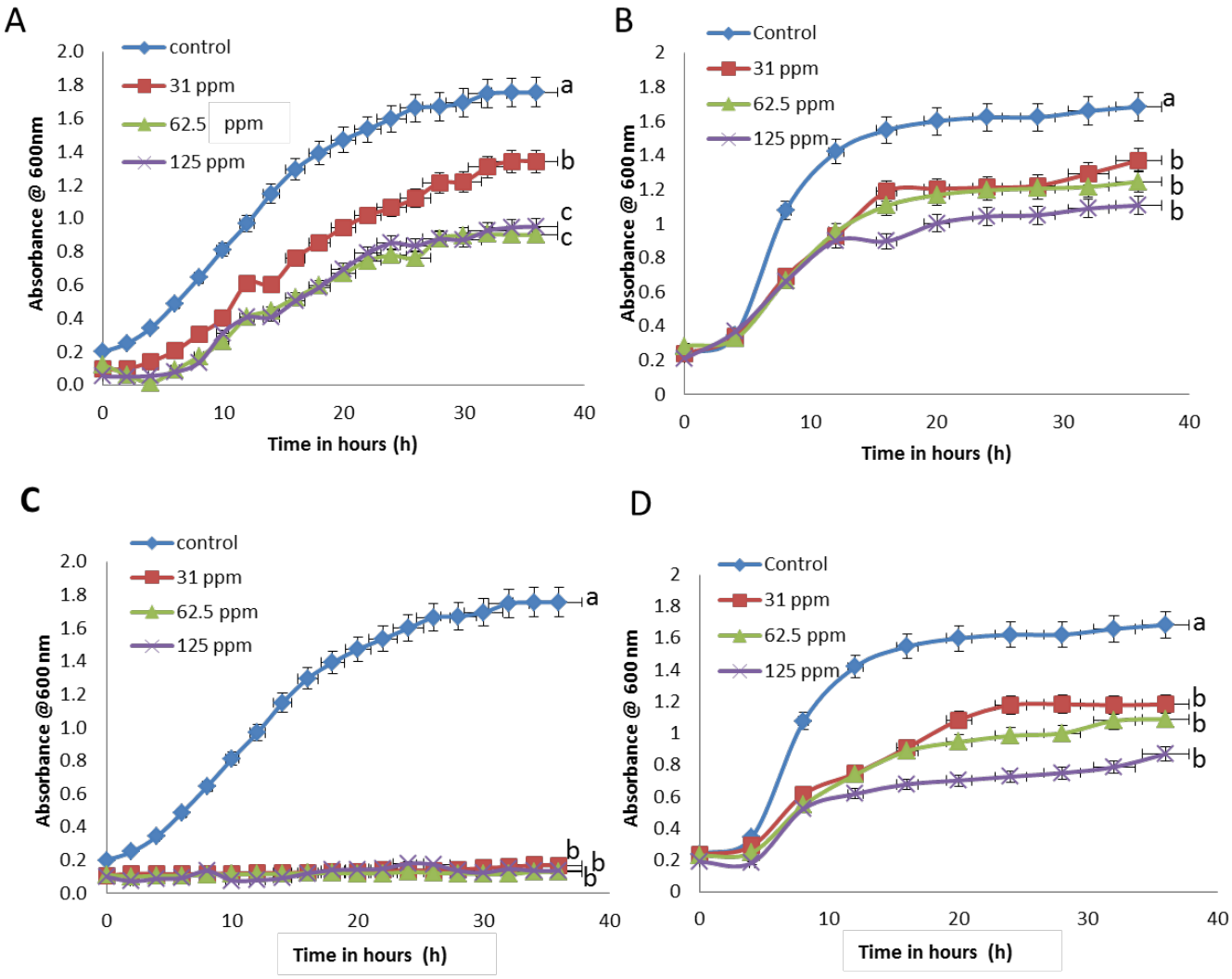

Figure 2.1. Dynamic growth curve of *S. meliloti* in YMB (A) growth inhibition of *S. meliloti* treated with CeO_2 NPs(B) treated with ionic cerium (C) growth inhibition of *S. meliloti* treated with ZnO NPs (D) and treated with ionic zinc. Lines with different letters are statistically significant.

The mechanism for the toxicity of ZnO NPs against *S. meliloti* is still unknown, but it could be attributed to either the presence of Zn^{2+} ions in solution (*13*, *14*, *34*) or disorganization of cellular membrane (*10*). But the bacteria grew in Zn^{2+} ions with slight inhibition (Figure 1D), which suggests some other factors are responsible for the higher toxicity of ZnO NPs apart from ionic zinc. In addition, CeO_2 NPs formed larger aggregates in solution compared to ZnO NPs (Table S1 and S2 of SI), which in turn decreased their bioavailability and toxicity.

2.4.3 TEM Imaging of Bacteria Treated with CeO_2 and ZnO NPs

Low voltage ultra-high resolution scanning electron microscopy of complete bacteria was used to investigate the potential uptake/adsorption of metal oxide nanoparticles. This technique has the advantage that requires no metal coating of the samples (*35*, *36*). In this particular case we avoided metal coating or commonly used heavy metal staining because it could interfere with EDX microanalysis of metal oxide nanoparticles used in the bioassays.

SEM provided surface imaging of bacteria, whereas with STEM mode it was possible to obtain high contrast images to assess location of metal oxide nanoparticles. Figure 2.2 A-B show STEM image taken in bright field (BF-STEM) and by using yttrium aluminum garnet - backscattered electron (YAG-BSE), respectively, of *S. meliloti* treated with CeO_2 NPs. BF-STEM image of complete bacteria treated with CeO_2 nanoparticles revealed some changes in cell morphology (Figure 2.2A-B), as a reduction in diameter and length (*35*, *36*); this could be due to high ionic strength achieved during treatments. BSE images obtained with YAG-BSE detector at low voltage (5 kV) (Figure 2.2-B), helped to reveal location of nanoparticles on bacterial surface. The contrast obtained on BSE images derives of interactions of electron beam with cerium oxide that emits backscattered electrons. BSE images obtained are qualitative compositional maps; bright areas correspond to materials with higher atomic number due to Z-contrast (*37*). In this

case, brighter spots correspond to sites of accumulation of cerium oxide on periphery of bacterial cell wall (Figure 2.2-B), confirming incorporation/binding of metal oxide nanoparticles used in the treatments.

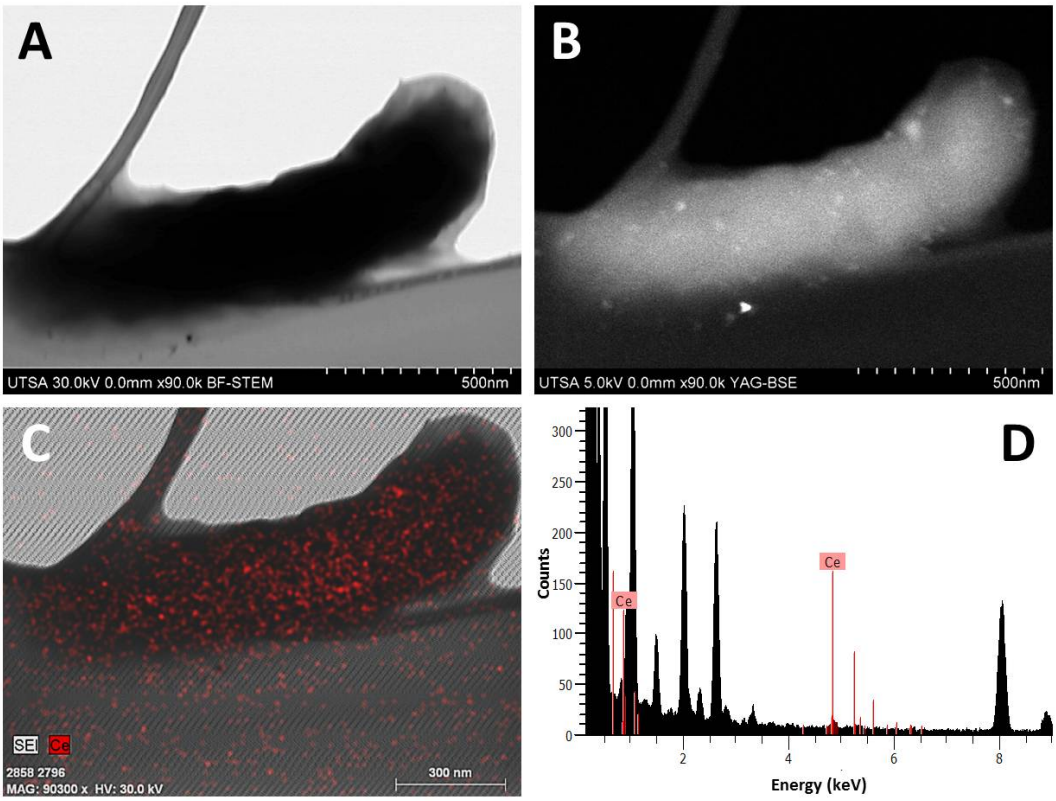

Figure 2.2. Imaging of bacteria treated with cerium oxide nanoparticles (125 mg/L) in YMB for 24 hours (A) BF-STEM, (B) YAG-BSE, (C) EDX mapping (the dots on the bacterial surface) of Ce, (D) EDX spectra.

Accumulation of NPs in the periphery of *S. meliloti* was confirmed by Energy Dispersive X-Ray (EDX) Spectroscopy obtained with QUANTAX Bruker detector coupled to FE-SEM. EDX mapping showed that the regions of high contrast observed with YAG-BSE correspond to Ce incorporated by cells during NP treatments (Figure 2.1-C-D). EDX microanalysis showed the presence of characteristic Ce peaks centered at 0.883 and 4.839 keV with a concentration equivalent to 3.29 ± 0.46 wt %.

High-contrast, low voltage STEM imaging is a new field of high-resolution electron microscopy and with the use of BF/DF Duo-STEM detector it is possible to obtain BF/DF images simultaneously. Figure 2.3 shows the morphological details of ZnO NP treated *S. meliloti* cell. High contrast regions showed that ZnO NPs are located inside and in the periphery of the cells. This confirms the incorporation/binding of these nanostructured materials mainly in the periplasmic region (*38*). Imaging with DF-STEM (Figure 2.3B) mode helped to clearly distinguish between the adsorbed and internalized ZnO NPs into the bacterial cells without using heavy metal staining or coating. In this mode, the strong contrast was due to Z^2 difference that is proportional to the atomic number of the metal. Therefore, this mode provides high contrast images of ZnO NPs located within ~100-200 nm depth. Elemental X-ray spectral mapping of Zn in complete bacteria was used to confirm the location of NPs observed by BF/DF-STEM (Figure 2.3-C). Integration of characteristic peaks of Zn centered at 1.012 and 8.637 keV in the EDX spectra indicated that sample contained 0.30 ± 0.04 wt % of Zn (Figure 2.3-D). We demonstrated that advanced analytical microscopy techniques allow to assess the location of ZnO NPs in complete cells without using negative staining. Apart from these, the STEM images showed very interesting morphological features onto the cell wall of CeO_2 treated bacteria (Figure 2.4). There were some spherical surface structures on the cell wall of *S. meliloti* that might be caused by the NPs toxicity. These surface structures need further investigation. In addition, ZnO NPs also resulted in irregular cellular surface with membrane damage (Figure 2.3A-B).

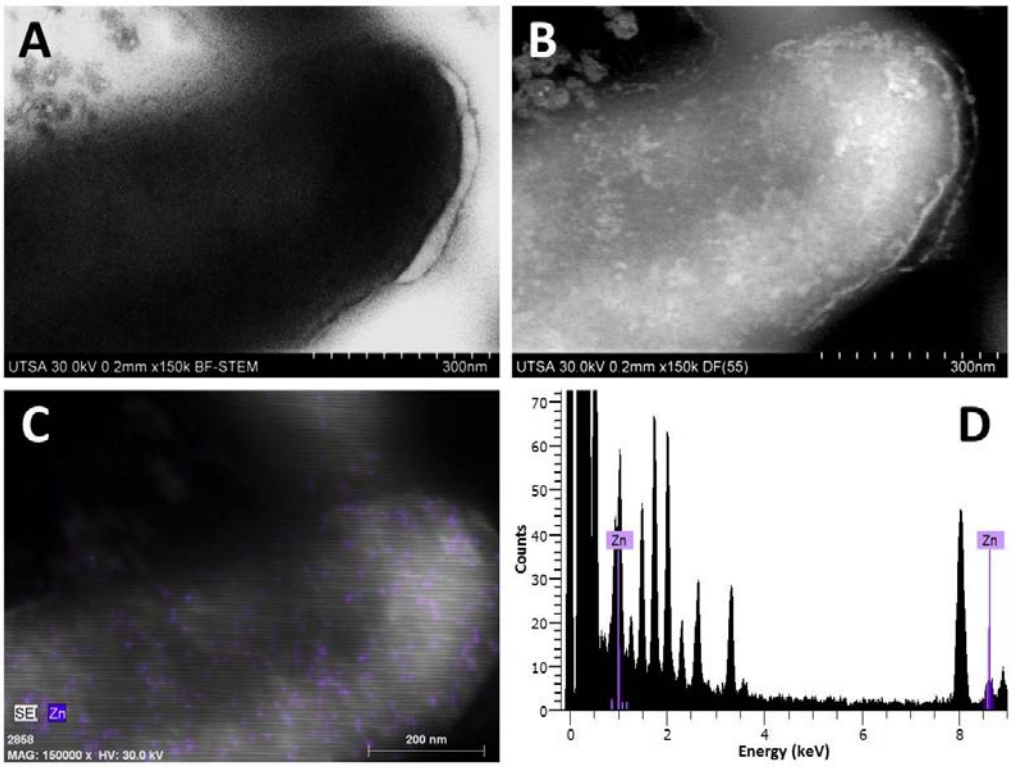

Figure 2.3. Imaging of bacteria treated with zinc oxide nanoparticles (31 mg/L) in YMB for 24 hours. (A) BF-STEM, (B) DF-STEM, (C) EDX mapping of Zn (the dots on the bacterial surface), (D) EDX spectra.

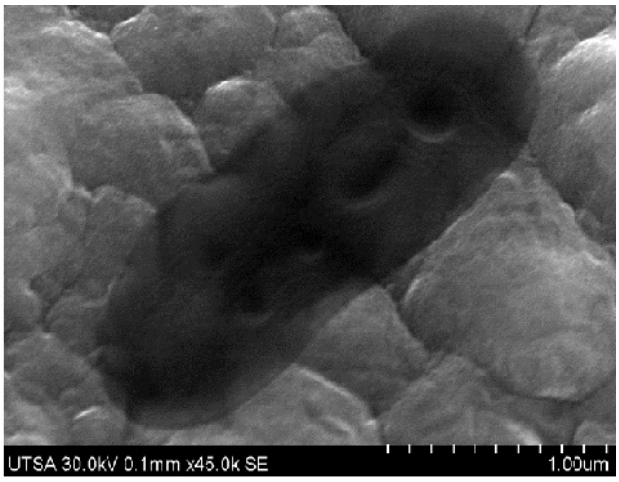

Figure 2.4. Spherical structures on the bacterial cell surface. Bacterial surface modified and the morphology changes upon treatment with NPs.

The accumulation/deposition of CeO_2 and ZnO NPs onto the cell surface suggests that the particles adsorbed to the bacterial cell surface at different concentrations. The adsorption may be due the electrostatic attraction between the NPs and the cell membrane (*10*). These could lead to production of ROS, which in turn cause the membranolytic damage of the bacterial cell surfaces by interacting with the protein and carbohydrate presents in the bacterial cell wall. This was further evidenced by the FT-IR of EPS extracted from treated cells.

Therefore, it was hypothesized that accumulation of CeO_2 and ZnO NPs on the surface and deposition of ZnO NPs within the periplasmic space of *S. meliloti* leads to inhibition of bacterial growth in both cases. The higher toxicity or antibacterial activity of ZnO NPs was likely due to: the smaller particle size which made NPs more bioavailable compared to CeO_2 NPs, their surface adsorption along with internalization inside the periplasm and corresponding membrane damage, and presence of ionic zinc in solution.

2.4.4. *FTIR* Analysis Results

The FTIR spectra from extracted EPS of treated and non-treated cells were examined separately. A number of absorption bands representative of various functional groups of polysaccharides and proteins present on the bacterial cell surface are shown in Figure 2.5-A-B. The FTIR spectra revealed distinct differences both in shape and absorbance intensity, which indicated the variation in composition and quantity of individual components present in EPS upon NPs application. The EPS from control shows a stretching frequency at 1098 cm^{-1} of C-O-C wagging frequency that represents the C-O-C group of polysaccharides (*39*). This peak shifted to 1045 cm^{-1}, 1007 cm^{-1} and 1014 cm^{-1} in case of ZnO NP treatments. The peak gets broaden at higher concentrations. Whereas, in case of CeO_2 the shift is less but the peaks area get broaden with increasing concentration of NPs in the solution (Figure 2.5 A). It is also reported that the band

vibration of polysaccharides appears in the frequency range 900-1200 cm^{-1} (*40*). Therefore, the overall changes in this region confirm changes in bacterial polysaccharide structures upon binding of NPs on cell surface. The C=O and C-N stretching appear near 1645 cm^{-1} and this represents the functional groups present in Amide-I of protein. The changes in Amide I band are associated with the conformational changes (*41-46*). Herein, we also observed the shift in intensities with changes in peak area in the amide I region .The band shifted to 1655 cm^{-1} and 1650 cm^{-1} for CeO_2 treatment whereas, the shift was significantly different (1633/1634 cm^{-1}) from the control for ZnO treatments. This suggests that the NPs toxicity might affect the α-sheet or β-helical structures of proteins. FTIR results of the present study corroborate the fact that attachment of NPs on bacterial cell surface resulted in a shift of Amide I band (*47*). The –OH stretching vibration (H-bonded) appears near 3243 cm^{-1} and the bands broaden and get shifted to 3268 cm^{-1}, 3259 cm^{-1}, and 3279 cm^{-1} with different concentrations of ZnO NPs. Whereas the CeO_2 treated samples show stretching frequencies at 3209 cm^{-1} and 3175 cm^{-1}. This represents the stretching vibration of –OH group presents in polysaccharides and proteins (*39*) long with the –OH of water molecules from the extraction process. The peak shifted more than 30 cm^{-1} in case of CeO_2 NP treatments. It should be noted that it is more than 7 times greater than the resolution of FTIR (4 cm^{-1}). C-H stretching frequencies of phenyl substitution also showed some changes. The peak appears near 881 cm^{-1} (control) and gets shifted to 868 cm^{-1}, 868 cm^{-1} and 872 cm^{-1}, with the treatment of 31, 62.5, and 125mg/L CeO_2 NPs, respectively. For the ZnO treatment, the same pattern was observed. The changes in peak intensities were different for ZnO NP treatments, which indicate the higher toxicity or interaction of ZnO NPs toward *S. meliloti*. The changes in the Amide I region inferred the adsorption of NPs induced changes in secondary and tertiary structures of proteins (*48-50*). The surface carboxylic groups of polysaccharides might

interact with the Zn or Ce atoms upon exposure to the NPs in solution. As a result, band gets shifted and the peak intensity also changed. These shifts in absorbance bands and decrease/increase in the peak intensities can be attributed to the interaction/binding of NPs with EPS and corresponding surface modifications. These changes in the EPS could impact the ability of this bacterium to colonize into the root surface, which directly affect the symbiotic nitrogen fixation in the system. Thereby nitrogen fixation will be distressed and in long term it will affect the global nitrogen cycle.

2.5. Conclusions

In summary, both the NPs have potential negative effects on *S. meliloti* (Rm 1021). CeO_2 NPs were found to be less toxic than ZnO NPs. The higher toxicity of ZnO NPs was attributed to the combined effect of surface attachment and internalization of the NPs and the corresponding ionic zinc through dissolution. The plausible mechanism of action of ZnO NPs towards bacterial cell encompasses direct interaction between the NPs and cell surface. Thereby Zn/ZnO NPs accumulates out/ inside cell wall, distressing the membrane chemistry by production of ROS, resulting in inhibition of the growth and viability of *S. meliloti*, and eventually cell death occurred. ZnO NPs were found to be bactericidal whereas the effect of CeO_2 NPs was bacteriostatic.

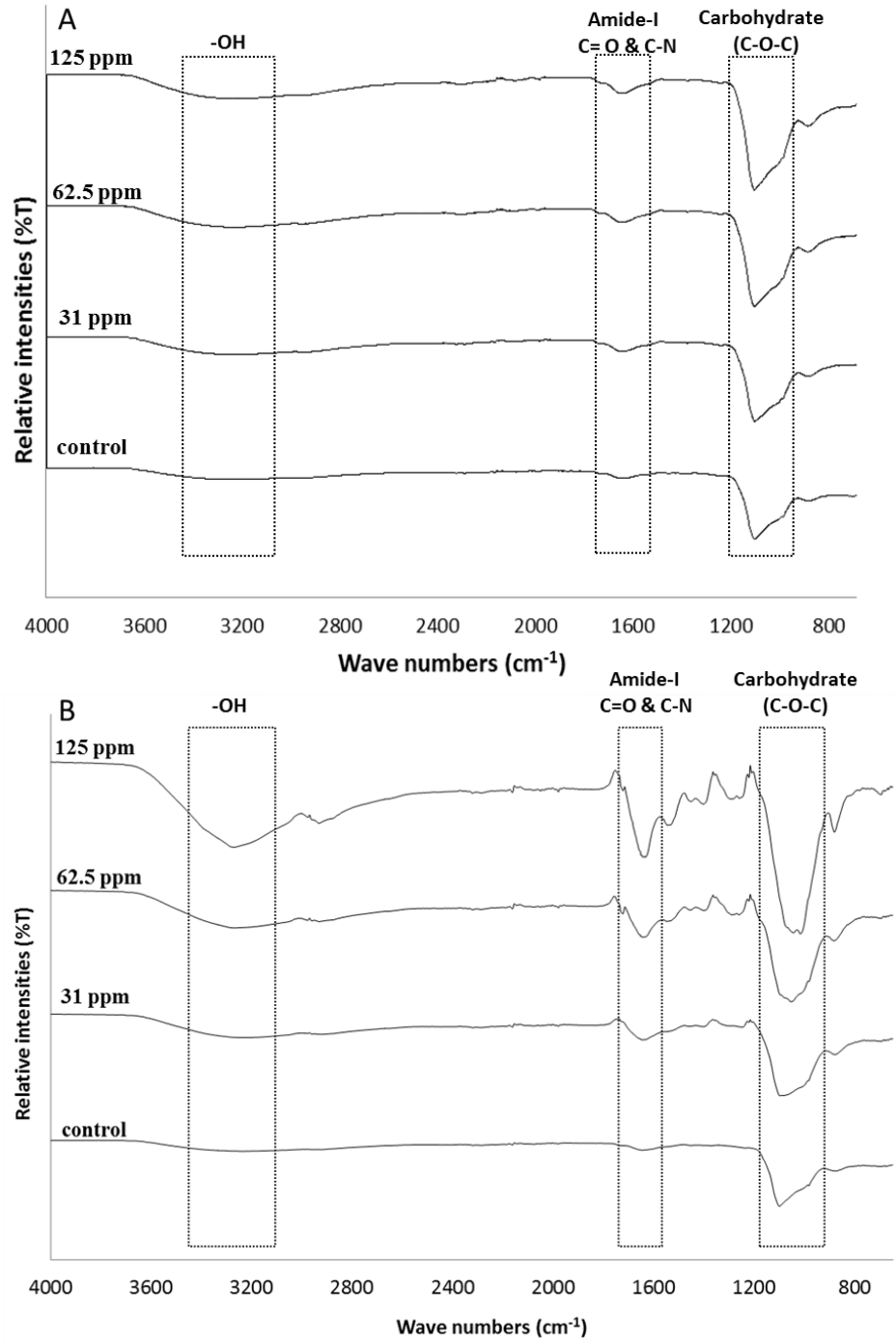

Figure 2.5. FT-IR spectra of bacterial extra cellular polysaccharides treated with (A) CeO_2 NPs and (B) ZnO NPs.

Chapter 3

Comparative phytotoxicity of ZnO NPs, bulk ZnO and ionic zinc onto the alfalfa-*Sinorhizobium meliloi* association in soil.

Abstract

Studies on ZnO nanoparticles (NPs) toxicity in a plant-bacterium association in soil matrix are limited. In this study, ZnO NPs, $ZnCl_2$, and bulk ZnO were exposed to the symbiotic alfalfa (*Medicago sativa* L.)-*Sinorhizobium meliloti* association at concentrations ranging from 0 to 750 mg/kg soil. Plant growth, Zn bioaccumulation, dry biomass, leaf area, total protein, and catalase (CAT) activity were measured in 30 day-old plants. Results showed 50% germination reduction by bulk ZnO at 500 and 750 mg/kg and all $ZnCl_2$ concentrations. ZnO NPs and ionic Zn reduced root and shoot biomass by 80% and 25%, respectively. Conversely, bulk ZnO at 750 mg/kg increased shoot and root biomass by 225% and 10%, respectively, compared to control. At 500 and 750 mg/kg, $ZnCl_2$ reduced CAT activity in stems and leaves. Total leaf protein significantly decreased as external $ZnCl_2$ increased. STEM analysis revealed the presence of ZnO particles in tissues, suggesting the uptake of NPs. However, ZnO NPs showed less toxicity compared to $ZnCl_2$ on measured traits. This study highlights the etiological issue about the phytotoxicity of NPs or that of Zn species derived from the NPs. The findings provide the insight of risk assessments of NPs and the ionic Zn species in soil.

Keywords: ZnO Nanoparticles, bulk ZnO, ionic Zn, leaf area, Zn uptake, toxicity

3.1 Introduction

Engineered nanoparticles (ENPs, NPs) are materials with at least two dimensions with a diameter of 100 nm or less. These materials have properties different from their bulk counterpart (*1*). Due to their novel and remarkable structural and physicochemical properties, these materials showed enhanced physical, chemical, and biomedical properties (*2*, *3*) with widespread application in different industrial and household sectors (*4*). ZnO NPs are one of the widely used metal oxide NPs for their photocatalyzing and photo-oxidizing abilities.[5] However, inappropriate handling and dumping of NPs and related wastes could result in environmental contamination (*6*). These certain the immediate need to assess the potential toxicological impact on human health and environment (*1, 3, 7, 8*). However, it is largely unknown whether the toxicity effects are same or different in terms of NPs or the released metal ions (*9*).

In the past few years, several reports have suggested that ENPs produce adverse effects in terrestrial plants (*10-16*). These studies reported that plants can accumulate high amount of metals in their tissues when exposed to ENPs. This not only impacts their physiological and biochemical factors (*11-14*), but could be the possible path of contamination to the food chain (*6*, *17*).

Reports indicate that ZnO NPs adversely affect plant growth of green pea, corn, cucumber rye, zucchini, soybean, and wheat, depending on the concentration of ZnO NPs (*6*, *11*, *13-16*). For example, Dimpka et al. reported that ZnO reduced wheat plant growth with increase production of ROS (*6*). Conversely, Lin and Xing (*14*) reported that ZnO NPs affected root elongation in ryegrass (*Lolium perenne*), radish (*Raphanus sativus*) and rape (*Brassica napus*) (*14*). The reported phytotoxicity was due to disruption in water and nutrient pathways (*14*). They also confirmed the adsorption and aggregation of the ZnO NPs to the root surface of ryegrass

where the high magnification TEM images showed the presence of NPs in the apoplast, cytoplasm and nuclei of the endodermal cells and the vascular cylinder (*15*). However, X-ray absorption confirmed the nonexistence of the NPs. Later, Kim et al (*19*), reported phytotoxic effects of ZnO NPs in *Cucumis sativus* due to excess Zn bioaccumulation (*19*); whereas, Lopez-Moreno et al. (*20*) reported the genotoxic effect of ZnO NPs to soybean (*Glycine max*) (*20*). Recently, Mukherjee et al. (*13*) reported the phytotoxic effect of ZnO NPs in green peas where ZnO NPs were found to be more toxic (compared to bulk ZnO) due to higher accumulation of ROS in different plant tissues (*13*). However, only one report was found where the interaction of NPs on symbiotic association (important in terms of nitrogen fixation) was studied (*21*). The authors reported that higher Zn was accumulated in above and below ground parts of soybean plants, including the nodules, which was confirmed through ICP analysis and electron microscopy imaging. The result showed that ZnO NPs adversely affect the plant growth; however the effect on nodulation/nitrogen fixation remained unaltered. The authors also confirm the Zn ions/ZnONPs accumulation in different parts of plants through ESEM and STEM (*21*).

To the best of the authors' knowledge, there are no reports on the comparative toxicological studies of ZnO NPs and their bulk/ionic counterpart and the probable phytotoxic mechanisms on the symbiotic association of alfalfa (*Medicago sativa* L.), the world's most important forage crop (*22, 23*) grown in association with *Sinorhizobium meliloti* (*S. meliloti*), a gram negative nitrogen fixing soil bacterium (*21*). Therefore, studies exploring this knowledge gap would be useful for a better understanding of plant− NP interactions in soil and the probable toxic species identification.

The present study was aimed to investigate the phytotoxic effect of 10 nm ZnO NPs towards alfalfa-*S. meliloti* association in soil. To discern phytotoxicity of ZnO NPs versus larger

particles or released (soluble) ions, both micron-sized bulk ZnO and soluble Zn salts (added as $ZnCl_2$) were tested separately. Plants were treated with ZnO NPs, bulk ZnO, and $ZnCl_2$ for 30 d and compared for bioaccumulation of Zn, plant growth, biomass, leaf area, leaf protein content, and catalase (CAT) activity. Bioaccumulation of Zn in different plant tissue was quantified through ICP-OES and the protein and catalase activity was measured through spectroscopic methods. High resolution Electron Microscopy (EM) techniques were used to confirm the aggregation of ZnO NPs in different plant tissues.

3.2 Materials and Methods

3.2.1Characterization of ZnO NPs

Ten nanometer ZnO NPs (Meliorum Technologies, Rochester, NY) were obtained from the University of California Center for Environmental Implications of Nanotechnology (UC-CEIN). The NPs were previously characterized by pXRD and TEM by Bandyopadhyay et al.(*7*). The desired amount of ZnO NPs were suspended in Millipore water (MPW) and applied to soil to have 250, 500, and 750 mg/kg of soil. Prior to soil application, NP suspensions were sonicated for 15 minutes in a water bath (Crest Ultrasonics, Trenton, NJ). Before choosing these concentrations, the plants were treated with lower concentrations (62.5 mg/kg and 125 mg/kg) but no visible sign of toxicity were found.

Three concentrations (250, 500, and 750 mg/kg of soil) of ZnO NPs, bulk ZnO and $ZnCl_2$ (Sigma–Aldrich) were prepared simultaneously in MPW and mixed with the soil.

3.2.2 Soil Sampling, Characterization, and Pot Preparation

The soil was collected from Fabens, Texas (top 20 cm) and mixed with organic soil (Scotts, premium potting soil to enhance soil fertility) in a ratio of 2:1 (v/v). The soil was air dried and sieved through a 2 mm mesh prior to characterization. The original (Faben, TX) soil type was

loam in texture, although very close to the border of sandy loam soil (based on the USDA soil classification scheme) (*24*). The soil pH was 7.75±0.4, CEC 8.21±0.2 and 28±0.5 mg/kg of Zn. Later, Zn content was reduced to 18.6±0.5 mg/kg after 30 days of harvesting.

The pots were prepared with soil mixtures amended with desired amount of nano, bulk ZnO, and $ZnCl_2$ (well mixed). The pots amended with ZnO NP, bulk ZnO and ZnCl2 were kept 24 h for conditioning. Next day, the alfalfa seeds were planted. Three replicates were prepared for each treatment.

3.2.3 Seed Germination

Alfalfa (*Medicago saliva L.*) seeds were purchased from Del Norte Seed & Feed (Vinton, TX, USA). The seeds were washed with 4% hypochlorite solution followed by washing with ethanol and MPW. Approximately 60 seeds of the same size were selected and sown in each pot. Alfalfa seeds were inoculated with *S. meliloti,* suspended in MPW for 2 h before being planted into the soil. The seeds were placed about 1 cm deep in the soil and covered with thin layer of soil. The ZnO treated pots with alfalfa seeds were placed in a growth chamber (Environmental Growth Chamber, Chagrin Falls, OH, USA) with a 14 h photoperiod, 25/20 °C day/night temperature, 65% relative humidity, and light intensity of 340 μmol s^{-1} m^{-2} for 30 days. The pots were watered with approximately 50 mL of MPW every day. The alfalfa sprouts appeared after one day of sowing, and after five days the number of germinated seeds was recorded.

3.2.4 Plant Growth

The plants were grown for 30 days and upon harvest, the root and shoot lengths were recorded for each plant separately (10-15 plants). The plants were washed with 4% HNO_3, followed by three rinsing with MPW. Shoots and roots were separated and dried at 70°C for 24 h and the biomass was recorded for each treatment.

3.2.5 Quantification of Zn in Dry Plant Tissues

Different parts of alfalfa plants (root, stem, and leaf) were digested and analyzed for Zn content by ICP-OES (Perkin-Elmer Optima 4300 DV, Shelton, CT equipped with a Burgener PEEK MiraMist nebulizer with argon flow) upon drying at 68 ^{0}C. Prior to ICP analysis, the plant tissue samples were microwave-assisted acid digested with concentrated plasma-pure HNO_3 and H_2O_2 (30%) (1:4) in a microwave acceleration reaction system (CEM Corp.; Mathews, NC). For QC check, Certified Reference Material (spinach leaves, NIST 1547) was processed as samples, and the Zn recovery rate was 99.82 ± 0.55.

3.2.6 Protein and Enzymatic Assays (CAT/APX)

Thirty-day-old fresh alfalfa plant samples were washed with 5% HNO_3 solution and three times with MPW to remove any external contaminant. 0.1 g of fresh plant tissues (roots, stems, and leaves) was used. The fresh tissue extracts were prepared using extraction buffer of 25 mM KH_2PO_4 at pH 7.4. Then, the extracts were centrifuged for 8 min at −4 °C and 9600 rpm (Eppendorf AG bench centrifuge 5417 R, Hamburg, Germany). The supernatants were collected to microcentrifuge tubes and stored at −20 °C until further analysis (*25*).

Total leaf protein content was determined according to the method of Bradford (26) with slight modifications using bovine serum albumin as standard. The absorbance kinetics (for protein and enzymes) was recorded in a Perkin Elmer Lambda 14 UV/Vis Spectrometer (single-beam mode, Perkin-Elmer, Uberlinger, Germany).

The catalase (CAT) activity was investigated by observing the degradation of H_2O_2 (extinction coefficient 39.4 mM^{-1} cm^{-1}) at 240 nm (*27*). Twenty μL crude enzyme extract was mixed with 980μL 10 mM H_2O_2 and the amount of enzyme necessary to decompose 1 μmol of H_2O_2 per minute was considered as one unit of CAT (*27*).

3.2.7 Electron Microscope Imaging

The ZnO treated alfalfa plants were used for EM imaging in order to see the aggregation of ZnO NPs within the plant tissues. Plant tissues were harvested (nodules, roots, stems and leaves) to determine location and accumulation of ZnO NPs. Samples were fixed with phosphate buffered 4% formaldehyde, 3% glutaraldehyde, pH 7.2 for 24 h prior resin embedding. Fixed tissues were rinsed with PBS and post-fixed with PBS+1% OsO_4 in 0.12 M phosphate buffer for 1 h at room temperature. After dehydration with increases series ethanol (75, 95, and 100%), samples were infiltrated with the resin Poly/Bed 812 plastic (Luft formulations; purchased from Polysciences, Inc.) prepared in acetone and cured for 24h at 60°C. Ultra-thin sections of 90 nm were cut with Leica Ultracut ultramicrotome using a 45° diamond knife. Sections were mounted on 200 mesh copper grids (2PSI) and dried at 37°C.

Tissue sections were imaged with HITACHI S-5500 In-Lens Ultra-high Resolution Field Emission Scanning Electron Microscope (UHR FE-SEM) coupled with BF/DF Duo-STEM, Low angle backscattered (LABE) and YAG-BSE detectors, and solid state EDX detector (Bruker), and microscope was operated with an accelerated voltage of 30 kV. Electron microscope images were analyzed with QUARTZ PCI and X-ray microanalysis acquired with QUANTAX EDS.

3.2.8 Statistical Analysis

Each concentration was set in triplicate including the control in a completely random design. Separate set of plants were used for Zn concentration, physiological measurements, and microscopy imaging. The data (means ± SE) were reported as averages of three replicates. A one-way ANOVA test was performed, and Tukey-HSD multiple comparisons conducted test performed using the statistical package SPSS version 12.0 (SPSS, Chicago, IL). Statistical

significance was based on probabilities of $p \leq 0.05$.

3.3 Results and Discussions

3.3.1 NP Characterization

ZnO NPs were characterized previously (*7*) where larger aggregation was found with increasing concentration. The initial size was 10 nm with a purity of 99%. Fig. S1 (SI) showed the TEM images of aggregated ZnO NPs with an average size of 322 ± 187 nm and the size range was from 94 nm to 1127 nm. After mixing with the soil, the physico-chemical behavior might change which affect the phytotoxicity of ZnO NPs. We also observed that the rate of dissolution was higher in bulk ZnO compared to ZnO NPs in soil medium (See SI). Though, it has been evident that NPs has higher dissolution than bulk ZnO due to their smaller size (*28*, *29*). Our result (S2, SI) is not in agreement with the previously reported results (*28*, *29*), maybe due to the fact that ZnO NPs aggregated during experimental condition (soil/water media). The formation of larger aggregates might hinder the dissolution kinetics by reducing the equilibrium solubility (*30*).

3.3.2 Effect on Seed Germination

Seed germination was differently affected by treatments (ZnO NPs, bulk ZnO, and $ZnCl_2$). ZnO NPs at 250 and 500 mg/kg did not affect germination rates (Fig. 3.1 and Fig. S3, SI), which followed previously described data of mung beans (*31*). However, at 750 mg/kg ZnO NP treatments germination rate was increased to 23% compared to control. Bulk ZnO treatments showed 50% lower germination rate at 500 and 750 mg/kg compared to control and the ionic treatments were found to be germination inhibitors with increased $ZnCl_2$ concentrations. At 500 and 750 mg/kg $ZnCl_2$ treatments, germination rates reduced to 50% and 80%, respectively. The ionic treatments showed lower germination rates in all three concentrations compared to control which clearly signifies the higher toxicity of ionic zinc. Although, Zn is an essential element for

plant growth, while higher concentration might result in growth inhibition and can produce phytotoxic symptoms (*32*). In addition, it should be mentioned that NP-stress response could be different for different plant species depending on other physical and biochemical onditions.

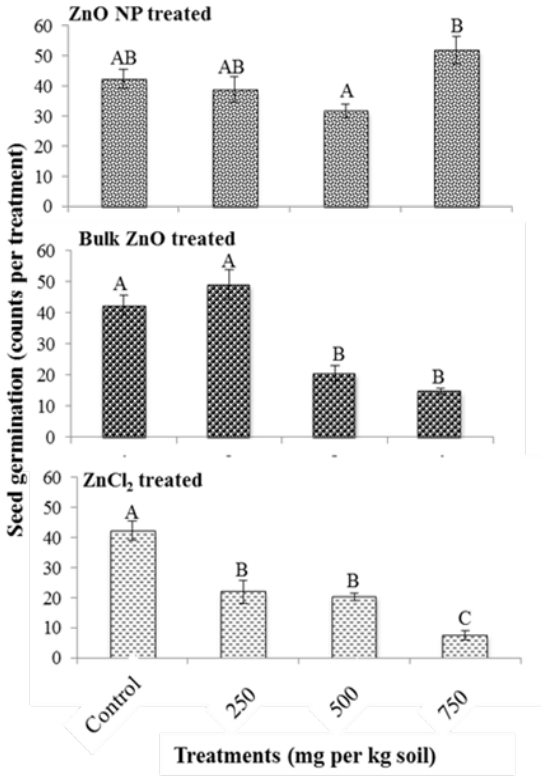

Figure 3.1. Germination of alfalfa seeds in soil treated with (A) ZnO (B) bulk ZnO (C) $ZnCl_2$ at 0, 250, 500, and 750 mg/kg. Means with the same letters are not significantly different at Tukey's test ($p \leq 0.05$). Evaluation was performed 5 days after sowing.

3.3.3 Zn Uptake and Translocation by Alfalfa

The Zn concentration in one month-old alfalfa plants are exhibited in Fig. 2(A-C). In each treatment, Zn level increased in alfalfa roots along with increasing dose of NPs, bulk ZnO, and ionic Zn when compared to control. The highest accumulation was observed at 750 mg of $ZnCl_2$ treatments with an average of 382 mg/kg of Zn in alfalfa roots (Fig. 3.2C). The higher root

uptake can be due to the fact that $ZnCl_2$ is fully ionized in soil and plants uptake more Zn and bio-accumulate it in root tissues. However, in comparison to bulk, higher root uptake was observed in NP treatments even though the dissolution of bulk ZnO was much higher than ZnO NPs in soil (Fig. S2, SI), suggested that smaller size of the NPs persuade more uptake than the bulk and hence more Zn bioaccumulated in roots of alfalfa.

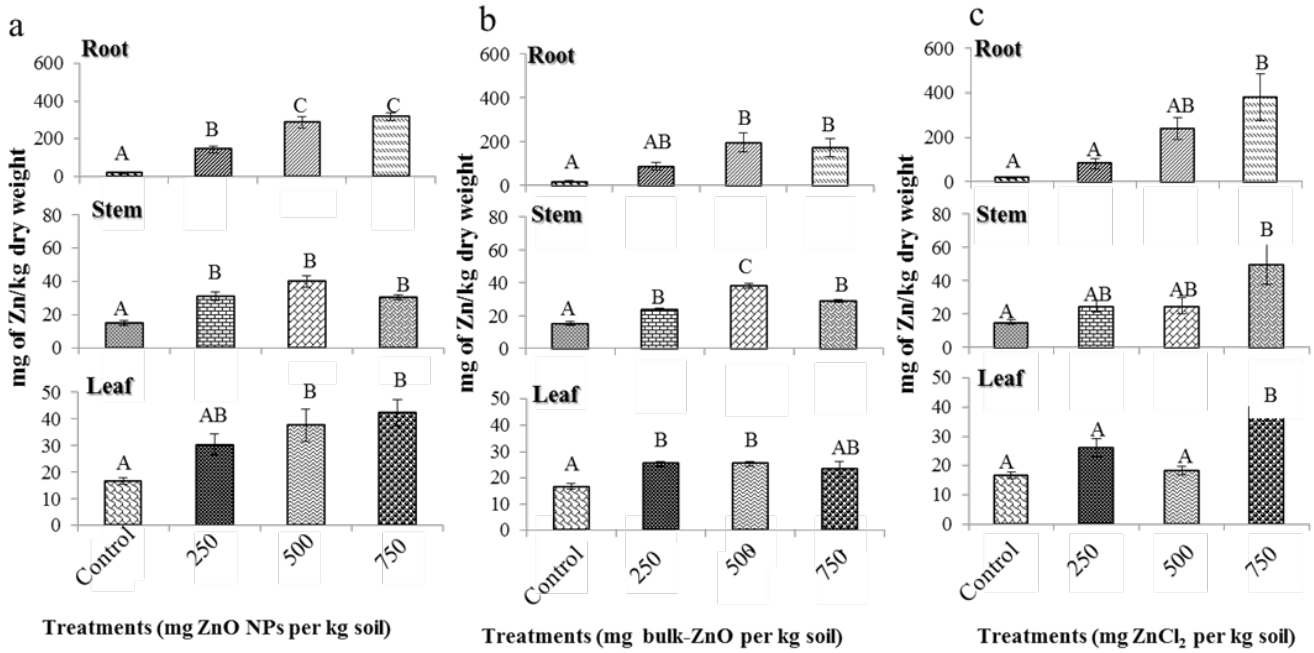

Figure 3.2. Bioaccumulation of Zn in roots, stems, and leaves of alfalfa plants grown for 30 days in soil treated with 0 (control), 250, 500, and 750 mg/kg ZnO NPs (**a**), bulk ZnO (**b**), and $ZnCl_2$ (**c**). Error bars stand for stadard deviations. Bars with the same letters/symbols show no statistically significant difference at $p \leq 0.05$. Comparisons were made between same plant tissues of different treatments.

In stem, the accumulation was higher at 250 and 500 mg/kg of ZnO NP treatments compared to bulk. Zn uptake from ZnO NPs increased to 106% and 166% compared to control, with treatment of 500 mg/kg>250~750 mg/kg. The Zn accumulation in stem was in same order of

control<250~750 mg/kg<500 mg/kg in case of NP and bulk treatments. However, ionic treatments showed a different accumulation trend of control<250<500<750mg/kg with significantly higher amount of Zn (3x increase at 750mg/kg treatment) in stems. The fig. 2 showed that in leaves NP treatments accumulated more Zn (about 2x higher) compared to bulk, ionic, and control. This is because of smaller size of ZnO NPs and biotransformation of Zn^{2+} from ZnO within the tissue (*6*). This signifies the different behavior of Zn^{2+} than ZnO NP. This can be inferred that the accumulated Zn was not only the dissolved Zn from ZnO NPs, but may be aggregated NPs in different parts of the plants. Otherwise the plants should respond similarly in different Zn treatments (ionic, bulk, and NPs).

The translocation factor (TF, Table 1, See SI) calculation showed that more Zn was translocated to alfalfa leaves at 500 and 750 mg/kg ZnO NP treatments (TF: 0.130, and 0.133) than $ZnCl_2$ treatments (TF: 0.0763, 0.104). However, at 250 mg/kg bulk and ionic treatments translocated more Zn (~0.3) to alfalfa leaves compared to ZnO NP treatment. Higher TF signifies more soluble Zn in leaves of NP treated plants compared to ionic treatment at 500 and 750 mg/kg treatments (*33*). The lower TF for ionic treatments explain the fact that possibly Zn complexes with organic acids/or amino acids and sequestered in root vacuoles and became less available for xylems (*33*, *34*), whereas the smaller size ZnO NPs enhances the transportation through vascular system and hence higher translocation was observed at 500 and 750mg/kg ZnO NP treatments. In addition, ZnO NPs may be bio-transformed to Zn^{2+} within the tissue giving higher Zn accumulation in terms of 42 mg of Zn/kg of dry alfalfa leaf biomass compared to what.

But, more elaborated studies are required in order to explain the higher bioaccumulation of Zn/ZnO NPs and related mechanisms in leaves compared to bulk and ionic treatments. In spite

of higher Zn accumulation in plant leaves, no visual sign of toxicity was observed in NP treated plant leaves; however, the ionic treated plants turned yellow after 3 weeks of germination (S6, A-C, SI, Appendix 2).

3.3.4 Effect on Biomass Production and Root-Shoot Length

Biomass production and plant growth are considered as indicators of plant health. Compared to control, alfalfa dry biomass significantly decreased (80%) at all ZnO NP concentrations (Fig.3 A-B). These results are in accordance with Priester et al. (*21*) who reported decreased root biomass of soybean with higher Zn accumulation (*21*). However, at 750 mg/kg bulk treatments, root biomass increased more than 2x ($p \leq 0.05$) and in case of ionic treatments dry biomass reduced to 70%, 72%, and 87% at 250~500>750mg/kg treatments respectively (Fig. 3.3A). Higher biomass reduction was observed at 250 and 500 mg/kg ZnO NPs treated alfalfa than the same ionic doses. These results confirm the phytotoxicity of ZnO NPs to alfalfa plants. Zn accumulation in the aerial parts also followed the same trend. In shoot, NP treatments showed 35% lower dry weight in all treatments (Fig. 3.3B). But, leaf biomass increased to 27%, 179%, and 223% at 250, 500, and 750 mg/kg ZnO bulk treatments, respectively, compared to control which was also confirmed visually (S2 A-C, SI). The alfalfa shoot biomass decreased to 43% at 750 mg/kg $ZnCl_2$ treatments which was also be visually confirmed by Fig. S5(SI).

Our results indicated that ZnO NPs induce the toxicity in terms of biomass reduction (*21*) and root elongation (*6*, *14*). The ionic treatments showed higher toxicity compared to NP treatments, conversely plants were healthy in bulk treatments in terms of root and shoot biomass production. It can be hypothesized that the amount of accumulated Zn might be crucial for alfalfa growth in bulk treatments and hence it acts as a growth promoting for alfalfa plants (*34*).

Fig. S4-A (S5, SI, Appendix 2) shows the changes in root length, where at 250 mg/kg of

ZnO NPs increased the root length (67%) while at 500 and 750 mg/kg no significant increase was observed compared to control. Bulk ZnO treatments followed different trend where 50% root elongation was observed at 500 and 750 mg/kg treatments, compared to control. The ionic treatments remained statistically unaltered. It is well known that Zn is one of the crucial micronutrients for optimum crop growth and it is possible that the dissolved Zn from bulk promote alfalfa's growth. In addition at lower concentration, ZnO NPs/dissolved Zn promote root elongation (*6*, *14*), however, at higher concentration, ionic Zn found to be toxic due to excess accumulation in root and shoots.

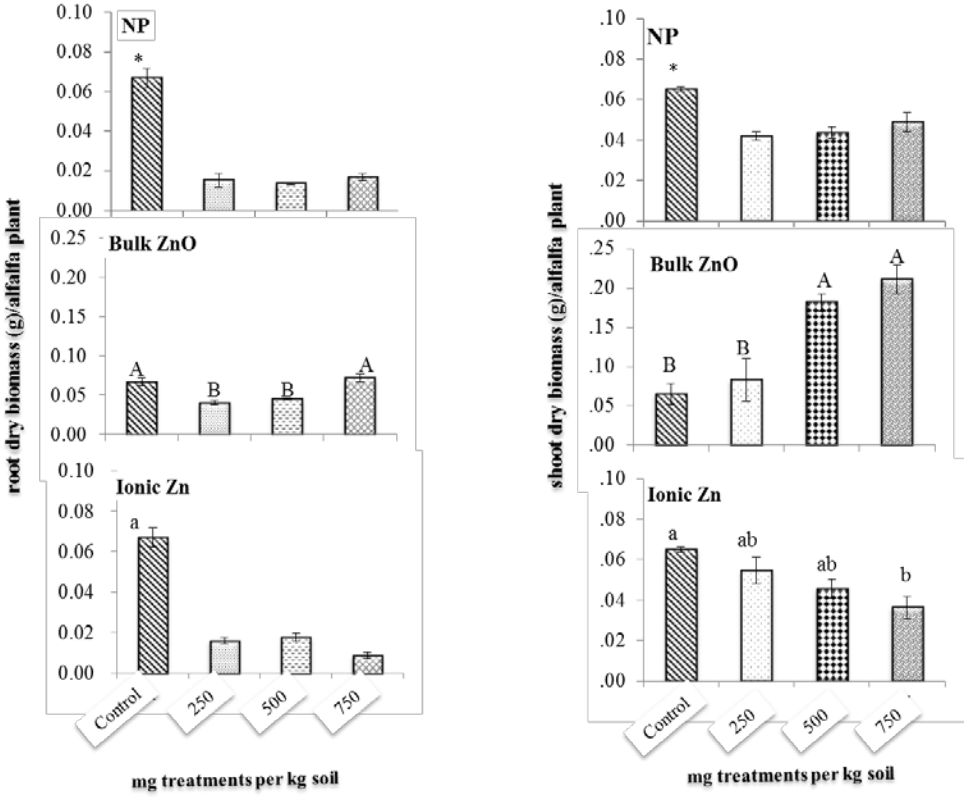

Figure 3.3. Root and shoot biomass (dry weight) of alfalfa plants treated with 0-750mg/kg of ZnO NPs (**A**), bulk ZnO (**B**), and $ZnCl_2$ (C) after 30 days of treatment. Bars with the same letters/symbols show no statistically significant difference at $p \leq 0.05$.

3.3.5 Changes in Alfalfa Leaf Area

Leaf area can be a good indicator of plant health (*36*, *37*). At 500 mg/kg bulk ZnO treatments, alfalfa leaf area significantly increased ($P \leq 0.05$) compared to NP, ionic treatments, and control (Fig. 3.4 and Fig S6, SI, Appendix 2). These results are confirmed by other research results reported recently (*38*, *39*).

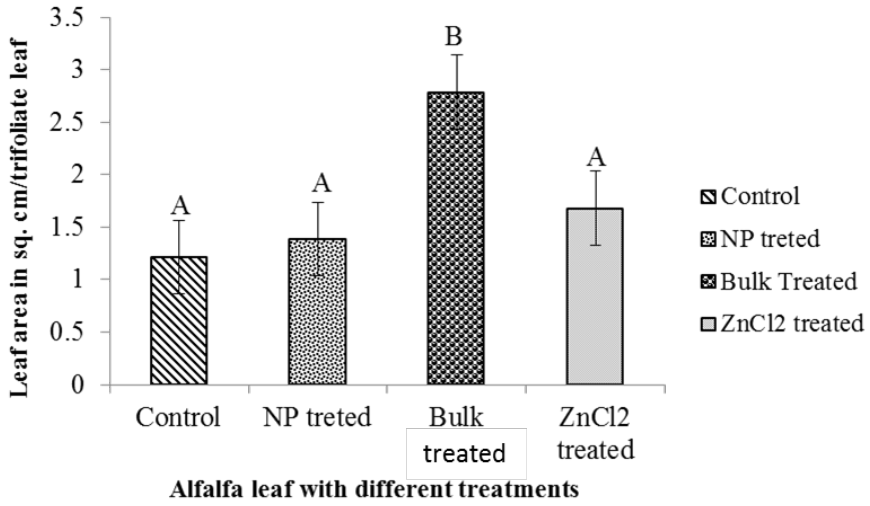

Figure 3.4. Total leaf surface area (sq. cm/trifoliate leaves) of alfalfa plants treated with 500 mg/kg of ZnO NPs, bulk ZnO, and $ZnCl_2$ for 30 days**.** Error bars stand for stadard deviations and bars with different letters show statistically significant difference at $p \leq 0.05$.

The Zn bioaccumulation in leaves was in an order of ZnO NPs>bulk ZnO> ionic Zn (37.65, 25.42, and 18.34 mg of Zn per kg of alfalfa leaf dry weight) at 500 mg/kg treatments. This can be concluded from the uptake and biotransformation of Zn (TF calculation: Table 1, SI) that at certain higher bulk ZnO treatment, accumulated Zn acts as growth promoting and possibly triggered the growth hormones which resulted in increased leaf area of alfalfa plants (*31*). We

also observed early flowering of alfalfa (in 2 months) in bulk treatments and it can be concluded that 500 mg bulk ZnO/kg treatment acts as growth enhancing for alfalfa plants for this particular phenotype.

3.3.6 Total Protein Content in Alfalfa Leaves

Alfalfa leaves contain approximately 30% crude protein and have been used widely as forage crop and high source of proteins in human diet (*40*). Therefore, total leaf protein content was measured to find out the impact of ZnO NPs and corresponding bulk and ionic Zn species on this particular crop plant. Fig. 3.5 showed that ZnO NP treatments, alfalfa leaf proteins (total) reduced but the change was statistically insignificant. Same trend was observed in bulk treatments. But, the ionic treatments showed a significant reduction in leaf protein content of ~ 17%, 28%, and 71% at 250, 500 and, 750 mg/kg $ZnCl_2$ treatments, respectively. Decrease in protein in ionic treatments suggests the phytotoxic effect of Zn^{2+}. Our results are in accordance with the previously reported studies where ionic zinc was found to be phytotoxic at higher concentration (*32*, *38*). At elevated Zn level in leaves, the phytotoxicity might be through displacement of essential elements in functional sites (*32*). In addition, ionic Zn/dissolved Zn^{2+} from ZnO NPs could hindered many biochemical function/s comprising proteins which are involved in different structural, transport or catalytic (enzymes) function (*32*). Therefore, decrease in leaf protein will directly affect the alfalfa food value (protein source) and is an indication of phytotoxicity.

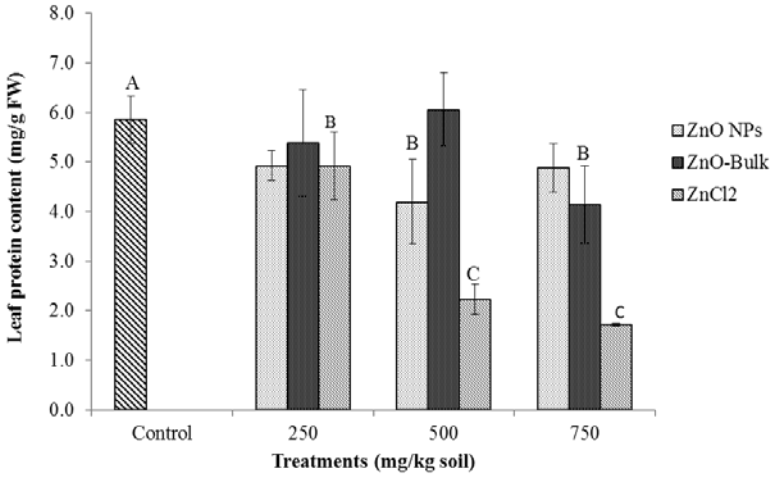

Figure 3. 5. Total leaf protein content (expressed in mg/g fresh weight; $p \leq 0.05$) of alfalfa treated with ZnO NPs (**A**), bulk ZnO (**B**), and $ZnCl_2$ (**C**) at 0 (control), 250, 500, and 750 mg/kg concentrations. Bars with different letters signify the statistical significant difference at $p \leq 0.05$.

3.3.7 CAT Activity

The main function of catalase (CAT) within cells is to prevent the accumulation of toxic levels of hydrogen peroxide, generated as a by-product of plant's metabolic processes and it can serve as a good indicator of plant's physiological responses (*41*). CAT activity is shown in Fig. 3.6 A-C. Statistically insignificant changes were observed in CAT level of root, stem, and leaves of alfalfa treated with ZnO NPs and bulk ZnO. However, the ionic treatments showed decreasing trends of CAT in stem and leaves at 500 and 750 mg/kg treatments compared to control (about 2x less). This was evident by inhibition of plant growth and yellow coloration of leaves at 500 and 750 mg/kg of $ZnCl_2$ treatments (Fig S7-C, SI, Appendix 2). Decreased plant size (shoot length, Fig 3.4B) implies lower cellular activity and higher H_2O_2 accumulation/generation. This is in accordance with other results (*11*, *13*) where lower CAT activity was reported with higher ZnO NPs concentrations. Mukherjee et al. (2013) reported decrease CAT activity in green pea leaves

with increase Zn doses (*13*). This inhibition of CAT activity might result in increase in H_2O_2 accumulation and hence plant's defense system might affect.[13] However, Hernandez-Viezcas et al. (*42*) reported an increase in CAT activity with increasing ZnO NP concentration in mesquite (*Prosopis juliflora-velutina*) plant (*42*). It is noteworthy to mention that different CAT activity can be dependent on type of treatments (NP, bulk and/or ionic Zn) and the physiological individuality of different plant species.

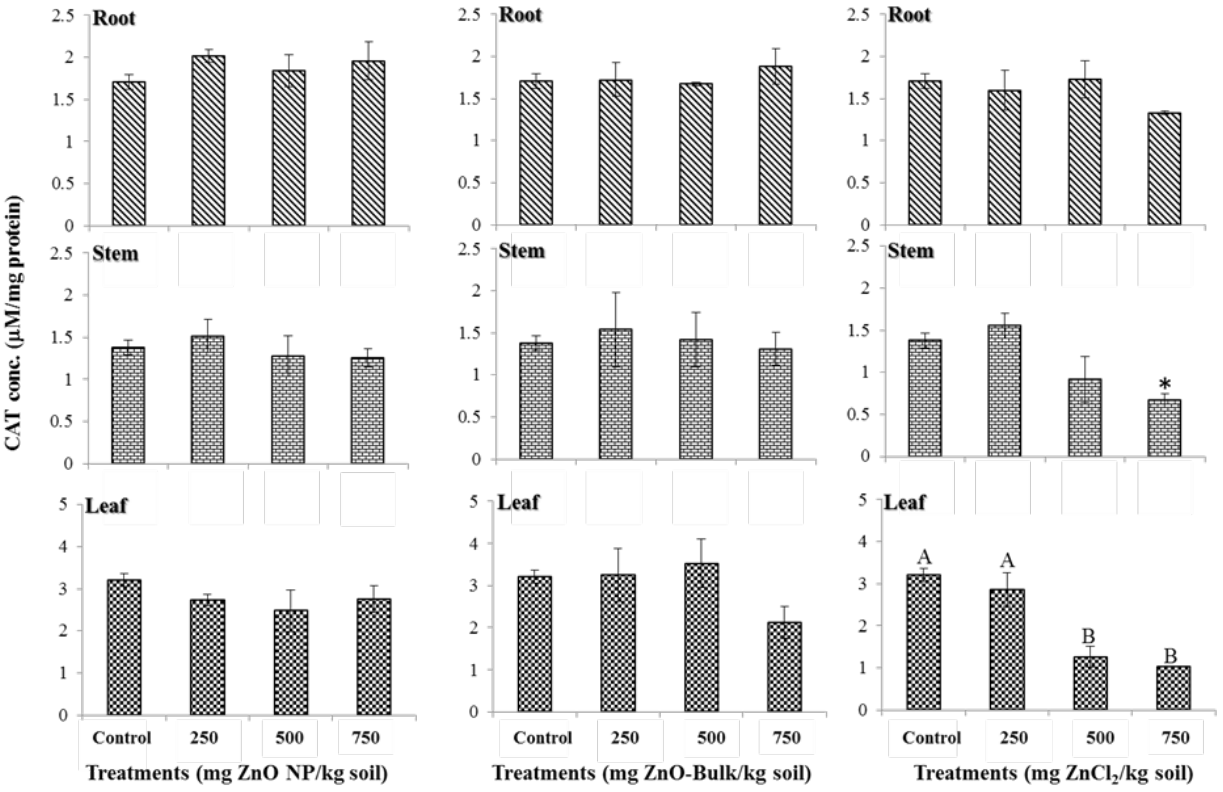

Figure 3.6. CAT activity in roots, stems, and leaves of alfalfa plants grown for 30 days in soil treated with 0 (control), 250, 500, and 750 mg/kg of ZnO NPs (**A**), bulk ZnO (**B**), ZnCl2 (**C**). One unit of CAT is the amount of enzyme necessary to decompose 1 µmol of H_2O_2 per minute. Error bars stand for stadard deviations and bars with the same letters/symbols show no statistically significant difference at $p \leq 0.05$.

3.3.8 Microscopy Imaging

To analyze effects of ZnO treatments on alfalfa plants, tissues were collected and processed for electron microscopy. Ultrathin sections of tissues were imaged with Ultra-high Resolution Field Emission Scanning Electron Microscope (UHR FE-SEM) coupled with Bright Field (BD) and Dark Field (DF) low voltage STEM, Backscattered electron imaging (LABE and YAG-BSE) and X-ray microanalysis.

STEM imaging of root nodules (Fig. 3.7) confirmed bioaccumulation of ZnO nanoparticles after the treatment. Low magnification DF-STEM helped to locate electrodense regions corresponding to metal oxide particles that possess high Z-contrast by their atomic number (Fig.8-A). ZnO NPs seemed to be accumulated primarily on cell periphery, high magnification BF-STEM of area selected in panel A revealed that aggregates were on cell walls and membranes (Fig. 3.8-B), and in some cases occurred nuclear invasion, as could be observed some particles on nuclear membrane and inside nucleus. Chemical composition was confirmed by X-ray microanalysis, EDX spectra (Fig. 3.8-D) showed peaks of Zn centered at 1.012 and 8.637 keV, whereas mapping of Zn (Fig. 3.8-C) confirmed distribution and sites of accumulation of particles observed by DF and BF-STEM. Backscattered electron imaging with Low Angle Backscattered (LABE) and high sensitivity YAG-BSE, and EDX mapping of Zn and O confirmed observations by DF/BF-STEM (Fig.S9, SI, Appendix 2).

In the case of tissue sections which come from alfalfa roots, ZnO particles appeared concentrated along cell walls and as aggregates clearly distinguished in DF-STEM imaging (Fig. 3.8-A). High resolution BF-STEM and EDX mapping confirmed that these high contrast aggregates corresponded to ZnO (Fig. 3.8-B-C-E). Zn signal was also obtained in the intra and extracellular regions, indicating that ZnO could be suffering dissolution into single particles and

finally into Zn ionic form that interact with cellular components (especially proteins and nucleic acids). No evident signs of apoptosis like DNA condensation, damaged organelles or compromised cell membrane were observed. Backscattered electron imaging (LABE and YAG-BSE) and EDX mapping of Zn and O confirmed observations by DF/BF-STEM (Fig. S10, SI).

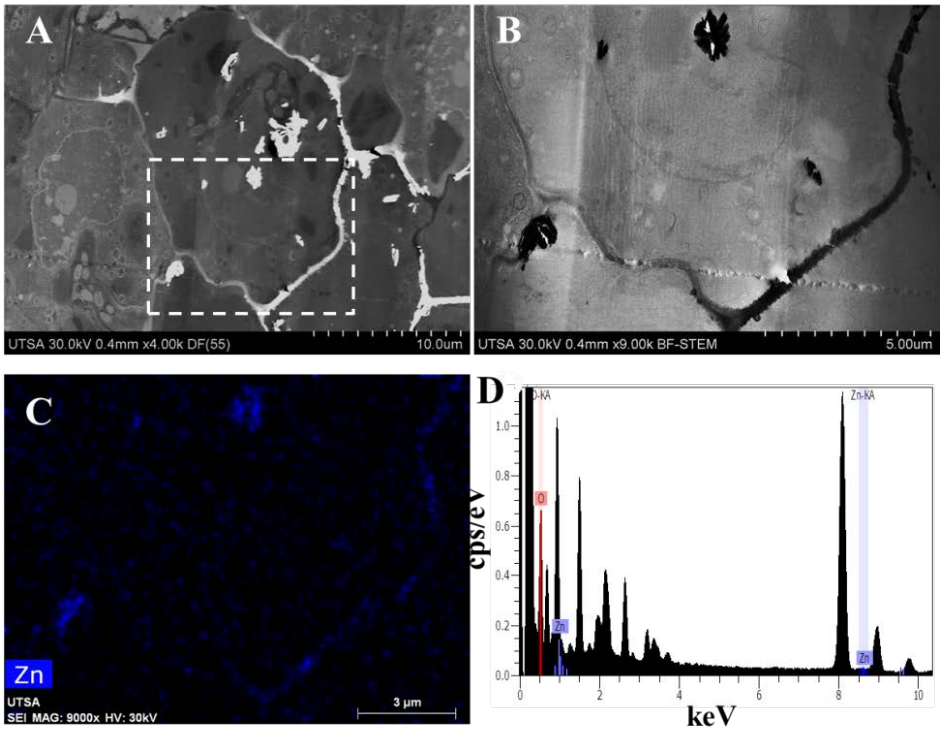

Figure 3.7. Electron microscope imaging of alfalfa nodules treated with 500 mg ZnO NPs/kg of soil for 30 days. (A) DF-STEM, (B) BF-STEM selected area in (A), (C) EDX mapping Zn (blue) (D) EDX spectra showing presence of Zn and O.

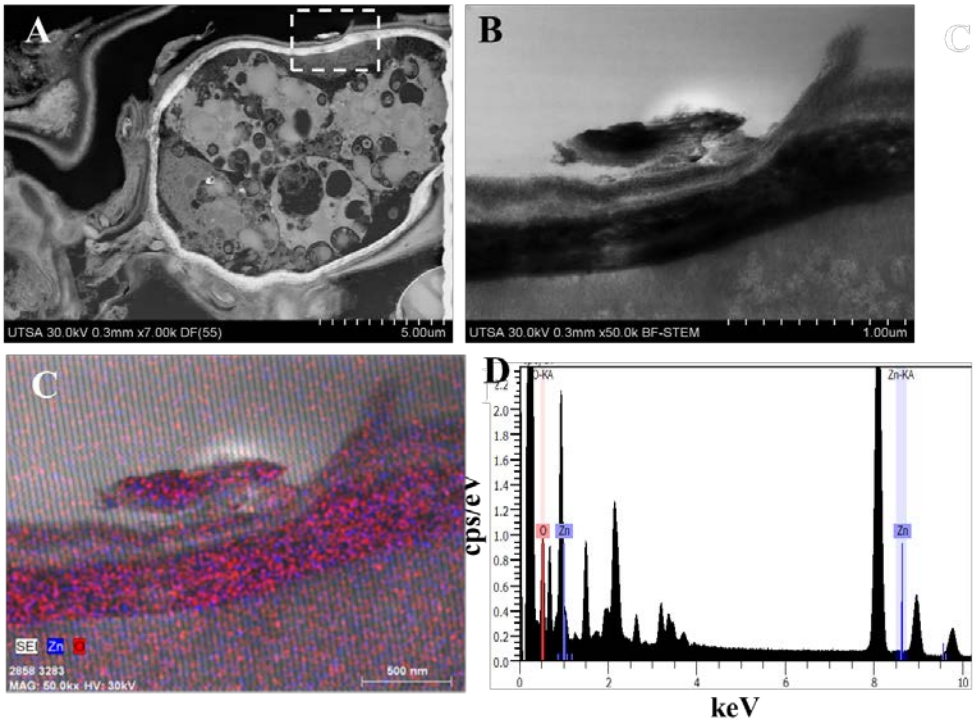

Figure 3. 8. Electron microscope imaging of alfalfa roots treated with 500 mg ZnO NPs/kg of soil for 30 days. (A) DF-STEM, (B) BF-STEM selected area in **(A)**, (C)EDX mapping of Zn and O combined showing the aggregation of ZnO NPs (F)EDX spectra showing Zn and O.

Imaging of alfalfa stem tissue revealed that ZnO accumulated along the cell walls, forming aggregates of ZnO particles (Fig. 3.9-A-B-C). DF-STEM that is sensitive to atomic number due to Z-contrast showed that these striations are formed by small particles of 9-12 nm (Fig. 3.9-D-E). Puntual EDX spectroscopy confirmed that these high contrast structures corresponded to Zn, other peaks that appear in spectra corresponded to osmium (1.91 and 8.9a keV) and copper (0.93 and 8.04 keV) (Fig. 3.9-F). STEM imaging of leaves showed regions of high contrast with electro-dense compounds located around the cell walls. We also observed bright nano size spots in leaf tissue epidermis with high resolution STEM (bright field) which corroborate with the STEM imaging of soybean leaves treated with ZnO NPs by Priester et al.

(*21*) However, EDX spectroscopy did not reveal Zn peaks due to low concentration, but DF and BSE imaging confirmed that accumulations observed by BF-STEM had high z-contrast (Fig.S8 A-F, Appendix 2). Figure S11 (Appendix 2) shows control tissues without ZnO treatment, these samples did not show high-contrast regions or accumulations in compassion with plats treated with nanoparticles.

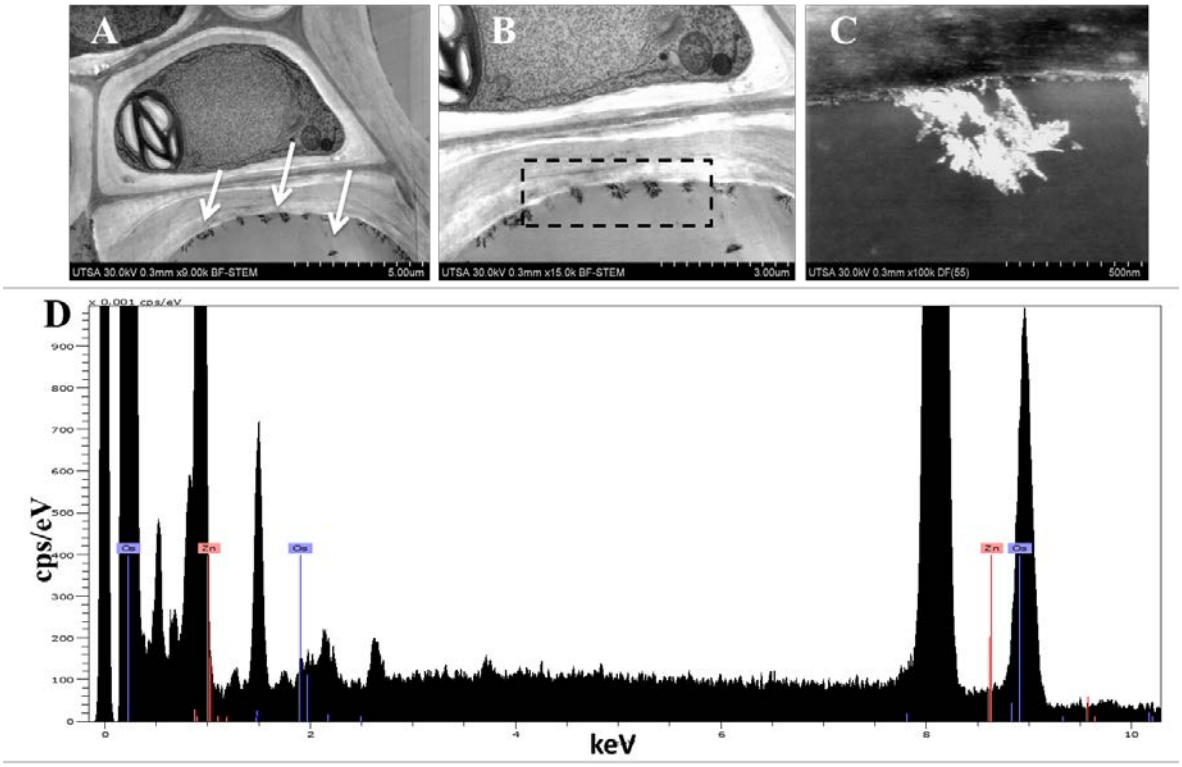

Figure 3. 9. STEM imaging of alfalfa stem treated with 500 mg ZnO NPs/kg of soil for 30 days confirming the presence of ZnO aggregates (A) ZnO nano-aggregates in cell walls of alfalfa stem cells. (B) BF-STEM of ZnO aggregates in cell wall (C) High magnification DF-STEM of selected area in (D), (F) EDX spectra showing Zn and O.

Electron microscopy results corroborate our Zn uptake data (Fig. 3.2A) where Zn accumulation was observed in root, stem, and leaves of alfalfa treated with ZnO NPs. Lin and Xing (2008) also confirmed the aggregation of ZnO NPs in root tissues of ryegrass and their cell organelles (*14*). However, it is important to know if those aggregations are ZnO NPs or some other Zn species. Dissolution data (S2, SI) showed that ZnO NPs releases Zn^{2+} in soil, which can be bio transformed to stem and leaves of alfalfa. However, the accumulation was high in ZnO NP treatments compared to bulk and ionic. Consequently, it can be hypothesized that root exudates dissolve a portion of the ZnO NPs on the root surface and both ZnO NPs and Zn^{2+} were transformed to steam and leaf tissues. The aggregation of ZnO/Zn species was confirmed by STEM imaging. Nonetheless, more extensive research is needed in order to confirm the biotransformation of the ZnO NPs and the associated mechanism. It is also necessary to confirm other factors affecting the ionization.

3.3.9. Conclusion

In summary, our study indicated the comparative phytotoxic effects of ZnO NPs, bulk ZnO, and ionic Zn ($ZnCl_2$) in alfalfa-*S. melilotti* association in terms plant growth, Zn uptake, dry biomass production, leaf area index, and changes in different biochemical parameters. $ZnCl_2$ found as phytotoxic at all concentrations whereas ZnO NPs was toxic at 500 and 750 mg/kg treatments by lowering the plant growth and biomass reduction. Conversely, bulk ZnO acts as alfalfa's growth promoter in certain concentrations. We also evident the aggregation of ZnO NPs in different parts of alfalfa plants along with root nodules, a place of nitrogen fixation. It is likely that in long term exposure, these particles/dissolved Zn species might affect the nitrogen fixation process and hence affect the soil fertility and plant growth.

Chapter 4

Secondary metabolites produced after the interaction of CeO_2 and ZnO nanoparticles with alfalfa (*Medicago sativa*)

Abstract

This research was aimed to study the differential phytotoxic behavior of ZnO and CeO_2 nanoparticles (NPs) towards antioxidative properties of different plant metabolites of alfalfa. Alfalfa plants were cultivated for one month in soil treated with 0, 250, 500, and 750 mg/kg ZnO and CeO_2 NPs. Total leaf chlorophyll, chlorophyll (*a* & *b*), carotenoids, total phenolic (roots and shoots) along with root and shoot flavonoids were quantified spectrophotometrically. Results showed that, compared to control, leaf chlorophyll *a* reduced to 60% and 40% at 750 mg/kg of CeO_2 and ZnO NP treatments, respectively. In addition, Chlorophyll *b* reduced by 64%, 48%, and 60% at 250, 500 and 750 mg/kg CeO_2 NP treatments, while it reduced to 40% with 750 mg/kg ZnO NPs. None of the treatments impacted total phenolic content. However, CeO_2 and ZnO NPs differently affected alfalfa's total root and shoot flavonoid content. While CeO_2 NPs enhanced the root flavonoid by 86% at 500 mg/kg, ZnO NP reduced root flavonoids by 49% at 750 mg/kg, compared to control. Surprisingly, at 250 mg/kg ZnO treatment, alfalfa shoot showed decreasing flavonoid content by 77%, compared to control. To the best of the authors' knowledge, this is the first report on the effects ZnO and CeO_2 NPs on alfalfa's secondary metabolites and chlorophyll contents.

Keyword: Cerium oxide nanoparticles; Zinc Oxide nanoparticles, secondary metabolites, flavonoids, chlorophyll

4.1 Introduction

Alfalfa (*Medicago sativa* L.) is a widely used forage crop and food crop used as nutritional supplement in human diet due to high protein content (*1*). In addition to protein and carbohydrate, it also contains vitamins, nutrients, and numerous secondary metabolites including flavonoids (*2*, *3*), and carotenoids (*4*) that are of attention in human nutrition. It is also reported that flavonoids produced by alfalfa's roots are signaling molecules for nodulation process, acting as chemoattractants (*5-7*). Flavonoids also induce nod gene for the symbiotic *Rhizobium* association in alfalfa (*5*, *6*). Therefore, any change in alfalfa's flavonoids and phenolic contents will directly impact its nutritional value as well as the biological nitrogen fixation process will be distressed.

Due to widespread use of ENPs, the environmental release is of great concern. Consequently, it is crucial to investigate their effects on the ecosystem and also on the quality of food crops, like alfalfa. Interaction of ENPs with higher plants and food crops is widely studied (*8-16*) in terms of bioaccumulation (*9*, *10*) and generation of reactive oxygen species (*11-13*). These plants are the essential components of ecosystems and play important role in the fate and transport of ENPs in the environment through uptake and translocation mechanisms (*17*). Reports have shown that CeO_2 and ZnO NP negatively affect plant growth (*12-14*), reduce total chlorophyll (*12*) and increase anti-oxidative enzyme activities through the generation of reactive oxygen species (ROS) (*11*, *12*).

But the understanding of ENP-plant interactions towards cellular metabolic processes in terms of secondary metabolites and anti-oxidant properties are still in its rudimentary stage. The interaction of phenolic compounds and their antioxidant activity in plants under heavy metal stress is well documented (*18*). However, only few studies have reported the interaction of ENPs

with plants phenolic and flavonoid contents (*18*). For example, Krishnaraj et al. (2012) reported an increase in total phenol content in leaves of the medicinal plant *Bacopa monnieri* (Linn.) Wettst. treated with AgNPs (*19*) . Recently, Rico et al. (2013) evidenced 12.5% increase in flavonoid concentration in grains of certain variety of rice treated with $nCeO_2$ (*20*).

However, to the best of our knowledge, no studies have been reported on the interaction of CeO_2 and ZnO NPs towards alfalfa's (*Medicago sativa L.*) antioxidative activities/secondary metabolites. These metabolites play very important role by maintaining plants physiological functions and protection from outside stress (*2*, *3*). Therefore, this research was aimed to investigate the phytotoxic effect of CeO_2 and ZnO NPs towards alfalfa in terms of changes in their anti-oxidants/secondary metabolites content. Plants treated with CeO_2 and ZnO NPs for 30 d were analyzed for Ce and Zn, chlorophyll (*a*, *b*, and total) content, carotenoids, total phenolic and flavonoids. ICP-OES was used to quantify the amount of Ce and Zn accumulated in root and shoot tissues of alfalfa. Leaf chlorophyll and carotenoids, phenolic and flavonoid content of roots and shoots were quantified by using UV-vis spectrophotometry.

4.2. Materials and Methods

4.2.1. Characterization of CeO_2 and ZnO NPs

Ten nanometer *n*CeO_2 and ZnO NPs (Meliorum Technologies, Rochester, NY) were obtained from the University of California Center for Environmental Implications of Nanotechnology (UC-CEIN). The NPs were previously characterized and published by Bandyopadhyay et al. (2011) (*21*) and Keller et al. (2010)(*22*). The desired amounts of NPs were suspended in Millipore water (MPW) and applied to soil to have 250, 500, and 750 mg/kg of soil. *n*CeO_2 and ZnO NPs suspensions were sonicated for 15 minutes in a water bath (Crest Ultrasonics, Trenton, NJ) and then mixed with soil.

4.2.2. Soil sampling, characterization, and pot preparation

The soil was collected from Fabens, Texas and top 10 cm soil was sampled and used for all the experiments. The plants were grown in 2:1 (v/v) mixture of organic potting soil (Scotts, premium potting soil to enhance soil fertility) and the regular soil. The soil was characterized before mixing for grain size. The original (Faben, TX) soil type was found sandy loam in texture (based on the USDA soil classification scheme) (*23*). The soil parameters were recorded as: pH 7.71±0.5, CEC 8.01±0.3 and 25±0.5 mg/kg of Zn. The pots were prepared with soil amended with desired amount of *n*CeO_2 and ZnO NPs to achieve the concentration of 250, 500, and 750 mg/kg soil. The soil mixed with NPs was kept overnight for stabilization and next day, alfalfa seeds were planted (50 seeds per pot). Three replicates were prepared for each treatment.

4.2.3. Plant growth

At harvest, the plant roots were washed with 4% HNO_3, followed by rinsing with MPW. Shoots and roots were separated and oven dried at 70°C for further analysis for elemental (Ce and Zn) constituents. For Chlorophyll estimation, fresh alfalfa leaves were used and for phenolic and flavonoid estimation, freeze dried alfalfa root and shoots samples were used.

4.2.4. Quantification of Zn and Ce in dry plant tissues

The above and below ground part of alfalfa plants were carefully washed with 4% HNO_3 followed by washing with $CaCl_2$ and DI water. Later, roots and shoots were separated and digested by microwave-assisted acid digestion with concentrated plasma-pure HNO_3 and H_2O_2 (30%) (1:4) in a microwave acceleration reaction system (CEM Corp.; Mathews, NC) (11, 12). The digested materials were analyzed for Ce and Zn content by ICP-OES (Perkin-Elmer Optima 4300 DV, Shelton, CT equipped with a Burgener PEEK MiraMist nebulizer with argon flow). To QC check of the analytical methods and digestion, blank, spiked, and Certified Reference Material (spinach leaves and peach leaves NIST 1547 and 1570) were processed as samples, and

the Zn and Ce recovery rate was 99.82 ± 0.55 and 98± 0.55 respectively.

4.2.5. Chlorophyll/carotenoids estimation

Alfalfa leaves (0.2g) were extracted in acetone and chlorophyll *a* and *b* were estimated by the formulae of Lichtenthaler and Wellburn (*24*) and Porra et al. (2002) (*25*). Total carotenoids were also measured by following Porra et al. (2002) (*25*).

4.2.6. Analysis of Antioxidant Property

For the phenolic and flavonoids determinations, freeze dried alfalfa root and shoot tissues were used. The extract for the phenolic and flavonoids estimation was prepared in methanol by following Adom and Liu (*26*) protocol. The total phenolic content was estimated by following Dewanto et al. (*27*) and flavonoid were estimated according to and Jia et al. (*28*).

4.2.7. Statistical Analysis

Each treatment was replicated three times. A one-way ANOVA test and Tukey-HSD multiple comparisons test were performed to analyze the results using SPSS statistical package 12.0 (SPSS, Chicago, IL). The data (means ± SE) were reported as averages of three replicates in all cases and were compared using Least Significant Differences. Statistical significance was based on probabilities of $p \leq 0.05$ except, when otherwise stated. All values were reported in dry weight basis, except chlorophyll and carotenoids.

4.3. Results and Discussions

4.3.1. Zn and Ce Bioaccumulation

Figure 4.1A shows the zinc concentration in dry alfalfa root and shoot tissues after one month treatment in soil. Compared to control, roots accumulated 8x, 15x, and 17x more Zn at 250, 500, and 750 mg/kg ZnO NP treatments; while shoot accumulated 2x and 2.5x more Zn at 250, 500~750 mg/kg treatment than control. However, in the case of CeO_2 NP treatments Ce level

increased to 39x, 48x, and 34x in roots compared to control (Figure 4.1B). Shoot accumulated 13x, 15x and 9x more Ce than in control. Previously, it has been evidenced that two and four fold increase in Zn uptake by green pea roots treated with 250 and 500 mg/kg of ZnO NP, compared to plants treated with 125 mg/kg (*12*). In addition, alfalfa accumulated higher Ce in roots compared other reported studies (*8*, *11*) as it is a well known hyperaccumulator. We also observed higher Zn translocation in shoot compared to cerium. This was also evident through the translocation factor (TF), where Zn has higher TF of 0.42 at 250 mg/kg compared to 500 and 750 mg/kg treatments (TF~0.27). But, the TF was almost the same for all three concentrations of CeO_2 NP treatments as 0.12, 0.11, and 0.11 for 250, and 500 and 750 mg/kg CeO_2 treatments. Higher TF signifies that Zn was taken up and distributed more in alfalfa shoots than in the case of Ce. Our results are in agreement with previously reported literature (*8*), where the majority of the Ce species accumulated in cucumber roots, compared to stem and leaves (*8*).

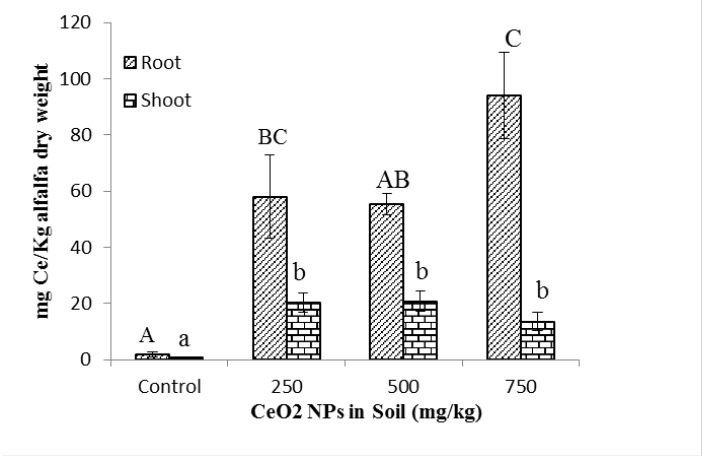

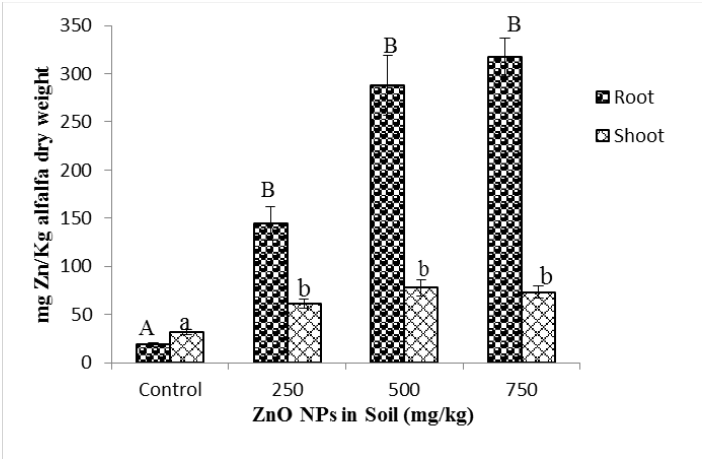

Table 4.1. Total leaf carotenoids represented as mg /g fresh alfalfa leaves treated with 0, 250, 500, and 750 mg of ZnO NPs and CeO2 NPs. Data are means ± standard error of four replicates.

4.3.2. Leaf Chlorophyll and Carotenoid Contents

Figure 4.2 shows chlorophyll concentrations in alfalfa leaves treated with CeO_2 and ZnO at 250, 500, and 750 mg/kg concentrations. As seen in Figure 4.2 (A-C), ZnO and CeO_2 differentially affected chlorophyll production. In the case of ZnO NPs, chlorophyll *a* was reduced by 40% at 750 mg/kg treatments whereas 60% less chlorophyll was produced at 750 mg/kg CeO_2NP treatment (Fig. 4.2A). Chlorophyll *b* reduced by 64%, 48%, and 60% at 250, 500 and 750 mg/kg CeO_2 NP treatments, and it remained the same in the case of the ZnO treatments, except with a 40% reduction at 750 mg/kg ZnO NP treatment, compared to control (Figure 4.2B).

Table 4.1. Total leaf carotenoids represented as mg /g fresh alfalfa leaves treated with 0, 250, 500, and 750 mg of ZnO NPs and CeO2 NPs. Data are means ± standard error of four replicates.

Treatments	Control	250 mg/kg	500mg/kg	750mg/kg
ZnO NPs	57.76±4.98a	50.73±1.45a	42.24±4.34b	43.78±2.87b
CeO_2 NPs	57.76±4.98a	21.25±5.43b	45.29±6.81a	38.80±6.38

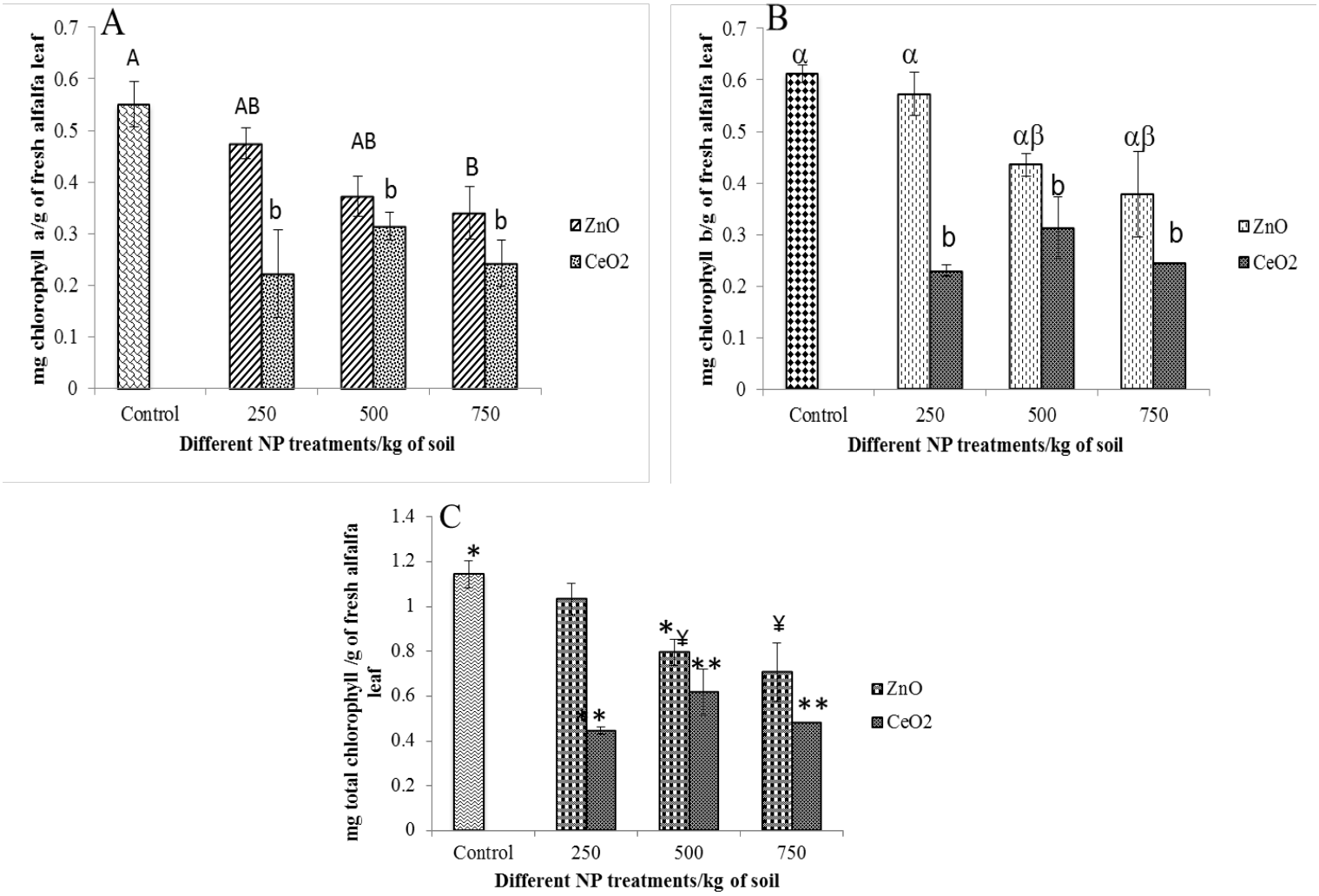

Figure 4. 2. (A) Chlorophyll *a*, (B) Chlorophyll *b*, and (C) total chlorophyll content in leaves of alfafa plants grown for 30days in soil treated with 0 (control), 250, 500, and 750 mg/kg of ZnO NPs and CeO_2 NPs. Error bars stand for standard errors and bars with different symbol/letters show statistically significant difference ($p \leq 0.05$).

Total chlorophyll content (Fig. 4.2C) showed the same trend at 750 mg/kg ZnO NP treatments with 38% reduction than control, while CeO_2 NPs reduced the total chlorophyll to

61%, 46%, and 58% at 250, 500, and 750 mg/kg treatments respectively. Conversely, the leaf carotenoids remain unaltered in all ZnO NP treatments and 63% reduction was observed in the case of the 250 mg/kg CeO_2 treatment (Table 4.1). Significant decrease in plant's carotenoid might have impacted the photosynthetic apparatus and light harvesting process (*29*) and hence the overall photosynthesis could have been disturbed. A decrease in chlorophyll content with increasing ZnO NPs was reported previously (*12, 29, 30*) and possibly due to substitution of the central magnesium of chlorophyll by Zn^{2+} (*30*).Thereafter, substitution might prevent photosynthetic light harvesting which resulted in chlorophyll decay and ultimately, interrupt the photosynthetic activity (*12, 30, 31*). However, lower chlorophyll and carotenoid contents with higher CeO_2 NPs were not well understood. We hypnotize that, like in the case of heavy metals, CeO_2 might reduce the photosynthetic pigments and/or inhibit the enzymes involved in chlorophyll biosynthesis (*32, 33*), hence, decreasing photosynthetic pigments.

4.3.3. Antioxidant Properties of Root and Shoot of Alfalfa Plants

Phenolic and flavonoid compounds in alfalfa possess antioxidative properties which make it a nutritional diet for humans (2-4). Therefore, these metabolites were quantified in alfalfa roots and shoot treated with CeO_2 and ZnO NPs. The effect of CeO_2 and ZnO NPs on alfalfa's total phenolic content in root and shoots are represented in Figure 4.3A and 4.3B, respectively. No statistically significant changes were observed in all the treatments except 20% increase in total phenolics in the 500 mg/kg CeO_2 NP treatment, compared to control.

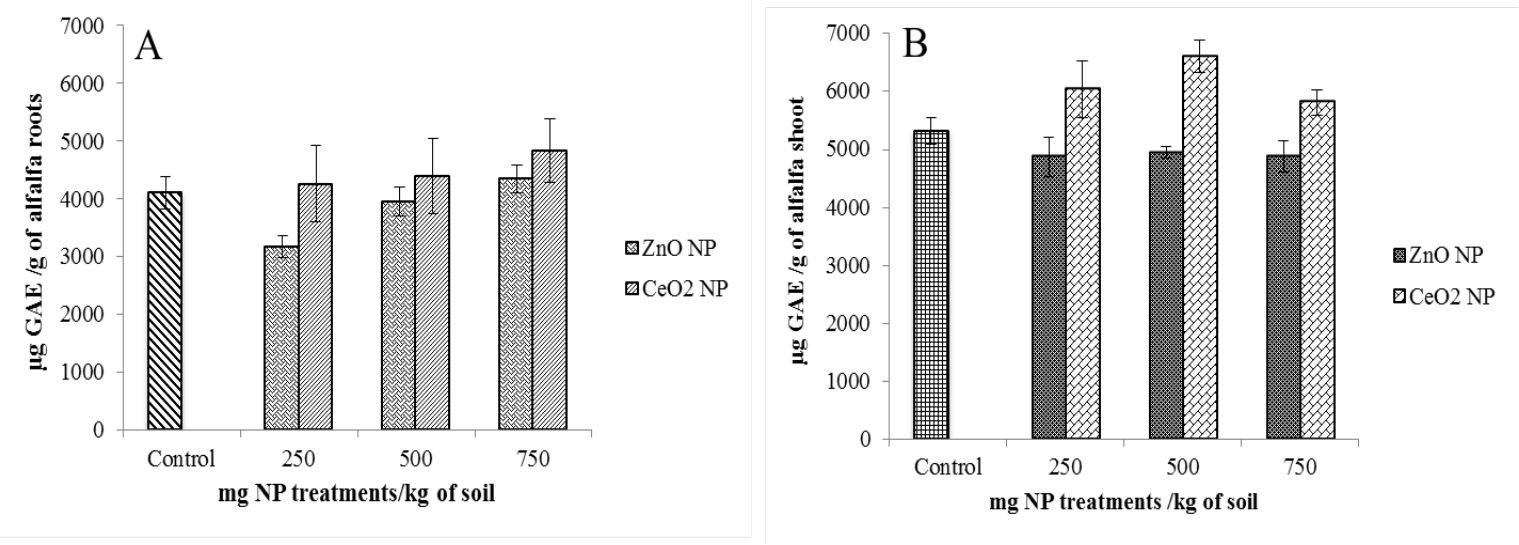

Figure 4. 3. Total phenolic content (represented as µg GAE/g) of freeze dried alfalfa plant's (A) roots, (B) Shoots, treated with 0 (control), 250, 500, and 750 mg/kg ZnO and CeO_2 NPs. GAE = gallic acid equivalent.

Root and shoot flavonoid contents are reported in Figure 4.4 (A-B). Our findings indicated an inverse relationship between CeO_2 and ZnO NPs treatments in roots and shoots flavonoids in alfalfa (Fig. 4.4A-B). CeO_2 NPs enhanced the root flavonoids content by 34% in the 750 mg/kg treatment and 86% in shoot in the 500 mg/kg treatment, compared to control (Fig. 4.4A). A decrease of 49% of total root flavonoids was observed at 750 mg/kg in the ZnO NP treatment, whereas total flavonoids in shoots remained almost the same to control, except in the 250 mg/kg treatment. Total flavonoid content decreased to 77% in shoots, compared to control. CeO_2 showed an increasing trend of root and shoot flavonoid whereas ZnO showed a decrease in root flavonoids. These results are in agreement with the reported results of Krishnaraj et al. (2012) where phenol content was increased in leaves of *Bacopa monnieri* (Linn.) Wettst. plant

treated with AgNPs (*19*). However, rice (*Oryza sativa*) treated with 500 mg/kg CeO_2 NPs showed a mixed trend of increasing flavonoids and decreasing phenolic content in certain concentrations, thus suggesting higher antioxidant activity in plants treated with CeO_2 NPs (*17*). However, the decrease in flavonoid content with high ZnO NPs suggest increase antioxidative activity of plants under metal stress (Zn/ZnO) since these molecules play a protective role in metal chelation and scavenging of reactive oxygen species (*18*). Conversely, an increase in flavonoids with higher concentration of CeO_2 NPs might correlate to the increased enzymatic activities; suggesting '*de novo*' synthesis of phenolic under stress (*18*) and/or result of conjugate hydrolysis (*34*). Reductions in root flavonoids of alfalfa with increasing dose of ZnO NPs cause concerns about the fact that it might interfere with biological nitrogen fixation processes and also can cause a negative effect in the nutritional value of alfalfa shoots. Additionally, it is hypothesized that there is a probability of increasing plant stress due to accumulation of reactive oxygen species (ROS) as flavonoids inhibit the generation of ROS and then reduce ROS once they are formed in plant tissues (*35*). However, more studies are needed in order to determine the effects of NPs on the alfalfa's flavonoids and radical scavenging ability. In summary, we conclude that the reducing functions of flavonoids along with the decrease in total leaf chlorophyll content suggests that alfalfa plants are affected from severe stress conditions due to exposure to the NPs.

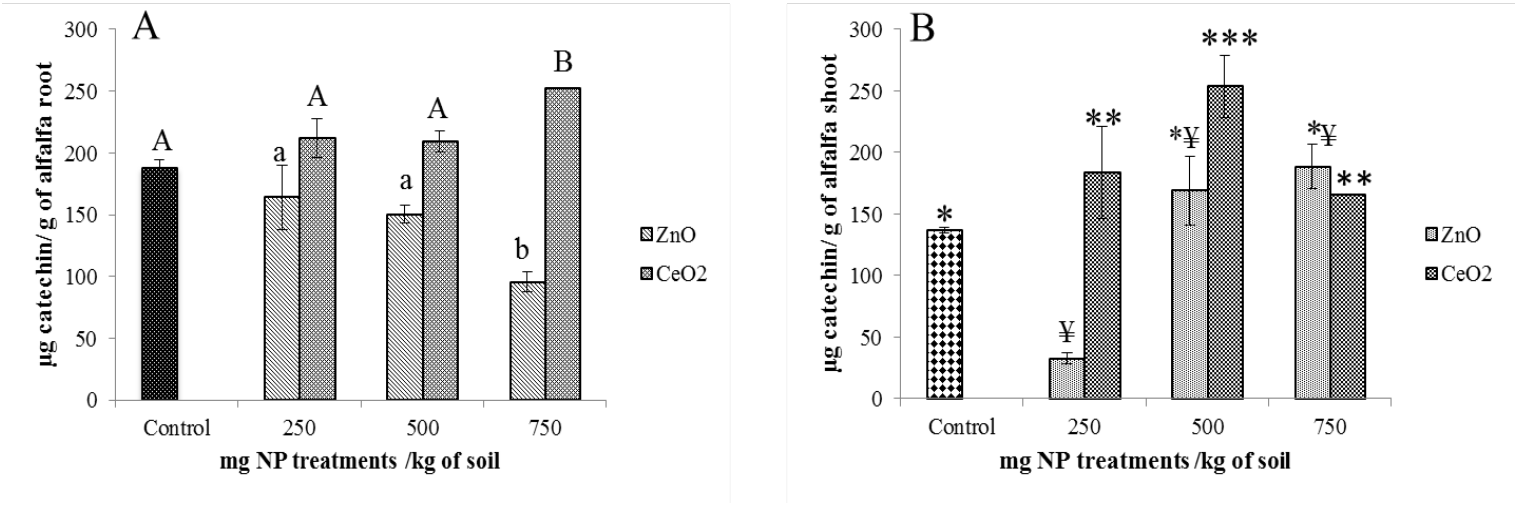

Figure 4.4. Changes in alfalfa's flavonoid content s expressed as µg catechin/g of freeze dried (A) root, and (B) shoot tissues. Plants were treated with 0 (control), 250, 500, and 750 mg/kg ZnO NPs and CeO_2 NPs respectively. Error bars stand for standard errors and bars with different symbol/letters show statistically significant difference ($p \leq 0.05$).

Chapter 5

Conclusion

To the best of authors knowledge, this is the first study where toxicity of two different NPs (CeO_2 and ZnO) and related bulk materials were tested in host plant alfalfa and the associated bacterium *S. meliloti*; separately and/or in symbiotic association. In phase I of this research, we found that these NPs showed differential bacteriological and phytotoxic effects in *S. meliloti* (Rm 1021). Assays in liquid cultures showed that CeO_2 NPs reduced bacterial growth at all concentrations. The growth profile for ionic cerium (Ce^{4+}) also showed same inhibitory effects the the NPs. Moreover, at the highest concentration (125 mg/L), CeO_2 NPs exhibited bacteriostatic effects against this bacterium. On the other hand, at all ZnO NPs concentrations, no bacterial growth were observed; suggesting bactericidal effect. This was also evidenced via the MIC and DIZ tests. The higher toxicity of ZnO NPs was attributed to the combined effect of surface attachment and internalization of the NPs (confirmed through STEM) and the corresponding ionic zinc. The plausible mechanism of action of ZnO NPs towards bacterial cell encompasses a direct interaction between the NPs and the cell surface. Thereby Zn/ZnO NPs accumulates out/ inside the cell wall, distressing the membrane chemistry by production of ROS, resulting in inhibition of the growth and viability of *S. meliloti*, and eventually cell death .

From the studies with ZnO NPs, bulk ZnO, and ionic Zn ($ZnCl_2$) in soil cultivated alfalfa-*S. melilotti* association (Phase II), we found that $ZnCl_2$ was phytotoxic at all concentrations, whereas ZnO NPs were toxic at 500 and 750 mg/kg treatments. Results showed 50% germination reduction by bulk ZnO at 500 and 750 mg/kg and at all $ZnCl_2$ concentrations. ZnO NPs and ionic Zn reduced root and shoot biomass by 80% and 25%, respectively. Conversely, bulk ZnO at 750 mg/kg increased shoot and root biomass by 225% and 10%, respectively,

compared to control. At 500 and 750 mg/kg, $ZnCl_2$ reduced CAT activity in stems and leaves. Total leaf protein significantly decreased as external $ZnCl_2$ doses increased. TEM images showed aggregation of ZnO NPs in different parts of alfalfa plants, along with root nodules, where nitrogen fixation occurs. It is likely that in long term exposures, these particles/dissolved Zn species might affect the nitrogen fixation process, and hence, affect the soil fertility and plant growth.

In Phase III, our extended studies showed that CeO_2 and ZnO have differential toxicity effects on chlorophyll and other secondary metabolites of alfalfa. At 750 mg/kg, both CeO_2 and ZnO NPs reduced chlorophyll *a* by60% and 40%, respectively. In addition, Chlorophyll *b* reduced by 64%, 48%, and 60% at 250, 500 and 750 mg/kg CeO_2 NP treatments, while it reduced to 40% with 750 mg/kg ZnO NPs. None of the treatments affected total phenolic content. However, CeO_2 and ZnO NPs impacted alfalfa's total root and shoot flavonoid content differently. CeO_2 NPs enhanced the root flavonoid by 86% at 500 mg/kg, ZnO NP reduced root flavonoids by 49% at 750 mg/kg, compared to control. Unexpectedly, at 250 mg/kg ZnO treatment, alfalfa shoot showed decreasing flavonoid content by 77%, compared to control. ZnO NPs decreased root and shoot flavonoids which indicate accumulation of H_2O_2 in tissues due to stress response of NPs. However, CeO_2 showed an increasing trend in alfalfa's total flavonoids production, which directly indicates higher ROS production. Our results indicate that alfalfa plants are affected from severe stress conditions due to NPs treatments, which in long term might affect nitrogen fixation processes and/or global nitrogen cycle. To, best of authors knowledge, this is the first study where toxicity of two different NPs (CeO_2 and ZnO) were tested in host plant alfalfa and the associated bacterium *S. meliloti*; separately and/or in symbiotic association in soil.

Acknowledgement

This material is based upon work supported by the National Science Foundation and the Environmental Protection Agency under Cooperative Agreement Number DBI-0830117. Any opinions, findings, and conclusions or recommendations expressed in this material are those of the author(s) and do not necessarily reflect the views of the National Science Foundation or the Environmental Protection Agency. This work has not been subjected to EPA review and no official endorsement should be inferred. The authors also acknowledge the USDA grant numbers 2008-38422-19138 and 2011-38422-30835 and the NSF Grant # CHE-0840525. J. L. Gardea-Torresdey acknowledges the Dudley family for the Endowed Research Professorship in Chemistry. The authors also acknowledge Dr. Guillermo Carrillo-Castaneda from Postgraduate College of Chapingo, Mexico who kindly supplied the bacterial cells and Dr. Jose Nunez for his help in the IR studies. The authors acknowledge Dr. Chuan (River) Xiao biochemistry research laboratory for spectroscopic measurements.

Chapter 6

References

Chapter 1

1. ASTM E2456-06. *Standard Terminology Relating to Nanotechnology* Available at:http://www.astm.org/Standards/E2456.htm(accessed November11, 2013).
2. Weinberg, H., Galyean, A. and Leopold, M. Evaluating engineering nanoparticles in natural waters. *Trends Anal. Chem.*, **2011**, 30(1): 72–83.
3. Huang, X., Neretina, S. and El-Sayed, M. A. Gold nanorods: From synthesis and properties to biological and biomedical applications. *Adv. Mater*, **2009**, 21: 4880–4910.
4. Nel, A.; Xia, T.; Madler, L.; Li, N. Toxic potential of materials at the nanolevel. *Science* **2006**, *311*, 622–627.
5. Pelletier, D. A.; Suresh, A. K.; Holton, G. A.; McKeown, C. K.; Wang, W.; Gu, B.; Mortensen, N. P.; Allison, D. P.; Joy D. C.; Allison, M. R.; Brown, S. D; Phelps, T. J.; Doktycz, M. J. Effects of Engineered Cerium Oxide Nanoparticles on Bacterial Growth and Viability, *App Environ. Microb*. **2010**, *75*, (24) 7981–7989.
6. Delay, M.; Frimmel, F.H. Nanoparticles in aquatic systems. *Anal Bioanal Chem* **2012** *402*,583–592.
7. Gaiser, B. K., Fernandes, T. F., Jepson, M. A., Lead, J. R., Tyler, C. R., Baalousha, M., Biswas, A., Britton, G. J., Cole, P. A., Johnston, B. D., Ju-Nam, Y., Rosenkranz, P., Scown, T. M. and Stone, V. Interspecies comparisons on the uptake and toxicity of silver and cerium dioxide nanoparticles. *Environ. Toxicol. Chem. 2012, 3, 144-154.*

8. Sharma, V.; Anderson, D. Alok, D.Zinc oxide nanoparticles induce oxidative DNA damage and ROS-triggered mitochondria mediated apoptosis in human liver cells (HepG2). *Apoptosis* 2012, 1-19 (DOI: 10.1007/s10495-012-0705-6).

9. Martha L. López-Moreno, M. L.; Guadalupe de la Rosa, G.; José.; Hernández-Viezcas, J.A.; Peralta-Videa, J.R.; Gardea-Torresdey, J.L. X-ray Absorption Spectroscopy (XAS) Corroboration of the Uptake and Storage of CeO2 Nanoparticles and Assessment of Their Differential Toxicity in Four Edible Plant Species. *J. Agri. Food Chem*. 2010 58 (6), 3689-3693.

10. Hawthorne, J.; Musante, C.; Sinha, S.K.; White, J.C. Accumulation and Phytotoxicity of Engineered Nanoparticles to Cucurbita Pepo. *Inter. J. Phytorem*. **2011**, *14*, 429-442.

11. Sinha, R.; Karan, R.; Sinha, A.; Khare, S.K. Interaction and nanotoxic effect of ZnO and Ag nanoparticles on mesophc and halophilic bacterial cells. *Bioresource Technol.* **2011,** 102, 1516–1520.

12. Lin, D.; Xing, B. Phytotoxicity of nanoparticles: inhibition of seed germination and root growth. *Environ. Pollut*. **2007**, 150, 243–250.

13. Lee, W. M.; An, Y. J.; Yoon, H.; Kweon, H. S. Toxicity and bioavailability of copper nanoparticles to terrestrial plants Phaseolus radiatus (mungbean) and Triticum aestivum (wheat); plant agar test for water-insoluble nanoparticles. *Environ. Toxicol. Chem*. **2008**, 27, 1915–1921.

14. Barrena, R.; Casals, E.; Colon, J.; Font, X.; Sanchez, A.; Puntes, V. Evaluation of the ecotoxicity of model nanoparticles. *Chemosphere* **2009**, 75, 850–857.

15. C. O. Dimkpa, J.E. McLean, D. W. Britt, and A.J. Anderson, *Ind. Biotechnol*, 2012, **8**, 344.

16. L. Zhao, J. A. Hernandez-Viezcas, J.R. Peralta-Videa, S. Bandyopadhyay, B. Peng, B. Munoz, A. A. Keller, and J.L. Gardea-Torresdey, *Environ. Sci.: Processes & Impacts*, 2013, **15**, 260.

17. A. Mukherjee, J. R. Peralta-Videa, S. Bandyopadhyay, C. M. Rico, L. Zhao and J.L. Gardea-Torresdey, *Metallomics*, 2014. **DOI:** 10.1039/C3MT00064H, available at: http://pubs.rsc.org/en/content/articlehtml/2014/mt/c3mt00064h.

18. D. Lin, D. and B. Xing, *Environ. Pollut.*, 2007, **150**, 243.

19. D. Lin, D. and B. Xing, *Environ. Sci. Technol.*, 2008, **42**, 5580.

20. D. Stampoulis, S. K. Sinha, J. C. White, *Environ Sci Technol.* 2009, **43**, 9473.

21. S. Kim, J. Kim, I. Lee, *Chem. Ecol.*, 2011, **27**, 49.

22. de la Rosa, G., López-Moreno, M.L., Hernández-Viescaz, J., Peralta-Videa, and J. R., Gardea-Torresdey, J. L. *Int. J. Nanotechnol*., 2011, **8**, 492.

23. J. H. Priester, Y.Ge, R.E. Mielke, A. M. Horst, S. Cole Moritz, K. Espinosa, J. Gelb, S.L. Walker, R.M. Nisbet, J. P. Schimel, R.G. Palmer, J.A. Hernandez-Viezcas, L. Zhao, J. L. Gardea-Torresdey and P. A. Holden, *Proc. Natl. Aca. Sci. USA. PNAS*, 2012, 109 (37), 2451.

24. Cherchi, C.; Chernenko, T.; Diem, M.; Gu, A. Z. Impact of nano titanium dioxide exposure on cellular structure of *Anabaena variabilis* and evidence of internalization. *Environ.Toxicol.Chem*. 2011, 30, 861-869.

25. Cherchi, C.; Gu, A.Z. Impact of Titanium Dioxide Nanomaterials on Nitrogen Fixation Rate and Intracellular Nitrogen Storage in *Anabaena variabilis. Environ. Sci. Technol.*, **2010**, 44 (21), 8302–8307.

26. Yang, Y.; Wang, J.; Zhu, H.; Colvin, V.L.; Alvarez, P.J. Relative Susceptibility and Transcriptional Response of Nitrogen Cycling Bacteria to Quantum Dots. *Environ. Sci. Technol*, **2012**, dx.doi.org/10.1021/es203485f

27. Premanathan, M.; Karthikeyan, K.; Jeyasubramanian, K.; Manivannan, G.; Selective toxicity of ZnO nanoparticles toward Gram-positive bacteria and cancer cells by apoptosis through lipid peroxidation. *Nanomed.: Nanotechnol., Biol. Med.* **2011**,*7*, 184–192.

28. Thill, A.; Zeyons, O.; Spalla, O.; Chauvat, F.; Rose, J.; Auffan, M.; Flank, A.M. Cytotoxicity of CeO_2 nanoparticles for *Escherichia coli.* Physico-chemical insight of the cytotoxicity mechanism. *Environ. Sci. Technol.* **2006**, *40*, 6151–6156.

29. Xie, Y.; He, H.; Irwin, P. L.; Jin, T. Antibacterial Activity and Mechanism of Action of Zinc Oxide Nanoparticles against *Campylobacter jejuni 201, Appl. Environ. Microbiol.* **2011**, *77*, 2325-2331.

30. Jiang, W.; Mashayekhi, H.; Xing, B. Bacterial toxicity comparison between nano- and micro-scaled oxide particles, *Environ. Pollution* **2009**, *157*, 1619–1625.

31. Li, M.; Zhu, L.; Lin, D. Toxicity of ZnO Nanoparticles to *Escherichia coli*: Mechanism and the Influence of Medium Components. *Environ. Sci. Technol.* 2011, *45*, 1977–1983.

32. Li, M.; Pokhrel, S.; Jin, X.; Mädler,L.; Damoiseaux, R.; Hoek R.M.V. Stability, Bioavailability, and Bacterial Toxicity of ZnO and Iron-Doped ZnO Nanoparticles in Aquatic Media. *Environ. Sci. Technol.* 2011, *45*, 755–761.

33. Gonzalez, J.E.; York, G.M.; Walker, G.C. *Rhizobium meliloti* exopolysaccharides: synthesis and symbiotic function**.** *Gene* **1996**, *179,*141-146.

34. Barnes, D.K.; Goplen, B. P.; Baylor, J.E. Highlights in the USA and Canada. In: Hanson AA, Barnes DK, and Hill RR, Jr. (eds) Alfalfa and alfalfa improvement. *Am. Soc. Agronom*. Madison, Wisconsin. Monograph, **1988**, *29*, 1-24.

35. Lopez, M.L., Peralta-Videa, J.R., Parsons, J.G., Gardea-Torresdey, J.L. Duarte-Gardea, M. Plant growth, uptake and translocation of lead, micro, and macronutrients in alfalfa treated with indole-3-acetic acid, kinetin, and ethylenediaminetetraacetic acid. International *Jour. Phytorem.* **2009**, 11(2), 131-149.

36. Peralta-Videa, J. R.; de la Rosa, R.; Gonzalez, J. H., Gardea-Torresdey, J. L. Effects of the growth stage on the heavy metal tolerance of alfalfa plants. *Adv. Environ. Res*. **2004**, 8, Issues 3–4, 679–685.

37. Miller, R.W., Al-Khazraji, M.L., Sisson, D.R.,Gardiner, D.T. Alfalfa growth and absorption of cadmium and zinc from soils amended with sewage sludge. *Agri. Eco. Environ.* **1995**, 53, 2, 179-184.

38. J.R. Peralta-Videa, J.L. Gardea-Torresdey, E. Gomez, K.J. Tiemann, J.G. Parsons, G. Carrillo, Effect of mixed cadmium, copper, nickel and zinc at different pHs. *Environ. Poln.* **2002**, 119, 3, 291–301.

39. Peralta-Videa, J.R., Gardea-Torresdey, J.L., de la Rosa, G., Gonzales, J.H., and Herrera, I. Effect of heavy metals on alfalfa plants at different growth stages. *Adv. Environ. Res.***2004**, 8(3-4), 679-685

40. Anderson, T.A., Guthrie, E.A., Walton, B.T. Bioremediation in the rhizosphere: plant roots and associated microbes clean contaminated soil. **1993**, *Environ Sci. Technol* 27: 2630–2636.

41. Botsford, A simple and rapid method to determine toxicity using a bacterial indicator organism, U.S. EPA (**2002**) El Paso County Metals Survey.

42. Wu, B.; Wang, Y.; Lee, Y.H.; Horst, A.; Wang, Z.P.; Chen, D.R.; Sureshkumar, R.; Tang, Y.J.J. Comparative eco-toxicities of nano-ZnO particles under aquatic and aerosol exposure modes. *Environ. Sci. Technol*. **2010**, *44*, 1484-1489.

43. Ruparelia, J.P.; Chatterjee, A.K.; Duttagupta, S.P.; Mukherji S. Strain specificity in antimicrobial activity of silver and copper nanoparticles. *Acta Biomaterialia* **2008**, *4*, 707– 716.

Chapter 2

1. A. Nel, T. Xia, L. Madler, N. Li, Toxic potential of materials at the nanolevel, *Science*, **2006**, 311, 622–627.

2. D.A. Pelletier, A. K. Suresh, G.A. Holton, C.K. McKeown, W.Wang, B. Gu, N. P. Mortensen, D. P. Allison, D. C. Joy, M. R. Allison, S.D. Brown, T. J. Phelps, M. J. Doktycz, Effects of Engineered Cerium Oxide Nanoparticles on Bacterial Growth and Viability. *App. Environ. Microb.* **2010**, **7,** 7981–7989.

3. M. Delay, F. H. Frimmel, Nanoparticles in aquatic systems, *Anal. Bioanal. Chem*. **2012**, 40, 583–592.

4. M.L. López-Moreno, G. Guadalupe de la Rosa, J.A. Hernández-Viezcas, J. R. Peralta-Videa, J.L. Gardea-Torresdey, X-ray Absorption Spectroscopy (XAS) Corroboration of the Uptake and Storage of CeO_2 Nanoparticles and Assessment of Their Differential Toxicity in Four Edible Plant Species, *J. Agri. Food Chem*. **2010**, 58, 3689-3693.

5. J. Hawthorne, C. Musante, S. K. Sinha, J. C. White, Accumulation and Phytotoxicity of Engineered Nanoparticles to *Cucurbita Pepo*, *Inter. J. Phytorem*. **2011**, 14, 429-442.

6. R. Sinha, R. Karan, A. Sinha, S. K. Khare, Interaction and nanotoxic effect of ZnO and Ag nanoparticles on mesophc and halophilic bacterial cells, *Bioresource Technol.* **2011**, 102, 1516–1520.

7. B. K. Gaiser, T. F. Fernandes, M. A. Jepson, J. R. Lead, C. R.Tyler, M.Baalousha, A. Biswas, G. J.Britton, P. A. Cole, B. D. Johnston, Y. Ju-Nam, P. Rosenkranz, T.M. Scown, V. Stone, Interspecies comparisons on the uptake and toxicity of silver and cerium dioxide nanoparticles, *Environ. Toxicol. Chem*. **2012**, 3, 144-154.

8. V. Sharma, D. Anderson, D. Alok, Zinc oxide nanoparticles induce oxidative DNA damage and ROS-triggered mitochondria mediated apoptosis in human liver cells (HepG2), *Apoptosis* , **2012**, 1-19 (DOI: 10.1007/s10495-012-0705-6).
9. M. Premanathan, K. Karthikeyan, K. Jeyasubramanian, G. Manivannan, Selective toxicity of ZnO nanoparticles toward Gram-positive bacteria and cancer cells by apoptosis through lipid peroxidation, *Nanomed. : Nanotechnol., Biol. Med.* **2011, 7**, 184–192.
10. Thill, O. Zeyons, O. Spalla, F. Chauvat, J. Rose, M. Auffan, A. M. Flank, Cytotoxicity of CeO_2 nanoparticles for *Escherichia coli.* Physico-chemical insight of the cytotoxicity mechanism, *Environ. Sci. Technol.* **2006**, 40, 6151–6156.
11. Y. Xie, H. He, P.L. Irwin, T. Jin Antibacterial activity and mechanism of action of zinc oxide nanoparticles against *Campylobacter jejuni* *Appl. Environ. Microbiol.* **2011,** 77, 2325–2331.
12. W. Jiang, H. Mashayekhi, B. Xing, Bacterial toxicity comparison between nano- and micro-scaled oxide particles, *Environ. Pollution.* **2009**, 157, 1619–1625.
13. M. Li, L. Zhu, D. Lin, Toxicity of ZnO Nanoparticles to *Escherichia coli*: Mechanism and the Influence of Medium Components, *Environ. Sci. Technol.* **2011**, 45, 1977–1983.
14. M. Li, S. Pokhrel, X. Jin, L. Mädler, R. Damoiseaux, R. M. V. Hoek, Stability, Bioavailability, and Bacterial Toxicity of ZnO and Iron-Doped ZnO Nanoparticles in Aquatic Media, *Environ. Sci. Technol.* **2011**, 45, 755–761.

15. A. Johansen, A.L. Pedersen, K.A. Jensen, U. Karlson, B.M. Hansen, J.J. Scoll-Fordsmand, A. Winding , Effects of C60 fullerene nanoparticles on soil bacterium and protozoans , *Environ. Sci. Technol.*, **2008**, 2, 1895–1903.

16. Y. Ge, J. P. Schimel, P. A. Holden, Evidence for Negative Effects of TiO_2 and ZnO Nanoparticles on Soil Bacterial Communities, *Environ. Sci. Technol.* **2011**, 45,1659–1664.

17. C. Cherchi', T. Chernenko, M. Diem, A. Z. Gu, Impact of nano titanium dioxide exposure on cellular structure of *Anabaena variabilis* and evidence of internalization, *Environ.Toxicol.Chem*. **2011**, 30, 861-869.

18. C. Cherchi', A. Z. Gu, Impact of Titanium Dioxide Nanomaterials on Nitrogen Fixation Rate and Intracellular Nitrogen Storage in *Anabaena variabilis*, *Environ. Sci. Technol.* **2010**, 44, 8302–8307.

19. Y. Yang, J. Wang, H. Zhu, V.L. Colvin, P.J. Alvarez. Relative susceptibility and transcriptional response of nitrogen cycling bacteria to quantum dots *Environ. Sci. Technol*. **2012,** 46 (6), 3433–3443.

20. J. E. Gonzalez, G. M.York, G. C.Walker, *Rhizobium meliloti* exopolysaccharides: synthesis and symbiotic function, *Gene* **1996**, 179, 141-146.

21. D. K.Barnes, B. P. Goplen, J. E. Baylor, Highlights in the USA and Canada. In: A. A. Hanson, D. K. Barnes, and R. R. Hill Jr. (eds) Alfalfa and alfalfa improvement. *Am. Soc. Agronom*. Madison, Wisconsin. Monograph, **1988**, 29, 1-24.

22. A. A. Keller, H.Wang, D. Zhou, H. S. Lenihan, G. Cherr, B. J. Cardinale, R.Miller, Z. Ji, Stability and aggregation of metal oxide nanoparticles in natural aqueous media. *Environ. Sci. Technol.* **2010**, 344, 1962-1967.

23. B. Wu, Y. Wang, Y. H. Lee, A. Horst, Z. P. Wang, D. R.Chen, R. Sureshkumar, Y. J. J. Tang, Comparative eco-toxicities of nano-ZnO particles under aquatic and aerosol exposure modes, *Environ. Sci. Technol*. **2010**, 44, 1484-1489.

24. J. P. Ruparelia, A. K. Chatterjee, S. P. Duttagupta, S. Mukherji, Strain specificity in antimicrobial activity of silver and copper nanoparticles, *Acta Biomat*. **2008**, 4, 707– 716.

25. J. M.Andrews, Determination of minimum inhibitory concentrations. *J. Antimicrob. Chemother*. **2011**, 48, 5−16.

26. A. Kumar, R. S.Kumar, N. Sakthivel, Compositional difference of the Exopolysaccharides produced by virulent and virulence-deficient strains *Xanthomonas oryzae pv. oryzae*. *Curr. Microbiol.* **2003**, 46, 251-255.

27. Y. Zhang, Y.Chen, P. Westerhoff, K. Hristovski, J. C.Crittenden, Stability of commercial metal oxide nanoparticles in water, *Water Res.* **2008**, 42, 2204– 2212.

28. R. C. Murdock, L. Braydich-Stolle, A. M.Schrand, J. J.Schlager, S. M. Hussain, Characterization of nanomaterials dispersion in solution prior to *in vitro* exposure using dynamic light scattering technique, *Toxicol. Sci.* **2008**, 101, 239-253.

29. S. Bayoudh, A. Othmane, L. Ponsonnet, H. Ben Ouada, Electrical detection and characterization of bacterial adhesion using electrochemical impedance spectroscopy-based flow chamber, *Colloids Surf., A: Physicochem. Eng. Aspects* **2008**, 318, 291–300.

30. A. Degen, M. Kosec, Effect of pH and impurities on the surface charge of zinc oxide in aqueous solution, *J. Eur. Ceram. Soc*. **2000**, 20, 667–673.

31. Y. Zhao, W. H. Xing, N. P. Xu, F. S.Wong, Effects of inorganic electrolytes on zeta potentials of ceramic microfiltration membranes, *Sep. Purif. Technol*. **2005**, 42, 117–121.

32. N. Jones, B. Ray, K. T. Ranjit, A. C.Manna, Antibacterial activity of ZnO nanoparticles suspensions on a broad spectrum of microorganisms, FEMS Microbial. Lett. **2008**, 279, 71-76.

33. Y. Liu, L.He, A. Mustakha, H. Li, J. Q. Hu, M. Lin, Antibacterial activity of ZnO nanoparticles against Escherichia coli 0157:H7, *J. Appl. Microbiol.* **2009**,107, 1193-1201.

34. L. Zhang, Y. Jiang, Y.Ding, M. Povey, D. J.York, Investigation into the antibacterial behavior of suspensions of ZnO nanoparticles (ZnO nanofluids), *Nanopart. Res*. **2007**, 9, 479–489.

35. D. Greif, D. Wesner, J.Regtmeier, D. Anselmetti, High resolution imaging of surface patterns of single bacterial cells, *Ultramicroscopy* **2010**, 110, 1290-1296.

36. D. Greif, D. Wesner, D. Anselmetti, J.Regtmeier, High-resolution imaging of dried and living single bacterial cells surfaces: artifact or not? *Microsc. Today* **2011**, 19, 22-25.

37. C. S. Schwandt, Characterizing nanometer-scale materials using a low-angle backscattered electron detector, Amer Lab. **2010**, 13-17.

38. M. E. Bayer, M. H.Bayer, Lanthanide accumulation in the periplasmic space of Escherichia coli B, *J. Bacteriol.* **1991**, 173, 141-149.

39. G. Sheng, H. Yu, C. Wang, FTIR-spectral analysis of two photosynthetic H_2- producing strains and their extracellular polymeric substances, *Appl Microbial Biot*. **2006**,73, 204-210.

40. A. Omoike, J. Chorover, Spectroscopic Study of Extracellular Polymeric Substances from *Bacillus subtilis*: Aqueous Chemistry and Adsorption Effects, *Biomacromolecules* **2004**, 5, 1219-1230.

41. C. Jung, Insight into protein structure and protein–ligand recognition by Fourier transforms infrared Spectroscopy, *J. Mol. Recognit*. **2000**, 13, 325-351.

42. A. Joachim, J.A. Hering, P.R. Innocent, P.I. Harris. Automatic amide I frequency selection for rapid quantification of protein secondary structure from Fourier transform infrared spectra of proteins. *Proteomics* **2002**, 2, 839–849.

43. M. van de Weert, P. I.Haris, W. E. Hennink, D. J. A. Crommelin , Fourier transform infrared spectrometric analysis of protein conformation: effect of sampling method and stress factors, *Anal. Biochem*. **2001**, 297, 160-169.

44. S. Krimm, J. Bandekar, Vibrational spectroscopy and conformation of peptides, polypeptides, and proteins, *Adv. Protein Chem*. **1986**, 38, 181-364.

45. W.K. Surewicz, H.H. Mantsch, D. Chapman. Determination of protein secondary structure by Fourier transform infrared spectroscopy: a critical assessment. *Biochemistry*, **1993**, 32, 389–394.

46. J. Grdadolnik, D. Hadzi, Conformational effects of metal salt binding to the polar head of phosphatidylcholines investigated by FTIR spectroscopy, *Chem. Phys. Lipids* **1993**, 65**,** 121-132.

47. G. Long, P. Zhu, Y. Shen, M.Tong, Influence of Extracellular Polymeric Substances (EPS) on Deposition Kinetics of Bacteria, *Environ. Sci. Technol*. **2009**, 43, 2308–2314.

48. K. P. Ishida,P. R. Griffiths, Comparison of the amide I/II intensity ratio of solution and solid-state proteins sampled by transmission, attenuated total refectance, and diffuse reflectance spectroscopy, *Appl. Spectrosc*. **1993**,47, 584-589.

49. T. J. Lenk, B. D. Ratner, R. M. Gendreau, K. K. Chittur, IR spectral changes of bovine serum albumin upon surface adsorption, *J. Biomed. Mater. Res*. **1989**, 23, 549-569.

50. C. E. Giacomelli, G. E. Maria, G.Bremer, W. Norde, ATR-FTIR study of IgG adsorbed on different silica surfaces, *J. Colloid Interface Sci*. **1999**, 220, 13-23.

Chapter 3

1. M. Auffan, J. R., J.-Y. Bottero, G. V. Lowry, J.-P. Jolivet, and M. R. Wiesner, *Nature Nanotechnology* **2009**, 4, 634.
2. S. K. Sahoo, S. Parveen, and J. J. Panda, *Nanomedicine*, **2007**, 3, 20.
3. A. Nel, T. Xia, L. Moedler, and N, Li, *Science*, **2006**, 311, 622.
4. S. Manzo, A. Rocco, R. Carotenuto, F. D. L. Picione, M. L. Miglietta, G. Rametta, and G. D. Francia, *Environ. Sci. Poll. Res*., **2011**, 18, 756.
5. T. Szabo, J. Nemeth, and I. Dekany, *Coll. Surf. A*, **2003**, 230, 23.
6. C. O. Dimkpa, J.E. McLean, D. W. Britt, and A.J. Anderson, *Ind. Biotechnol*, **2012**, 8, 344.
7. S. Bandyopadhyay, J.R. Peralta-Videa, G. Plascencia-Villa, M. José-Yacamán, and J.L. Gardea-Torresdey, *J. Hazard. Mater*, **2012**, 30, 379.
8. Y. Ge, J. P. Schimel, and P. A.Holden, *Environ. Sci. Technol.* **2011**, 45, 1659.
9. J. G. Parsons, M.L. Lopez, C. M.Gonzalez, J. R. Peralta-Videa, and J. L.Gardea-Torresdey, *Environ Toxicol Chem.* **2010**, 29,1146.
10. R. Nair, S. H.Varghese, N. G.Nair, T. Maekawa, Y.Yoshida, and D. S.Kumar, *Plant Sci.* **2010**, 179,154.
11. L. Zhao, J. A. Hernandez-Viezcas, J.R. Peralta-Videa, S. Bandyopadhyay, B. Peng, B. Munoz, A. A. Keller, and J.L. Gardea-Torresdey, *Environ. Sci.: Processes & Impacts*, **2013**, 15, 260.

12. M. I. Morales, C. M. Rico, J. A. Hernandez-Viezcas, J. E. Nunez, A. C. Barrios, A. Tafoya, J. P. Flores-Marges, J. R. Peralta-Videa, J. L. Gardea-Torresdey, *J Agric Food Chem.* **2013**, 61(26), 6224.

13. A. Mukherjee, J. R. Peralta-Videa, S. Bandyopadhyay, C. M. Rico, L. Zhao and J.L. Gardea-Torresdey, *Metallomics*, **2014**, DOI: 10.1039/C3MT00064H, available at: http://pubs.rsc.org/en/content/articlehtml/2014/mt/c3mt00064h.

14. D. Lin, D. and B. Xing, *Environ. Pollut.*, **2007**, 150, 243.

15. D. Lin, D. and B. Xing, *Environ. Sci. Technol.*, **2008**, 42, 5580.

16. D. Stampoulis, S. K. Sinha, J. C. White, *Environ Sci Technol.* **2009**, 43, 9473.

17. S. Asli, and P. M. Neumann, *Plant Cell Environ.* **2009**, 32, 577.

18. R. C. Monica and R. Cremonini, *Caryologia* , **2009**, 62 (2), 161.

19. S. Kim, J. Kim, I. Lee, *Chem. Ecol.*, **2011**, 27, 49.

20. de la Rosa, G., López-Moreno, M.L., Hernández-Viescaz, J., Peralta-Videa, and J. R., Gardea-Torresdey, J. L. *Int. J. Nanotechnol*., **2011**, 8, 492.

21. J. H. Priester, Y.Ge, R.E. Mielke, A. M. Horst, S. Cole Moritz, K. Espinosa, J. Gelb, S.L. Walker, R.M. Nisbet, J. P. Schimel, R.G. Palmer, J.A. Hernandez-Viezcas, L. Zhao, J. L. Gardea-Torresdey and P. A. Holden, *Proc. Natl. Aca. Sci. USA. PNAS*, 2012, 109 (37), 2451.

22. J. E. Gonzalez, G. M. York, and G. C. Walker, *Gene* **1996**, 179, 14.

23. D.K. Barnes, B. P. Goplen, J.E. Baylor, *Am. Soc. Agronom*. Madison, Wisconsin. Monograph, **1988**, 29, 1-24.

24. M. Sperazza, J. N. Moore, and M. S. Hendrix, *J. Sediment. Res*., **2004**, 74(5) 736.

25. D. H. Lee, and C.B. Lee, *Plant Sci.*, **2000**, 159, 75.

26. M. M. Bradford, *Anal. Biochem.*, **1976**, 72, 248.

27. H. Aebi, **1974**, Catalases, in: H.U. Bergmeyer (Ed.), *Methods of enzymatic analysis, vol. 2*, Academic Press, NY, 673.

28. P. Born, F. C. Klaessig, T. D. Landry, B. Moudgil, J. Pauluhn, K. Thomas, R. Trottier, and S. Wood. Research strategies for safety evaluation of nanomaterials, part V: role of dissolution in biological fate and effects of nanoscale particles. *Toxicol Sci*, **2006**, 90(1), 23.

29. Z. Young and C. Xie, *Colloids Surf., B,* **2006**, 47, 140.

30. N. M. Franklin, N. J. Rogers, S. C. Apte, G. E. Batley, G. E. Gadd, and P. S. Casey, *Environ. Sci. Technol.*, **2007**, 41 (24), 8484.

31. P. Patra, S. Roy Choudhury, S. Mandal, A. Basu, A. Goswami, R. Gogoi, C. Srivastava, R. Kumar and M. Gopal, *Adv.Nanomat. and Nanotechnol*. in Springer Proceedings in Physics **2013**, 143, 301-309.

32. G. R. Rout, and P. Das, *Agronomie*. **2003**, 23, 3.

33. X. Jiang, and C. Wang, C., J. Plant Physiol. **2008**,165, 697.

34. A. Straczek, G. Sarret, A. Manceau, P. Hinsinger, N. Geoffroy, and B. Jaillard, *Environ. Exp. Bot.* **2008**, 63, 80.

35. F. Skoog, *Am. J. Bot*., **1940**, 27, 939.

36. F. H. Gutierrez-Boem, and G. W.Thomas, *J Plant Nutr.*, **2001**, 24,1711.

37. E. Weryszko-Chmielewska, and M. Chwil, *Soil Sci Plant Nutr.*, 51,203.

38. H. M. H. Salama, *Int. Res. J. Biotechnol*. **2012**, 3, 10, 190.

39. S. K. R. Namasivayam and K. Chitrakala, *J. Biopest*., 2011, 4 (1), 97.

40. M.A. Jorgensen, J.M. Akayezu, J.G. Linn and H.G. Jung, US Dairy Forage Research Center, Research Report, 1997), 81(Unpublished data).

41. Panda, S. K.; Choudhury, S. Chromium stress in plants *J. Plant Physiol.* **2005**, 17, 95–102.

42. J. A. Hernandez-Viezcas, H. Castillo-Michel, A.D. Servin, J.R.Peralta-Videa, J. L. Gardea-Torresdey, *Chem. Eng J.* **2011**, 170(1-3), 346.

Chapter 4

1. Stochmal, A.; Piacente, S.; Pizza, C.; De Riccardis, F.; Leitz, R.; Oleszek, W. Alfalfa (*Medicago sativa* L.) flavonoids. 1. apigenin and luteolin glycosides from aerial parts. *J. Agric. Food Chem.* **2001**, *49*, 753-758.
2. Hernandez, T.; Hernandez, A.; Martinez, C. Polyphenols in alfalfa leaf concentrates. *J. Agric. Food Chem.* **1991**, *39*, 1120-1122.
3. Bisby, F. A., Buckingham, T., Harborne, T. B., Eds. *Phytochemical Dictionary of the Leguminosae*, Vols. 1 and 2; Chapman and Hall: London, 1994.
4. Livingston, A. L.; Kohler, G. D.; Kuzmicky, D. D. Comparison of carotenoid storage stability in alfalfa leaf protein (Pro-Xan) and dehydrated meals. *J. Agric. Food Chem.* **1980**, *28*, 652-656.
5. Jones K. M.; Kobayashi, H.; Davies, B. W.; Taga, M. E.; Walker, G. C. How rhizobial symbionts invade plants: the *Sinorhizobium–Medicago* model. *Nat. Rev. Microbiol.* **2007**, *5*, 619–633.
6. Dharmatilake, A. J.; Bauer, W. D. Chemotaxis of *Rhizobium meliloti* towards nodulation gene-inducing compounds from alfalfa roots. *Appl. Environ. Microb.* **1992**, *58*, 41153-41158.
7. Hirsch, A. M. Developmental biology of legume nodulation. *New Phytol.* **1992**, *122*, 211–237.
8. Zhang, P.; Ma, Y.; Zhang, Z.; He, X.; Zhang, J.; Guo, Z.; Tai, R.; Zhao, Y.; Chai, Z. Biotransformation of ceria nanoparticles in cucumber plants. *Environ. Sci. Technol.* **2012**, *6*, 9943-9950.

9. Priester, J. H.; Ge, Y.; Mielke, R. E.. Horst, A. M.; Cole Moritz, S.; Espinosa, K.; Gelb, J.; Walker, S. L.; Nisbet, R. M.; An, Y.J.; Schimel, J. P.; Palmer, R. G.; Hernandez-Viezcas, J. A.; Zhao, L.; Gardea-Torresdey, J. L.; Holden P. A. Soybean susceptibility to manufactured nanomaterials: evidence for food quality and soil fertility interruption. *P. Natl. Acad. Sci. USA* **2012**, *109*, E2451–E2456.
10. Hernandez-Viezcas, J. A.; Castillo-Michel, H.; Andrews, J. C.; Cotte, M.; Rico, C.; Peralta-Videa, J. R.; Ge, Y.; Priester, J. H.; Holden, P. A.; Gardea-Torresdey, J. L. In situ synchrotron x-ray fluorescence mapping and speciation of CeO_2 and ZnO nanoparticles in soil cultivated soybean (*Glycine max*). *ACS Nano* **2013**, *7*, 1415-1423.
11. Zhao, L.; Peng, B.; Hernandez-Viezcas, J. A.; Rico, C.; Sun, Y.; Peralta-Videa, J. R.; Tang, X.; Niu, G.; Jin, L.; Varela-Ramirez, A.; Zhang, J.; Gardea-Torresdey, J. L. Stress response and tolerance of *Zea mays* to CeO_2 nanoparticles : cross talk among H_2O_2, heat shock protein, and lipid peroxidation. *ACS Nano* **2012**, *6*, 9615-9622
12. Mukherjee, A.; Peralta-Videa, J. R.; Bandyopadhyay, S.; Rico, C. M.; Zhao, L.; Gardea-Torresdey, J. L. *Metallomics*, **2013**, DOI:10.1039/C3MT00064H.
13. Morales, M. I.; Rico, C. M.; Hernandez-Viezcas, J. A.; Nunez, J. E.; Barrios, A. C.; Tafoya, A.; Flores-Marges, J. P.; Peralta-Videa, J. R.; Gardea-Torresdey, J. L. Toxicity assessment of cerium oxide nanoparticles in cilantro (*Coriandrum sativum* L.) plants grown in organic soil. *J. Agric. Food Chem.* **2013,** *61*, 6224-6230.
14. Dimkpa, C. O.; McLean, J. E.; Britt, D. W., Anderson, A. J. Bioactivity and biomodification of Ag, ZnO, and CuO nanoparticles with relevance to plant performance in agriculture. *Ind. Biotechnol.* **2012**, *8*, 344-357.

15. Wang, Q.; Ma, X.; Zhang, W.; Pei, H.; Chen, Y. The impact of cerium oxide nanoparticles on tomato (*Solanum lycopersicum* L.) and its implications for food safety. *Metallomics* **2012**, *4*, 1105-1112.

16. Liu, D.; Wang, X.; Lin, Y.; Chen, Z.; Xu, H.; Wang, L. The effects of cerium on the growth and some antioxidant metabolisms in rice seedlings. *Environ. Sci. Pollut. Res.* **2012**, *19*, 3282-3291.

17. Monica, R. C.; Cremonini, R. Nanoparticles and higher plants. *Caryologia* , **2009**, *62*, 161-165.

18. Michalak, A. Phenolic compounds and their antioxidant activity in plants growing under heavy metal stress. *Pol. J. Environ. Stud.* **2006**, *15*, 523-530.

19. Krishnaraj, C.; Jagan, E. G.; Ramachandran, R.; Abirami, S. M.; Mohan, N.; Kalaichelvan, P. T. Effect of biologically synthesized silver nanoparticles on *Bacopa monnieri* (Linn.) Wettst. plant metabolism. *Process Biochem.* **2012**, *47*, 651-658.

20. Rico, C. M.; Morales, M. I.; Barrios, A. C.; McCreary, R.; Hong, J.; Lee, W. Y.; Nunez, J.; Peralta-Videa, J. R.; Gardea-Torresdey, J. L. Effect of cerium oxide nanoparticles on the quality of rice (*Oryza sativa* L.) grains. *J. Agric. Food Chem.* **2013**, DOI: 10.1021/jf404046v

21. Bandyopadhyay, S.; Peralta-Videa, J. R.; Plascencia-Villa, G.; José-Yacamán, M.; Gardea-Torresdey, J. L. Comparative toxicity assessment of CeO_2 and ZnO nanoparticles towards *Sinorghizobium meliloti*, a symbiotic alfalfa associated bacterium: use of advanced microscopic and spectroscopic techniques. *J. Hazard. Mater.* **2012**, *30*, 379-386.

22. Keller, A. A.; Wang, H.; Zhou, D.; Lenihan, H. S.; Cherr, G.; Cardinale, B. J.; Miller, R.; Ji, Z. Stability and aggregation of metal oxide nanoparticles in natural aqueous media. *Environ. Sci. Technol.* **2010**, *344*, 1962−1967.

23. Sperazza, M.; Moore, J. N.; Hendrix, M. S. High resolution particle size analysis of naturally occurring very fine-grained sediment through laser diffractometry. *J. Sediment. Res*. **2004**, *74*, 736-743.

24. Lichtenthaler, H. K.; Wellburn, A. R. Determinations of total carotenoids and chlorophylls *a* and *b* of leaf extracts in different solvents. *Biochem. Soc. T.* **1983**, *11*, 591-592.

25. Porra, R. J. The chequered history of the development and use of simultaneous equations for the accurate determination of chlorophylls *a* and *b*. *Photosynth. Res.* **2002**, *73*, 149-156.

26. Adom, K. K.; Liu, R. H. Antioxidant activity of grains. *J. Agric. Food Chem.* **2002**, *50*, 6182-6187.

27. Dewanto, V.; Wu, X.; Adom, K. K.; Liu, R. H. Thermal processing enhances the nutritional value of tomatoes by increasing total antioxidant activity. *J. Agric. Food Chem.* **2002**, *50*, 3010-3014.

28. Jia, Z.; Tang, M.; Wu, J. The determination of flavonoid contents in mulberry and their scavenging effects on superoxide radicals. *Food Chem.* **1999**, *64*, 555-559.

29. Hartel, H.; Grimm, B. Consequences of chlorophyll deficiency for leaf carotenoid composition in tobacco synthesizing glutamate 1-semialdehyde aminotransferase antisense RNA: dependency on developmental age and growth light. *J. Exp. Bot.* **1998**, *49*, 535–546.

30. Küpper, H.; Küpper, F.; Spiller, M. Environmental relevance of heavy metal substituted chlorophylls using the example of water plants. *J. Exp. Bot.* **1996**, *47*, 259-266

31. Prasad, M. N. V.; et al. Impact of Heavy Metals on Photosynthesis. In *Heavy Metal Stress in Plants*; Prasad, M. N. V., Hagemeyer, J., Eds.; Springer: Berlin 1999; pp. 117-138.

32. Van Assche, F.; Clijsters, H. Effects of metals on enzyme activity in plants. *Plant Cell Environ.* **1990**, *13*,195–206.

33. De Filippis, L.F.; et al. Heavy metals: Sources and biological effects. In *Algae and Water Pollution*; Rai, L. C., Gaur, J. P., Soeder, C. J., Eds.; E. Schweizerbartsche, Verlagsbuchhandlung: Stuttgart 1994; pp 31-77.

34. Krystofova, O.; Sochor, J.; Zitka, O.; Babula, P.; Kudrle, V.; Adam, V.; Kizek, R. Effect of magnetic nanoparticles on tobacco BY-2 cell suspension culture. *Int. J. Environ. Res. Public Health* **2013**, *10*, 47-71.

35. Parry, A. D.; Tiller, S. A.; Edwards, R. The effects of heavy metals and root immersion on isoflavonoid metabolism in alfalfa (*Medicago sativa* L.). *Plant Physiol.* **1994**, *106*, 195-202.

36. Agati, G.; Azzarello, E.; Pollastri, S.; Tattini, M. Flavonoids as antioxidants in plants: location and functional significance. *Plant Sci.* **2012**, *196*, 67–76.

Appendix I

Characterization of NPs

Transmission electron microscopy (TEM) characterization.

For the TEM characterization, the NPs were suspended in absolute ethanol at a concentration of 250 mg/L and sonicated for 15 min. Subsequently, aliquots of 10 µl from each sample were loaded on 300 mesh carbon/formvar copper grids (ElectronMicroscopySciences) and dried before electron microscopy imaging. The TEM analysis of both NPs was performed with a high resolution TEM (HRTEM), JEOL 2010F at 200 kV. TEM micrographs of CeO_2 and ZnO NPs were analyzed with digitalMicrosgraph (Gatan) and MacBiophotonics Image *J*.

X-ray diffraction analysis (XRD).

Powder XRD analysis was performed in order to determine the purity and crystalinity of the NPs. The XRD patterns were obtained using a Siemens D5000 X-ray diffractometer (Bruker AXS GmbH, Germany) equipped with a Braun position sensitive detector. Before loading, the dry samples were weighted and placed on the flat sample holder. Patterns were collected over the angular range between 5° to 80° at 0.02° per step.

Imaging of bacteria-NP interaction

Field emission- scanning electron microscopy (FE-SEM) imaging and energy dispersive x-ray (EDX) analysis.

For the SEM study, *S. meliloti* cells were harvested after treatment with the NPs by centrifugation at 5000 rpm for 5 min; exhausted media was rinsed and cell pellet resuspended in fixative buffer (phosphate buffered 4% formaldehyde, 1% glutaraldehyde, pH 7.2) and incubated at room temperature for 2 h. Fixed cells were pelleted, re-suspended in sterile double distilled water (ddH_2O) and loaded on 300 mesh carbon/formvar copper grids

(ElectronMicroscopySciences). Finally, samples were stored in a desiccation chamber under vacuum before FE-SEM imaging and EDX microanalysis.

The SEM analysis was carried out with a HITACHI S-5500 In-Lens FE-SEM coupled with LABE (Low Angle Backscattered Electron), YAG-BSE (Yttrium-Aluminum-Garnet Backscattered Electron), BF/DF-STEM detectors and EDX spectrometer (Bruker), operated with an accelerating voltage of 5-30 kV. SEM imaging of complete cells was obtained by collecting high quality micrographs optimizing illumination, contrast, magnification, and working distance for further analysis.

Results and Discussion

Characterization of CeO_2 and ZnO NPs.

To test the purity of both CeO_2 and ZnO NPs, the powder XRD patterns were analyzed. **Figure S1A** represents the XRD pattern of CeO_2 NPs. Peaks located near 28.8^o, 33^o, 47.5 ^{o} and 56.5 ^{o} 59.1 ^{o}, 69.5 ^{o}, 76.7 ^{o}, 79.1 ^{o}, and 88.5 ^{o} correspond to the (111), (200), (220), (311), (222), (400), (331), (420), and (422) planes of CeO_2. There is also a resemblance with *a=5.412* which confirm the space group *Fm3jm* of CeO_2 unit cell [1]. There were no unindexed reflections in the XRD results, which also show the purity of CeO_2 NPs. For the ZnO NPs, the peaks at 36 ^{o}, 47.5 ^{o}, 56.5 ^{o} and 63^o correspond to 101, 102, 110 and 103 planes respectively [2]. The XRD pattern shows solid lines which corroborate with tetragonal ZnO phase with parameter *a*=3.249 Å, *c* = 4.206 Å and spacegroup (*P*63*mc*). However, ZnO NPs show some impurity with two unindexed Bragg peaks near 31.5 ^{o} and 34.5 ^{o} (Figure S1B).

Dissolution of CeO_2 and ZnO NPs in YMB and water.

The dynamic dissolution of both the NPs shows that ZnO released higher numbers of ionic zinc than that of CeO_2. The released Zn^{2+} ions ranged from 8-9.9 mg/L whereas the dissolution of

nano-ceria was almost negligible (Figure S3AB). Furthermore, we studied the dissolution of ZnO in both YMB and ultrapure water for 24 h and there were huge significant difference observed. The dissolution in YMB was significantly higher (59-61 mg/L) compared to ultrapure water (2 mg/L). Higher numbers of Zn^{2+} ions in the media might be one contributing factor for greater toxicity, among others.

Table S1. Physicochemical characteristics of CeO_2 NPs in dry, aqueous, and cell culture medium (YMB).

Particle	Primary particle size	pH		Size (nm)		Zeta Potential (mV)	
CeO_2	10 nm	DI H_2O	YMB	DI H_2O	YMB	DI H_2O	YMB
31 mg/L	-	6.32	6.70	1698	1758	31.7	-19.6
62.5 mg/L	-	6.19	6.71	1654	2174	25.5	-18.0
125 mg/L	-	5.48	6.78	1307	2773	25.3	-17.1
250 mg/L	-	5.35	6.70	966	2252	43.5	-17.6

Table S2: Physicochemical characteristics of ZnO NPs in dry, aqueous, and cell culture medium (YMB).

Particle	Primary particle size	pH		Size (nm)		Zeta Potential (mV)	
ZnO	10 nm	DI H_2O	YMB	DI H_2O	YMB	DI H_2O	YMB
10 mg/L	-	7.21	6.76	410	893	34.3	-25.1
31 mg/L	-	7.47	6.81	441	682	30.1	-25.9
62.5 mg/L	-	7.51	6.76	596	618	12.5	-26.2
125 mg/L	-	7.89	6.80	452	1302	14.1	-19.5

Table S3: Diameter of Inhibition Zones (DIZ in mm) for CeO_2 and ZnO NP treatments (After 24 incubation)

Concentrations	DIZ (mm)for ZnO NPs treatment	DIZ (mm) for CeO_2 NPs treatment
10 mg/L	10.4±.5	No inhibition
31 mg/L	15.5±.5	No inhibition
62.5 mg/L	No colony formation	9.75±.5
125 mg/L	No colony formation	12.25±.5
250 mg/L	No colony formation	No colony formation

A

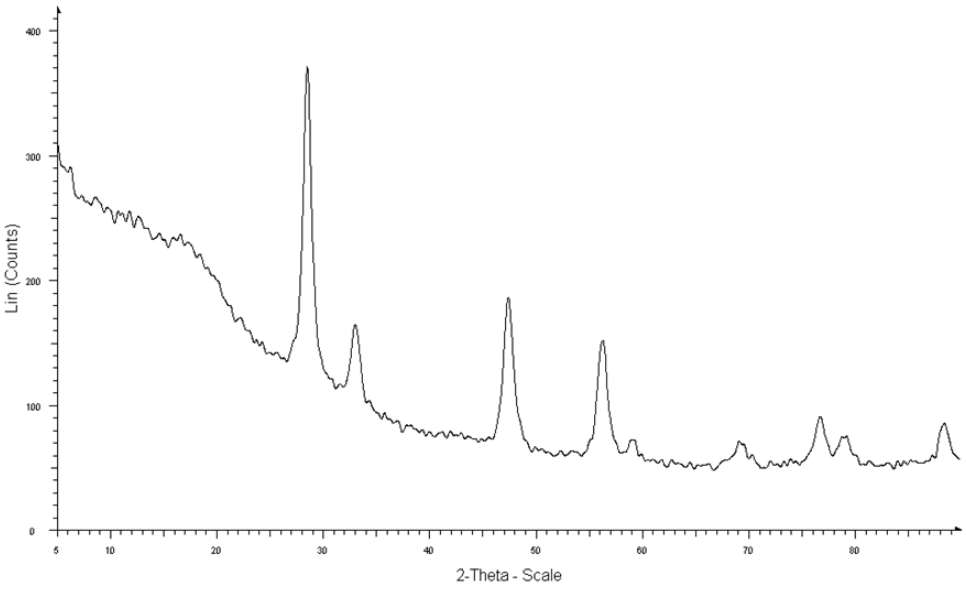

B

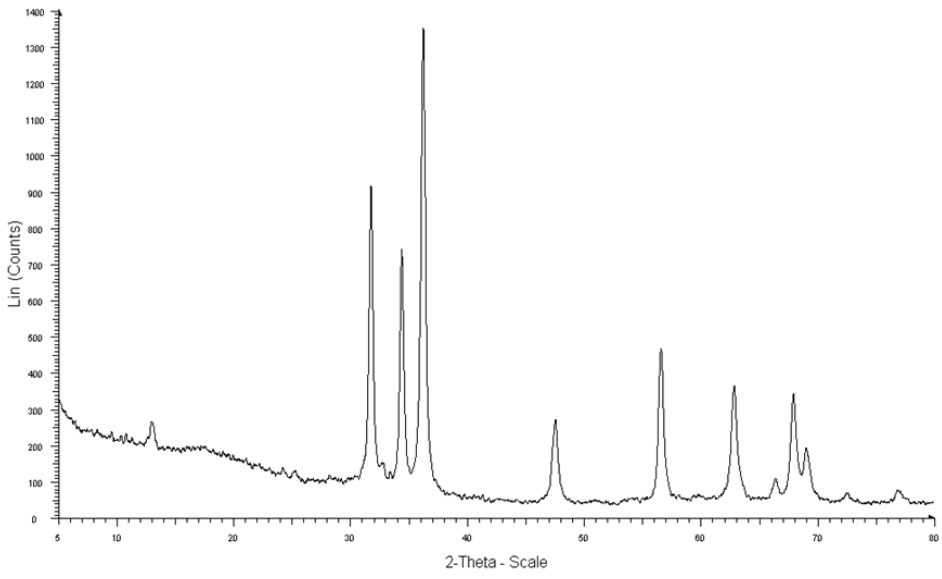

Figure S1. Powder X-Ray Difration (pXRD) pattern of (A) CeO_2 NPs and (B) ZnO NPs collected over the angular range between 5° to 80° at 0.02° per step.

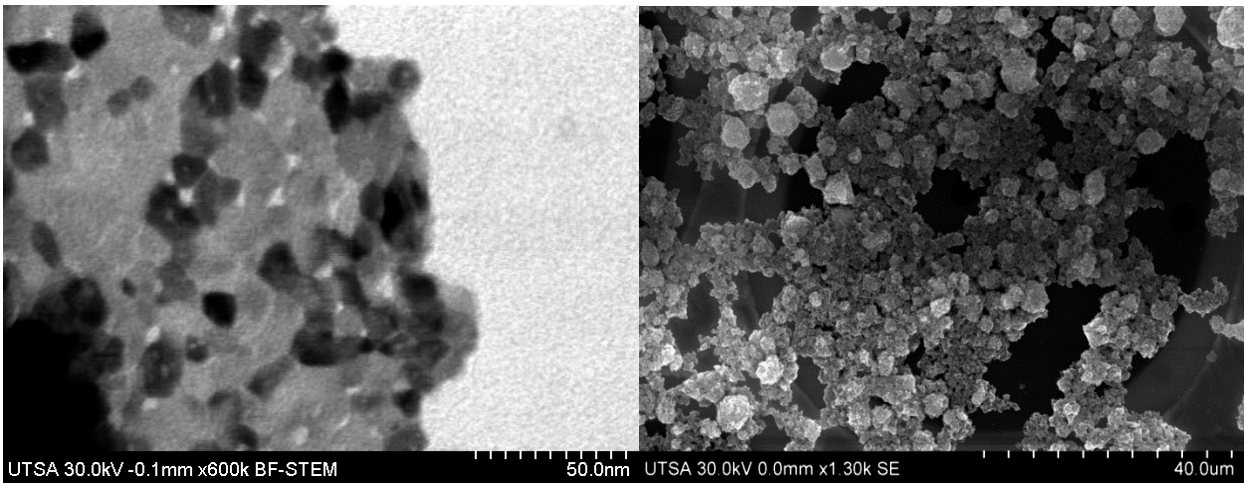

Figure S2. TEM micrographs of nanoparticles dispersed in ethanol. (Left) Aggregated CeO_2 NPs, (right) aggregated ZnO NPs

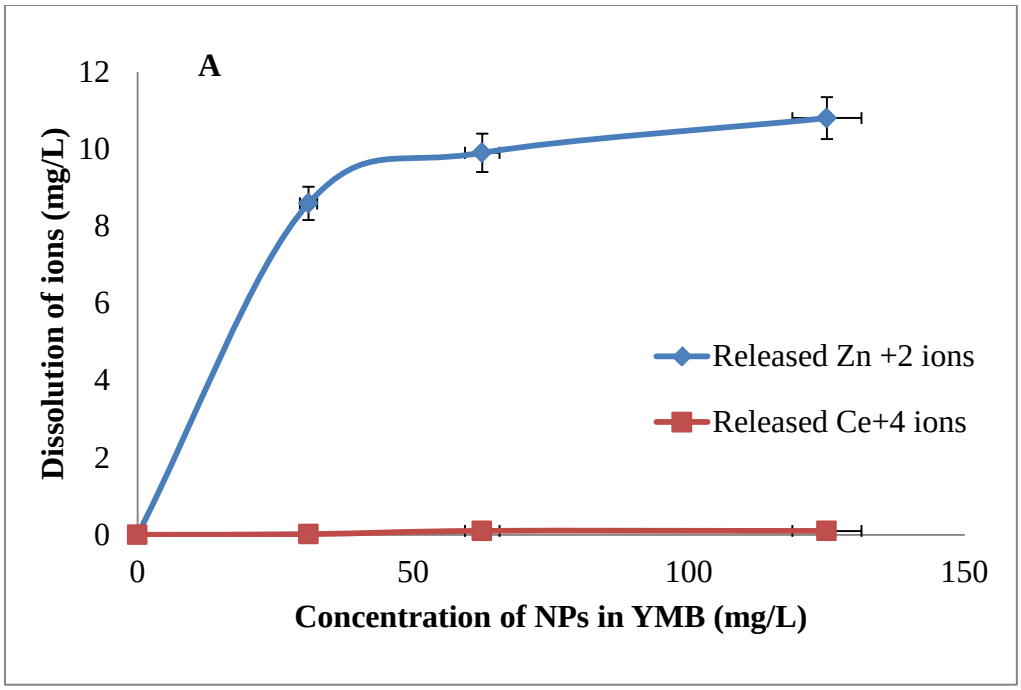

A

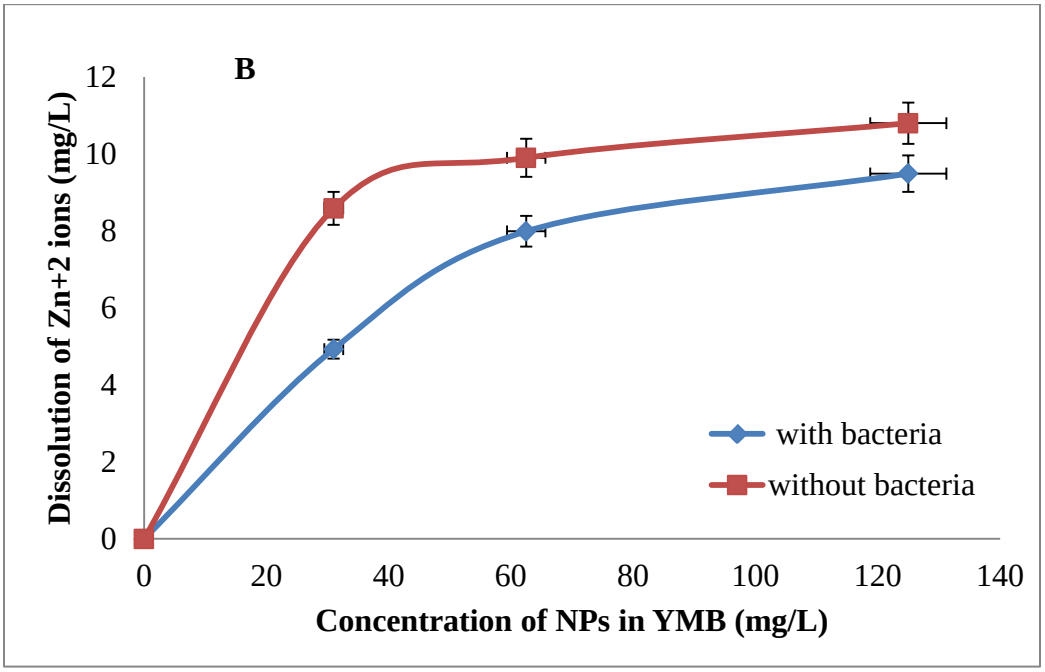

Figure S3. (A) Dissolution kinetics of CeO_2 and ZnO NPs in YMB in three different concentrations. (B) Dissolution of ZnO NPs in YMB in presence and absence of bacteria.

Appendix 2

Comparative phytotoxicity of ZnO NPs, bulk ZnO and ionic zinc onto the alfalfa-*S. meliloti* association in soil.

Supporting Information

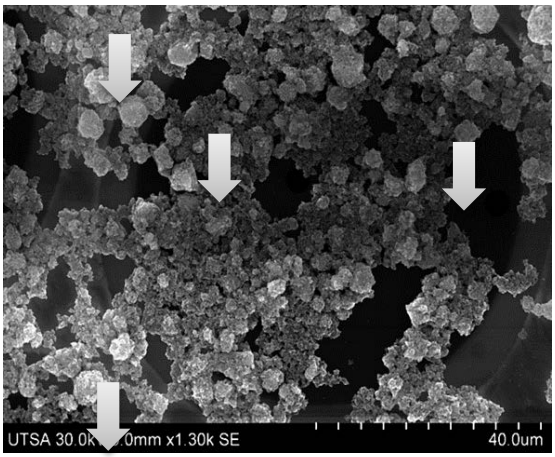

Fig.S1. TEM of ZnO NPs dispersed in ethanol.

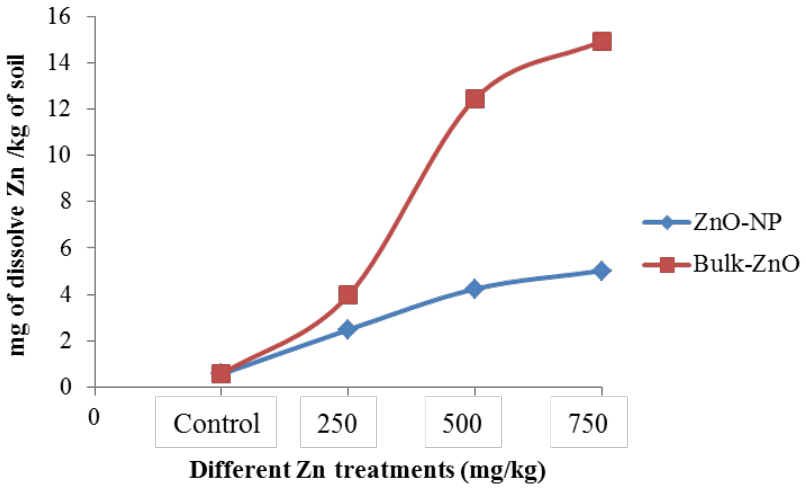

Fig. S2. Dissolution of Zn in soil treated with 0. 250, 500 and 750 mg/kg of ZnO NPs and bulk ZnO after 30days of treatments.

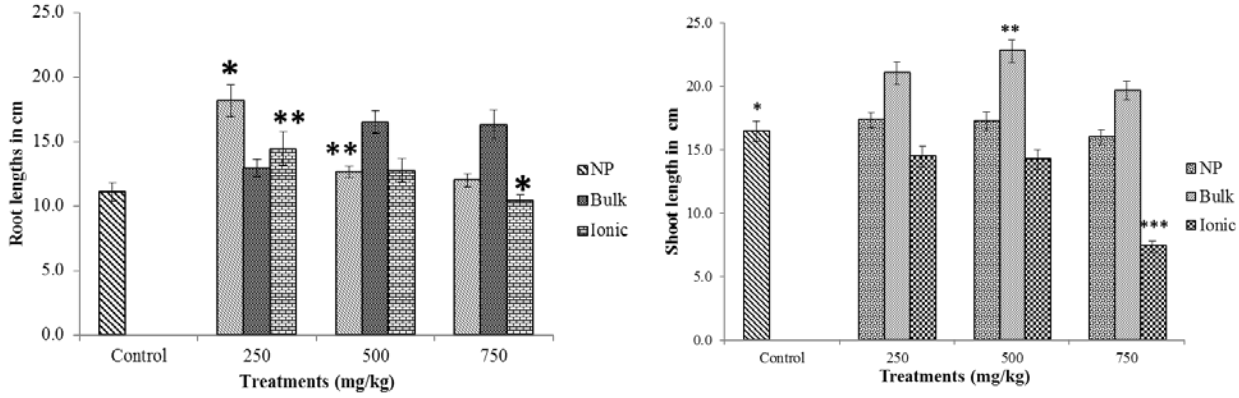

Fig. S3. Changes in root and shoot lengths of alfalfa treated with with 0 (control), 250, 500, and 750 mg/kg of A. ZnO NPs, B. Bulk ZnO, and C. $ZnCl_2$. Error bars stand for stadard deviations. Bars with the same letters show no statistically significant difference at $p \leq 0.05$.

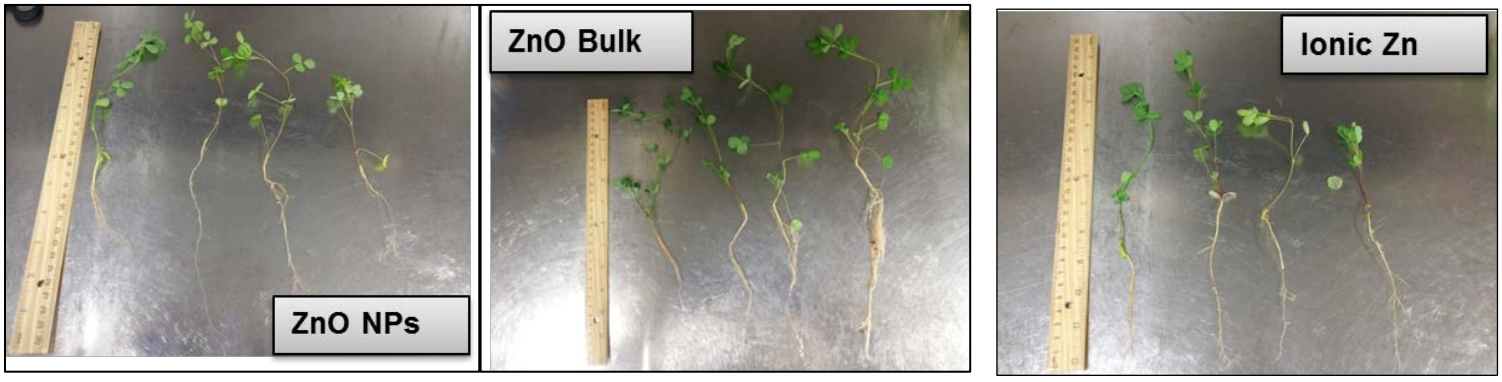

Fig. S3. Changes in root and shoot length of alfalfa plants treated with A. ZnO NPs, B. ZnO bulk, and $ZnCl_2$

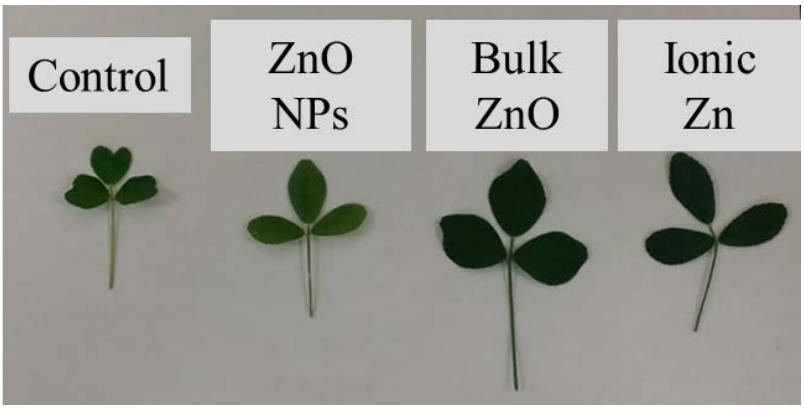

Fig. S4. Changes (visual image) in total leaf surface area of alfalfa leaves treated with 500 mg/kg of ZnO NPs, bulk ZnO bulk, and $ZnCl_2$

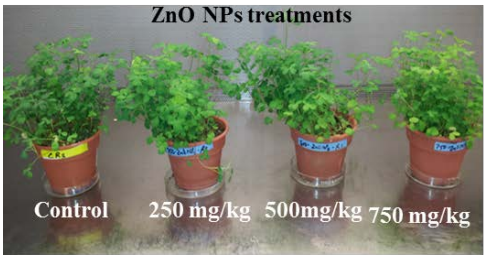

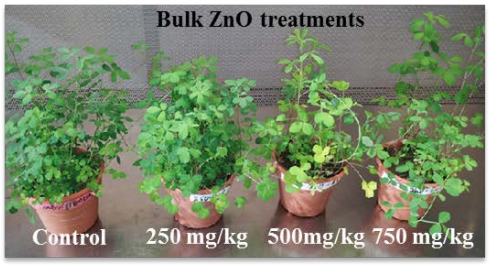

Fig. S5. Pots showing the difference in alfalfa's overall plant growth and health after 30 days of treatment with A. ZnO NPs, B. ZnO bulk, and C. Ionic Zinc ($ZnCl_2$) at 0(control), 250, 500, and 750 mg/kg of ZnO NPs.

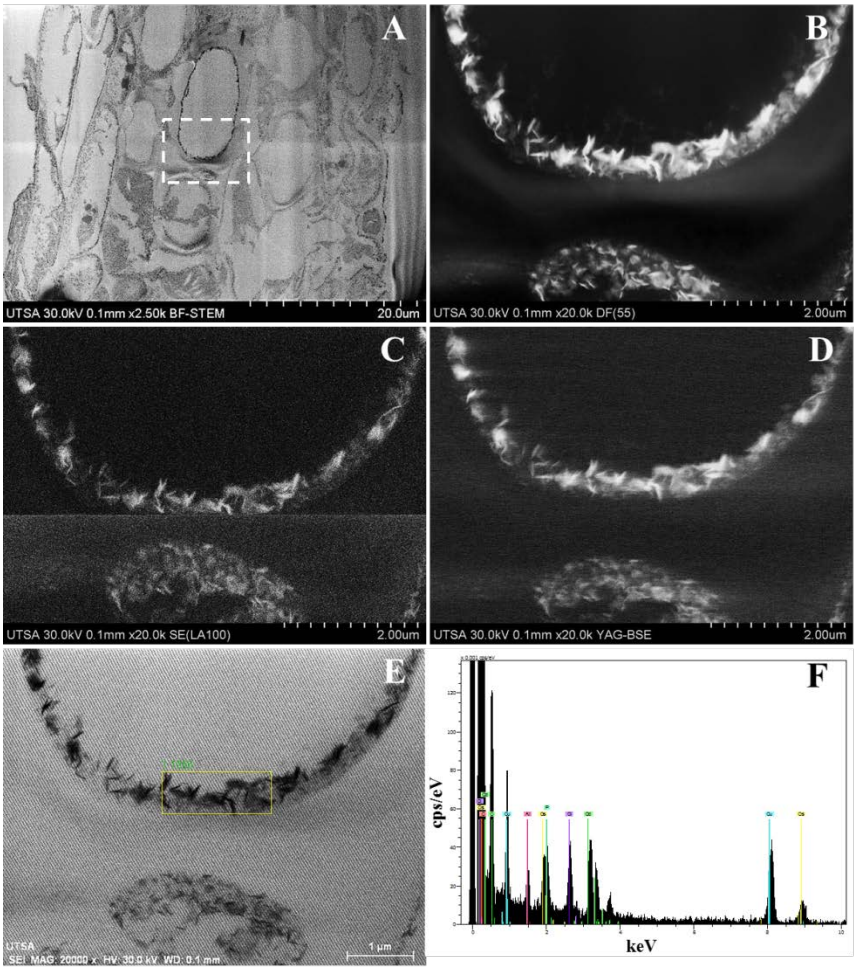

Fig. S6. STEM imaging of alfalfa leaf treated with 500 mg/kg ZnO NPs. (A) BF-STEM, (B) DF-STEM, (C) LABE, (D) YAG-BSE, (E) EDX spectroscopy, (D) EDX spectra.

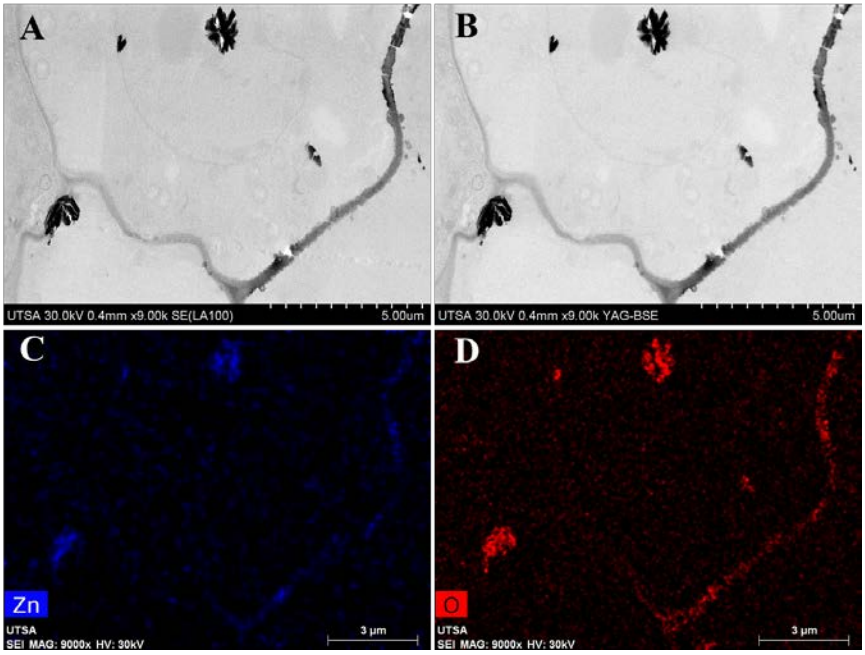

Fig.S7. Electron microscope imaging of alfalfa nodules treated with 500 mg/kg ZnO NPs. (A) LABE, (B) YAG-BSE, (C) EDX mapping of Zn, (D) EDX mapping of O.

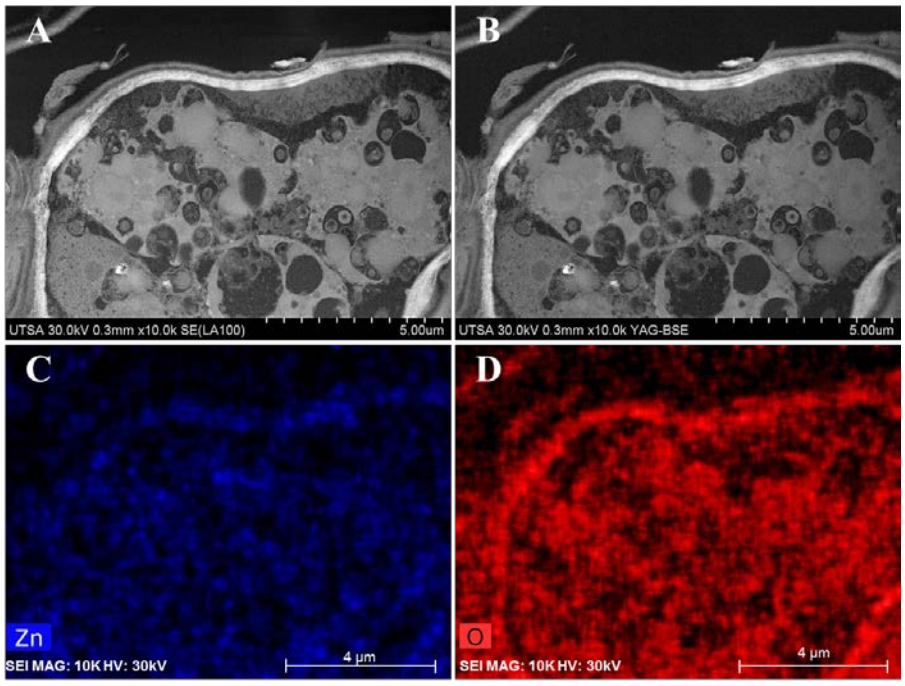

Fig.S8. Electron microscope imaging of alfalfa roots treated with 500 mg/kg ZnO NPs. (A) LABE, (B) YAG-BSE, (C) EDX mapping of Zn, (D) EDX mapping of O.

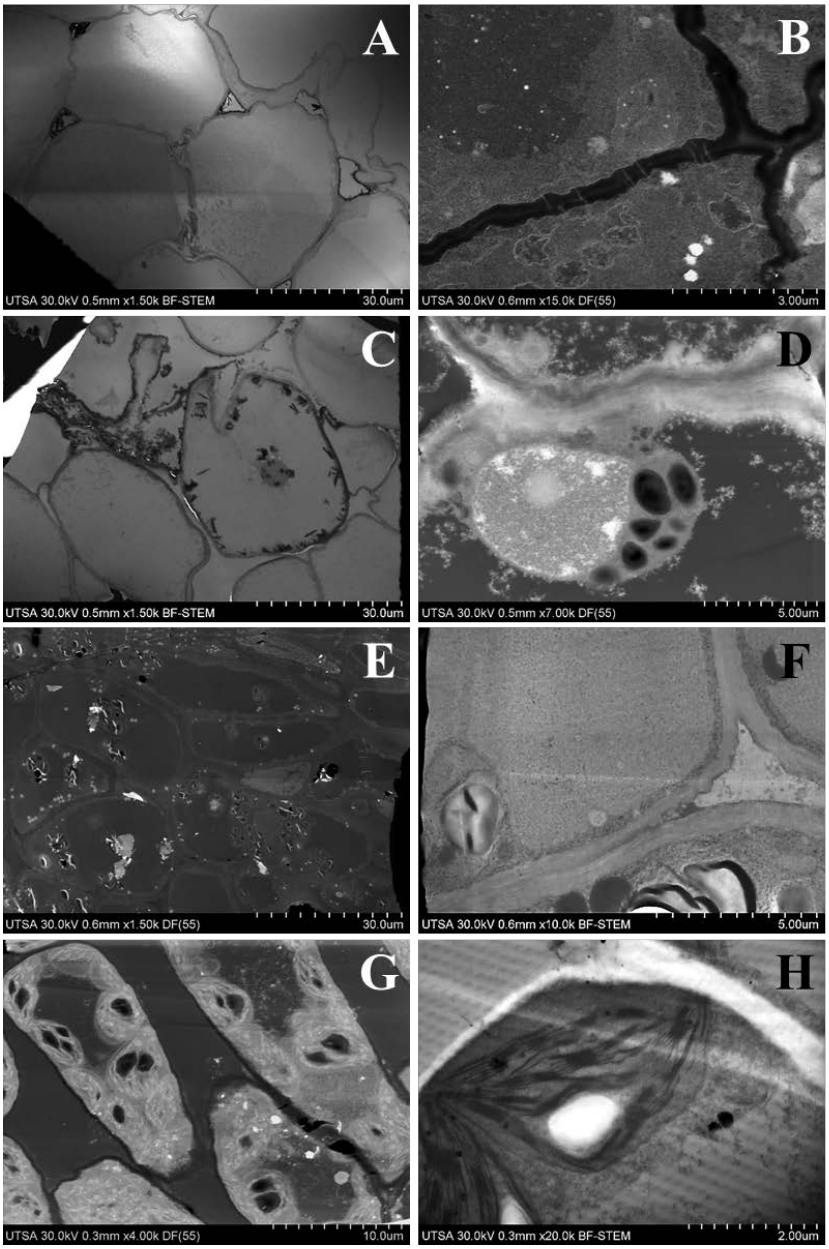

Fig. S9. Control alfalfa tissues. (A-B) Nodule, (C-D) Root, (E-F) Stem, (G-H) Leaf.

Vita

Susmita Bandyopadhyay was born and raised in a small town in India (Ukhradihi, Dist: Bankura; State West Bengal). She was only daughter of Mr. Ramlochan Bandyopadhyay and Ruplekha Bandyopadhyay. Ms. Bandyopadhyay received her Bachelor of Science in Chemistry (with Physics and Mathematics) from the University of Burdwan, India in 2002. She received her Master of Science in Environmental Science in 2005 from Visva Bharati, India and she was awarded the university merit scholarship and gold medal for being the **first class first (top)** in MS level. In 2011, she joined the doctoral program in Environmental Science and Engineering at The University of Texas at El Paso under the supervision of Dr. Jorge Gardea Torresdey.

Ms. Bandyopadhyay has been the recipient of numerous honors and awards including UTEP Graduate School '**Dodson Research Grant**' and **'Franck B Cotton Trust'** Scholarship. She was also a recipient of **Dodson Travel** awards from the College of Science, UTEP. Her scholastic achievements placed her among top five graduate students of the '**Dean's List**' by College of Engineering. She was awarded Frank and Polly Ann Morrow **Outstanding International Student Award** at UTEP (AY 2012-2013). She also served as a member of '**Faculty Senate Committee'** and **Women Advisory Council to the President** at UTEP as a graduate student representative.

While pursuing her PhD, Ms. Bandyopadhyay worked as a research associate and teaching assistant for the chemistry department. She interned at Freeport McMoran Copper and Gold Inc. as a quality chemist in 2013 summer. Recently, she has been offered a full time position of environmental manager in a consulting firm. Ms. Bandyopadhyay has presented her research at national conference meetings including the American Chemical Society's National Meeting. Additionally, Ms. Bandyopadhyay has published her research in many high impact peer

reviewed journals. She has published three articles as principle author and three others as co-authors (**six manuscripts**). In addition she has two other manuscripts in the process of reviewing and two in preparation. Ms. Bandyopadhyay's dissertation, "*Interaction of CeO_2 and ZnO NPs towards the symbiotic association of Alfalfa and Sinorhizobium meliloti in soil"*, was supervised by Dr. Jorge Gardea-Torresdey.

Achievements and Awards:

- Frank and Polly Ann Morrow **Outstanding International Student Award** at the University of Texas at El Paso (AY 2012-2013).
- Recognized as one of the **TOP FIVE graduate students** (2012) at the University of Texas at El Paso (College of Engineering Dean's List).
- Recipient of Graduate School **Dodson Research Grant** (**Top ten outstanding proposals**) for the year 2012-2013 at the University of Texas at El Paso.
- Received **Franck B Cotton Trust** Scholarship at the University of Texas at El Paso for the year 2012-2013.
- Recipient of **Dodson Travel Grant** from the College of Science, the University of Texas at El Paso.
- Selected student member of '**Faculty Senate Committee**' (Graduate Research division) at the University of Texas at El Paso (**Student Government Association**).
- Selected student member of the **Women Advisory Council to the President** at UTEP
- Research was highlighted on UCLA website for the month of July, 2013 (Research spotlight) (http://www.cein.ucla.edu/new/p126.php); can be accessed at

https://www.youtube.com/watch?list=PL6XoOarfZTxEeNX3o2LFpw2aYkTbNoM0O&v=1h1JdHBqcxU

- Qualified the **National Eligibility Test** (NET, December 2004, and June 2005) in Environmental Sciences for consecutive two times; conducted by the University Grants Commission, Govt. of India. (**Ranked among top five students in India**).
- **First class first** in MS and awarded the university **Merit Scholarship** in Visva Bharati, India.

Activities:

- Serving **Women Advisory Council to the President** Dr. Diana Natalicio**,** UTEP.
- Active member (selected) of '**Faculty Senate Committee**' (Graduate Research division) at the University of Texas at El Paso.
- Reviewer of UTEP Provost's **Summer Student Research Assistant Program.**
- Official reviewer of American Chemical Society's (**ACS**) peer reviewed journals.
- Volunteering science outreach program (STEM) for Transmountain Early College High School (http://tmechs.episd.org*) kids*, El Paso, TX.
- Participating "Environmental Awareness" program among local school kids.
- Active participant in the Chemistry Research Day (ACS) organized by the department of Chemistry, UTEP.
- Chemistry demo presented to the school kids on WMU Chemistry Day, April 2010.
- Invited speaker in International workshop for Chemist and Chemical Engineers, WMU, summer, 2009.

- Served as **General Secretary** of Chemistry Graduate Student Association (CGSA), WMU June 2009-April 2010.
- The only **student member** for Central Universities Samsad court, VIsva Bharati, India, during year 2004-2005.

Professional memberships

- American Chemical Society (ACS).
- Golden Key International Honor Society.
- Sigma Xi Scientific Research Society
- University of California-Center for Environmental Implication of Nanotechnology (UC-CEIN)

Publications:

1. **Bandyopadhyay, S.** Peralta-Videa, J.R., Hernandez-Vieazcas, J.A., Montes, M., Keller, A.A., Gardea-Torresdey, J.L. 2011. Microscopic and spectroscopic methods applied to the measurements of nanoparticles in the environment. *Applied Spectroscopy Reviews,* Volume 47, Issue 3, 180-206, **2012.**
2. **Bandyopadhyay, S.** Peralta-Videa J. R., Germán P. Villa., Yacaman, M. Jose. Gardea-Torresdey, J.L. 2012. Comparative toxicity assessment of CeO_2 and ZnO nanoparticles towards *Sinorhizobium meliloti*, a symbiotic alfalfa associated bacterium: Use of advanced microscopic and spectroscopic techniques. *Journal of Hazardous Materials*, Volumes 241–242, 379–386, **2012**.
3. Zhao, L. Hernandez-Viezcas, J.A. Peralta-Videa, J. L. **Bandyopadhyay, S.** Peng, B. Munoz, B., Keller, A. A. Gardea-Torresdey, J. L. ZnO nanoparticle fate in soil and zinc

bioaccumulation in corn plants **(***Zea mays***)** influenced by alginate. *Environ. Sci.: Processes Impacts*, **2013**, 15 (1), 260 – 266.

4. **Bandyopadhyay S.**, Peralta-Videa, J. R., Gardea-Torresdey, J. L Advanced Analytical Techniques for the Measurement of Nanomaterials in Food and Agricultural Samples: A Review. *Environmental Engineering Science*; Special Issue, **2013,** 30(3):118-125.
5. Zhao, L., Peralta-Videa, J.R., Peng, B., **Bandyopadhyay, S**., Corral-Diaz, B., Keller, A.A., Gardea-Torresdey, J.L. **2013**. Alginate modifies the physiological impact of CeO_2 nanoparticles in corn seedlings cultivated in soil, *Journal of Environmental Science.* (In press)
6. Mukherjee, A.; Peralta-Videa, J. R.; **Bandyopadhyay, S**.; Rico, C. M.; Zhao, L.; Gardea-Torresdey, J. L. .ZnO nanoparticles induce phytotoxicity and differential ant-oxidative stress response in green peas (Pisum sativum L.) cultivated in soil. *Metallomics*, **2013**, DOI:10.1039/C3MT00064H
7. Majumdar, S., Peralta-Videa, J.R., **Bandyopadhyay, S.**, Castillo-Michel, H., Hernandez, J.A., Sahi, S., Gardea-Torresdey, J.L. 2013. Localization and biotransformation of cerium oxide nanoparticles in Red kidney bean plants and their in vivo antioxidative properties. *Environmental Science and Technology* (Under Review)
8. **Bandyopadhyay, S.,** Plascencia-Villa, G., Mukherjee, A. Peralta-Videa, Rico, C., José-Yacamán, M. and J. R., Gardea-Torresdey. Comparative phytotoxicity of ZnO NPs, bulk ZnO, and ionic zinc onto the alfalfa-*Sinorhizobium meliloi* association in soil. (Ready to submit, November, 2013).

9. **Bandyopadhyay, S.,** Mukherjee, A. Rico, C., . Peralta-Videa, J. R, Gardea-Torresdey J.L. Differential interaction of CeO_2 and ZnO nanoparticles on alfalfa's (*Medicago sativa*) secondary metabolites (Ready to submit, November, 2013).
10. **Bandyopadhyay S.**, Mukherjee, A. Majumdar, S. Peralta-Videa, J. R., Gardea-Torresdey, Interaction of CeO_2 NPs towards symbiotic nitrogen fixation between alfalfa (*Medicago sativa*) and associated bacterium (In preparation).

Poster and Presentations:

1. **Susmita Bandyopadhyay**, Arnab Mukherjee, Jose R. Peralta-Videa, Germán Plascencia-Villa, Cyren Rico, Miguel José-Yacamán and Jorge L. Gardea-Torresdey. Eco-toxicological effects of ZnO nanoparticles onto Medicago sativa-Sinorhyzobium meliloti association: An essential symbiotic association towards N-fixation; UC CEIN Nano EHS Forum: Scientific Advances towards Reducing Complexity in Nano EHS Decision Making. May 8, 2013 at **UC-CEIN, UCLA California NanoSystems Institute.**
2. **Susmita Bandyopadhyay**, Jose R. Peralta-Videa, German Plascencia Villa, Jorge L. Gardea-Torresdey. Toxicity assessment of CeO_2 and ZnO nanoparticles towards nitrogen fixing gram negative bacteria *Sinorhizobium meliloti* (Rm 1021); 244^{th} ACS National Meeting, August 2012.
3. **Susmita Bandyopadhyay**, Jose R. Peralta-Videa, German Plascencia Villa, Jorge L. Gardea-Torresdey. Toxicity of CeO_2 and ZnO nanoparticles towards *Sinorhizobium meliloti* (Rm 1021), Presented on 'Chemistry Research Day' (ACS) at UTEP, El Paso, TX, April 14^{th}, 2012.
4. **Susmita Bandyopadhyay** and S. Obare "Facile room temperature synthetic procedure for well-defined palladium nanocubes" ACS National Meeting, March 2010.

5. **Bandyopadhyay, S** and Chattopadhyay, G, “Impact of Organic Manuring in the Health of agricultural Soils in Red and Lateritic Soils Zone” NCOF National Seminar on Technology Options of Organic Inputs for Sustaining Soil Health in Indian Agriculture, Nov. 2006.
6. **Bandyopadhyay, S** “Effect of Persistent Organic Pollutants (POPs) on Coastal Environment-A threat to mankind”, accepted in the National Conference on “Environmental Hazards/Disaster and Its Management”, February 2007.

Permanent address: 6/A G P Singha Road
PO + Dist. Bankura, W.B
India
Pin: 722101

This dissertation was typed by Susmita Bandyopadhyay.